TABLE OF CONTENTS

Section			Page	
0		EXECUTIVE SUMMARY	0-1	1/B2
1.0		INTRODUCTION	1-1	1/B14
	1.1	Background Information	1-4	1/C4
2.0		PHASE AND AMPLITUDE TRACKING DEVELOPMENT AND DEMONSTRATION	2-1	1/D3
	2.1	Introduction and Summary of Results	2-1	1/D3
	2.2	Phase and Amplitude Tracking Data	2-5	1/D9
	2.3	Description of the Demonstration Test Bed, the Integration of the Magnetron with the Buck-Boost Coil, and Other Supporting Data	2-13	1/E5
	2.3.1	Physical Description of the Demonstration Test Bed	2-13	1/E5
	2.3.2	Description of the Magnetron with Buck-Boost Coil; Buck-Boost Coil Characteristics	2-15	1/E7
	2.3.3	Description of the Sensors, Comparators, and Other Components in the Phase and Amplitude Feedback Control	2-18	1/E11
	2.4	Analysis of the Microwave Power Amplitude Control System	2-23	1/F2
	2.5	Analysis of the Microwave Power Phase Control System	2-31	1/F10
	2.6	Documentation of the Electronic Circuits in the Amplifier for Phase and Amplitude Control Circuitry	2-31	1/F10
	2.7	Suggested Approach for a Phase Shift Device in the SPS Architecture	2-34	1/G1
3.0		MAGNETRON STARTING	3-1	1/G5
4.0		CONCEPT OF THE POWER MODULE AND ITS INTERFACE WITH THE REST OF THE SATELLITE	4-1	1/G9
	4.1	Definition of the Power Module and Its Interface with the Subarray	4-1	1/G9
	4.2	Interface of the Power Module with the Thermal Environment and with the Auxiliary DC Power Sources	4-6	2/A6
5.0		AUXILIARY POWER SOURCE STUDY	5-1	2/A13
	5.1	Introduction	5-1	2/A13
	5.2	Application of Microwave-to-DC Power Conversion as a Source of Auxiliary Power	5-3	2/B3
	5.3	Scenario of Start-Up Procedure in Subarray that Supplies its Own Auxiliary Power	5-10	2/B13

TABLE OF CONTENTS (Continued)

Section			Page
6.0		NOISE MEASUREMENTS	6-1 2/C6
	6.1	Introduction and Summary	6-1 2/C6
	6.2	Description of the High Sensitivity Noise Measuring Equipment	6-6 2/C13
	6.3	Description of the First Magnetron Configuration Tested	6-6 2/C13
	6.4	Results from the Magnetron Directional Amplifier Using the Raytheon QKH2000 #13	6-13 2/D9
	6.5	Description of and Test Results from the Second Magnetron Configuration	6-15 2/D11
7.0		DESIGN OF THE SPS MAGNETRON	7-1 2/E5
	7.1	Introduction	7-1 2/E5
	7.2	Study of Pyrographite Heat Radiator Design and Its Manufacture and Cost	7-5 2/E9
	7.2.1	Heat Radiator Design	7-5 2/E9
	7.2.2	Bonding Pyrolytic Graphite to the Magnetron Anode	7-11 2/F3
	7.2.3	The Manufacture of Pyrolytic Graphite and Its Fabrication into Radiators	7-12 2/F4
	7.3	Magnetic Circuit Study	7-15 2/F9
	7.4	Design of Interaction Areas of Magnetron	7-19 2/F13
	7.5	Design of Cathode for Long Life	7-23 2/G4
	7.6	Mechanical Design of the Magnetron	7-24 2/G5
	7.7	Projection of the Characteristics of the Magnetron Package	7-26 2/G7
8.0		HARMONIC SUPPRESSION BY COAXIAL STUB FILTERS	8-1 3/A7
9.0		THE USE OF THE AMPLITUDE CONTROL FEATURE IN THE MAGNETRON DIRECTIONAL AMPLIFIER TO OPTIMIZE THE OVERALL SYSTEM EFFICIENCY AND TO PROVIDE DIRECT CONTROL OF SPS SYSTEM DC POWER OUTPUT BY THE ELECTRIC UTILITY	9-1 3/B6
	9.1	Experimental Verification with a Simulated Voltage-Current Characteristic of the Solar Cell Array	9-6 3/B11

TABLE OF CONTENTS (Continued)

Section			Page	
10.0		DEFINITION OF TECHNOLOGY DEVELOPMENTS FOR THE MAGNETRON PACKAGE AND MAGNETRON DIRECTIONAL AMPLIFIER	10-1	3/B14
	10.1	Introduction	10-1	3/B14
	10.2	Unresolved Issues and Additional Investigations	10-2	3/C1
	10.3	The Proposed Development Program for the Magnetron Package	10-5	3/C4
	10.4	The Proposed Development Program for the Magnetron Directional Amplifier	10-5	3/C4
11.0		ESTIMATED MAGNETRON PACKAGE PRODUCTION COSTS	11-1	3/C10
APPENDIX A		THEORY OF OPERATION OF THE MAGNETRON DIRECTIONAL AMPLIFIER	A-1	3/C13
APPENDIX B		DATA COMPARISON	B-1	3/C14

NAS 1.26:3383

NASA Contractor Report 3383

ORIGINAL
COMPLETED

Satellite Power System (SPS) Magnetron Tube Assessment Study

William C. Brown

CONTRACT NAS8-33157
FEBRUARY 1981

MICROFILMED FROM
BEST AVAILABLE COPY

NASA

NASA Contractor Report 3383

Satellite Power System (SPS) Magnetron Tube Assessment Study

William C. Brown
Raytheon Company
Waltham, Massachusetts

Prepared for
Marshall Space Flight Center
under Contract NAS8-33157

National Aeronautics
and Space Administration

**Scientific and Technical
Information Branch**

1981

BLANK PAGE

BLANK PAGE

TABLE OF CONTENTS

Section			Page
0		EXECUTIVE SUMMARY	0-1
1.0		INTRODUCTION	1-1
	1.1	Background Information	1-4
2.0		PHASE AND AMPLITUDE TRACKING DEVELOPMENT AND DEMONSTRATION	2-1
	2.1	Introduction and Summary of Results	2-1
	2.2	Phase and Amplitude Tracking Data	2-5
	2.3	Description of the Demonstration Test Bed, the Integration of the Magnetron with the Buck-Boost Coil, and Other Supporting Data	2-13
	2.3.1	Physical Description of the Demonstration Test Bed	2-13
	2.3.2	Description of the Magnetron with Buck-Boost Coil; Buck-Boost Coil Characteristics	2-15
	2.3.3	Description of the Sensors, Comparators, and Other Components in the Phase and Amplitude Feedback Control	2-18
	2.4	Analysis of the Microwave Power Amplitude Control System	2-23
	2.5	Analysis of the Microwave Power Phase Control System	2-31
	2.6	Documentation of the Electronic Circuits in the Amplifier for Phase and Amplitude Control Circuitry	2-31
	2.7	Suggested Approach for a Phase Shift Device in the SPS Architecture	2-34
3.0		MAGNETRON STARTING	3-1
4.0		CONCEPT OF THE POWER MODULE AND ITS INTERFACE WITH THE REST OF THE SATELLITE	4-1
	4.1	Definition of the Power Module and Its Interface with the Subarray	4-1
	4.2	Interface of the Power Module with the Thermal Environment and with the Auxiliary DC Power Sources	4-6
5.0		AUXILIARY POWER SOURCE STUDY	5-1
	5.1	Introduction	5-1
	5.2	Application of Microwave-to-DC Power Conversion as a Source of Auxiliary Power	5-3
	5.3	Scenario of Start-Up Procedure in Subarray that Supplies its Own Auxiliary Power	5-10

TABLE OF CONTENTS (Continued)

Section			Page
6.0		NOISE MEASUREMENTS	6-1
	6.1	Introduction and Summary	6-1
	6.2	Description of the High Sensitivity Noise Measuring Equipment	6-6
	6.3	Description of the First Magnetron Configuration Tested	6-6
	6.4	Results from the Magnetron Directional Amplifier Using the Raytheon QKH2000 #13	6-13
	6.5	Description of and Test Results from the Second Magnetron Configuration	6-15
7.0		DESIGN OF THE SPS MAGNETRON	7-1
	7.1	Introduction	7-1
	7.2	Study of Pyrographite Heat Radiator Design and Its Manufacture and Cost	7-5
	7.2.1	Heat Radiator Design	7-5
	7.2.2	Bonding Pyrolytic Graphite to the Magnetron Anode	7-11
	7.2.3	The Manufacture of Pyrolytic Graphite and Its Fabrication into Radiators	7-12
	7.3	Magnetic Circuit Study	7-15
	7.4	Design of Interaction Areas of Magnetron	7-19
	7.5	Design of Cathode for Long Life	7-23
	7.6	Mechanical Design of the Magnetron	7-24
	7.7	Projection of the Characteristics of the Magnetron Package	7-26
8.0		HARMONIC SUPPRESSION BY COAXIAL STUB FILTERS	8-1
9.0		THE USE OF THE AMPLITUDE CONTROL FEATURE IN THE MAGNETRON DIRECTIONAL AMPLIFIER TO OPTIMIZE THE OVERALL SYSTEM EFFICIENCY AND TO PROVIDE DIRECT CONTROL OF SPS SYSTEM DC POWER OUTPUT BY THE ELECTRIC UTILITY	9-1
	9.1	Experimental Verification with a Simulated Voltage-Current Characteristic of the Solar Cell Array	9-6

TABLE OF CONTENTS (Continued)

Section			Page
10.0		DEFINITION OF TECHNOLOGY DEVELOPMENTS FOR THE MAGNETRON PACKAGE AND MAGNETRON DIRECTIONAL AMPLIFIER	10-1
	10.1	Introduction	10-1
	10.2	Unresolved Issues and Additional Investigations	10-2
	10.3	The Proposed Development Program for the Magnetron Package	10-5
	10.4	The Proposed Development Program for the Magnetron Directional Amplifier	10-5
11.0		ESTIMATED MAGNETRON PACKAGE PRODUCTION COSTS	11-1
APPENDIX A		THEORY OF OPERATION OF THE MAGNETRON DIRECTIONAL AMPLIFIER	A-1
APPENDIX B		DATA COMPARISON	B-1

LIST OF ILLUSTRATIONS

Figure		Page
1-1	Activity Flow Chart for Tasks 1.0 and 2.0	1-3
1-2	An Early Packaging Concept for Combining the Microwave Generator, its Heat Radiator, and a Section of Slotted Waveguide Radiator of Nearly the Physical Size of the Heat Radiator. In the Illustration Six Radiating Waveguides are Fed at Their Centers from a Slot in a Feed Waveguide. In the Case of the Magnetron Directional Amplifier the Feed Waveguide is Closed at Both Ends and is Fed at its Center from the Output of the Ferrite Circulator Attached to the Magnetron. Compare with Figure 4-1.	1-8
1-3	Slotted Waveguide Radiator Made from Thin Aluminum Sheet Stock by Novel Fabrication Method Developed at Raytheon. The Fabrication Method was Applied to a JPL Electrical Design to Produce the 8 x 8 Array (Eight Waveguides with Eight Slots in Each) that is Fed from a Single Port at the Middle and which can be Coupled Directly to the Magnetron Directional Amplifier.	1-9
1-4	Early Concept of Assembly of Packaged Crossed-Field Generator and Slotted Waveguide Units into a Power Module. Compare with Updated Concept in Figure 4-1.	1-10
1-5	Theoretical and Experimentally Observed Electronic Efficiencies of Conventional Microwave Oven Magnetron and 915 MHz Magnetron. Electronic Efficiency is Efficiency of Conversion of DC Power into Microwave Power. Overall Efficiency Includes Circuit Inefficiencies which can be Ascertained from Cold Test Data.	1-12
2-1	Schematic Diagram of Phase and Amplitude Control of Output of Magnetron Directional Amplifier. The Proposed Packaged Unit is Enclosed in Dotted Line. Relationship to SPS Overall System is Indicated Outside the Dotted Line.	2-3
2-2	Photograph of Test Bed for Phase and Amplitude Tracking Demonstration	2-4
2-3	Test Arrangement for Evaluating the Magnetron Directional Amplifier with Phase and Amplitude Tracking Feature	2-6
2-4	Phase Tracking of Output Phase to Reference Phase and Phase Shift through Magnetron Directional Amplifier as Function of Anode Voltage Level. Amplitude of Microwave Output is Held Constant.	2-9

LIST OF ILLUSTRATIONS (Continued)

Figure		Page
2-5	Phase and Amplitude Tracking Data with Series Resistance Reduced to 100 ohms to Simulate Operation Across a Hard Voltage Bus-10 Watts of Drive.	2-10
2-6	Phase and Amplitude Tracking Data with 50 Watts of Drive	2-11
2-7	Phase and Amplitude Tracking Data with 2.5 Watts of Drive	2-12
2-8	Overall View of Phase and Amplitude Control Circuits on Test Bed	2-14
2-9	Closeup View of Magnetron with Buck-Boost Coil Fitted to Waveguide in Phase and Amplitude Tracking Test Bed.	2-16
2-10	Modification of Microwave Oven Magnetron Showing (1) Magnetron Stripped of Cooling Fins and Ceramic Magnets (2) Buck-Boost Coil, (3) Cold-Rolled Steel Shell, and (4) Samarium Cobalt Magnets (Inside Ends of Each Portion of Shell).	2-17
2-11	Conventional Microwave Oven Magnetron Whose Magnetic Circuit has been Modified by the Addition of Coils which can be Used to Buck or Boost the Residual Magnetic Field Established by Permanent Magnets of the Original Packaged Tube.	2-19
2-12	Magnetron Anode Voltage and Power Dissipated in Buck-Boost Coil as Function of Current in Buck-Boost Coil. The Relationship of Anode Voltage to Coil Current is Very Linear as Shown.	2-20
2-13 a&b	Characteristics of ANAREN 70116 Crystal Mixer at 2.45 GHz.	2-21
2-14	Schematic Diagram of Amplifier in Phase Tracking Feedback Loop.	2-32
2-15	Schematic Diagram of Amplifier in Amplitude Tracking Feedback Loop.	2-33
2-16	A Comparison of Present Phase Control Arrangement with Proposed Magnetron Tuning which Provides Fast, Frictionless, Response and Broad Operating Range.	2-36
3-1	Transient Starting Behavior of Magnetron Directional Amplifier.	3-4
4-1	Assembly Architecture for the Magnetron Directional Amplifier in the Antenna Subarray. Two Power Modules are Shown. Microwave Drive and All References and Auxiliary Power are Inserted from the "Backbone" of the Subarray. The Array has Two Distinct Temperature Zones. The Top is Used to Radiate the Heat. The Bottom is Used for Mounting of Solid State Components.	4-2

LIST OF ILLUSTRATIONS (Continued)

Figure		Page
4-2	Schematic of Subarray Made from Power Modules.	4-3
4-3	Simplified Layout of Subarray Using Assumption that One Microwave Drive Source will Drive All of the Power Modules in the Array.	4-5
4-4	Schematic Diagram of Microwave Circuit for One Subarray.	4-7
4-5	Thermal Interfaces in Power Module.	4-8
4-6	Electrical Input Interface with Subarray Showing Use of RF to DC Conversion for Auxiliary DC Power.	4-9
5-1	Cross Section and Schematic of Rectenna Element that Efficiently Converts Microwave Power into DC Power.	5-4
5-2	Close-Up View of the "Split" Rectenna Element Mounted on the Ground-Plane. Diode is Cooled by Intimate Contact with Ground-Plane.	5-5
5-3a	Figure 5-3a Shows an Assembled Model of a Proposed Microwave-to-DC Source of Power for Transient Starting of Magnetrons.	5-6
5-3b	Indicates How Diodes of Existing Design Could be Efficiently Used.	5-7
5-4	Exploded View of the Model of the Proposed Arrangement for Obtaining High Current at Low Voltage from a 50 ohm Source of Microwave Power.	5-8
5-5	Schematic of Arrangement for Containing All Sources of Auxiliary Power within the Subarray.	5-11
6-1	DC to RF Converter Spectral Noise Power Density in 4 kHz Bandwidth.	6-3
6-2	Improved Notched Filter Functional Test Block Diagram for Increased Sensitivity of Noise Measurements. Power not Getting through High Power Waveguide Filter is Reflected Back into a Ferrite Circulator and Absorbed. Total Filter Consists of a Cascade Combination of a "T" Section of WR 430 Waveguide with a Short in One Arm Adjusted to Give Minimum Power Transmission and a Resonate Cavity Made from WR 284 Tightly Coupled to 3/4 Inch Coaxial Line. A Ferrite Circulator is Interposed Between Them to Prevent Coupling.	6-7
6-3	Attenuation of Notch Filter as Function of Frequency as Viewed on Hewlett Packard Spectrum Analyzer and Using Swept Oscillator as Signal source.	6-8

LIST OF ILLUSTRATIONS (Continued)

Figure		Page
6-4	Assembly of Tube Under Test. A Special Microwave Circuit is Attached to the Cathode Circuit. The Microwave Output of the Tube Feeds into a Coaxial Circuit which is then Coupled into Waveguide that is Attached to Noise Measuring Equipment.	6-10
6-5	Assembly of Tube in its Magnetic Circuit. From Top to Bottom (1) Coaxial Output, (2) Top Cold-Rolled Steel Flange, (3) Upper Samarium Cobalt Magnet, (4) Torus which is Combination Water Cooling Jacket or Magnetron and "Buck-Boost" Coil and (5) Lower Samarium Cobalt Magnet, (6) Lower Cold-Rolled Steel Flange, (7) Special Circuitry Added to Cathode Lead.	6-11
6-6	Cathode Plunger-Probe Set-Up.	6-12
6-7	Signal to Noise Ratio Measurements of Improved Sensitivity. Spectral Noise Density of 196 dB Below Carrier was Measured.	6-14
6-8	Data Indicating Impact of Positioning Cathode Circuit Short Circuit and Applying Heater Power.	6-16
6-9a	Magnetron with an Optical Window for Viewing Filament Temperature.	6-18
6-9b	Leeds and Northrup 86226 Optical Pyrometer.	6-18
6-10	Experimentally Observed and Theoretically Predicted Relationship Between Cathode Temperature and Anode Current for Two Magnetrons with Optical Window.	6-19
6-11	Spectra as a Function of Anode Current.	6-21
6-12	Spectrum Appearance as Function of Position of Movable Short in Circuitry Attached to Cathode.	6-22
7-1	Cross Section of Magnetron Design Showing Permanent Magnets, Buck-Boost Coils for Amplitude Control, and "Voice Coil" Driven Tuner for Phase Control.	7-3
7-2	Thermal Conductivity of Pyrographite in the "a" Direction as a Function of Temperature.	7-7
7-3	Drawing of the Shape of the Cooling Fin for the Microwave Generator. Heat Flows Radially from the Generator at Radius r_i, and is Radiated from the Top Surface. There will be a Temperature Drop T_d from r_e and r_i. Diameter of Radiator is Determined by Dimensions of the Slotted Waveguide Radiator.	7-9

LIST OF ILLUSTRATIONS (Continued)

Figure		Page
7-4	Information Chart for Selection of Pyrographite Radiator and Determination of its Mass. First, Determine Desired Temperature at Inner Radius of Radiator. Then Select the Desired Value of power to be Dissipated by the Radiator and Project this Value Horizontally Until it Intersects with the Inner Radius Temperature Curve. Vertical Projection of this Point Determines both the Thickness of the Radiator at its Inner Edge and the Mass of the Radiator in Grams. Temperature at Edge of Radiator May also be Estimated.	7-10
7-5	Magnetic Circuit Used for Computer Simulation and Experimental Measurement of Field in Interaction Area by Probe. The Scale of the Illustration is 40% Oversize.	7-16
7-6	Computer Field Plots for Magnetic Circuit.	7-18
3-1	Coaxial Output Fitted Directly to the Microwave Oven Magnetron.	8-2
8-2	Arrangement for Investigating Stub-Type Filter for Reducing Harmonic Level.	8-3
8-3	Proposed Reflection Filters to Minimize Second and Third Harmonic Power	8-4
8-4	Experimental Arrangement for Measuring Additional Attenuation of Second Harmonic Power by Coaxial Stub in 7/8 Inch Coaxial Line Tuned to Reflect Second Harmonic Power.	8-5
9-1	Overall Control System Showing How the Varying Demands of the Utility Power Grid can be Interfaced with the SPS Facility	9-2
9-2	Control of Illumination Distribution by Logic and Control Center to Command Amount of Power Radiated from Each Step-Taper Level.	9-3
9-3	Interface between Solar Cell Array and Magnetron Directional Amplifier.	9-5
9-4	Test Arrangement for Evaluation of Amplitude Control. See Also Figures 2-1 and 2-3.	9-7
9-5	Experimental Data on the Amplitude Control System Shown in Figures 9-4 and in More Detail in Figures 2-1 and 2-3.	9-8
10-1	Proposed Development of SPS Magnetron Package.	10-6

LIST OF TABLES

Table		Page
5-1	Auxiliary Power in Subarray.	5-2
6-1	Radiated Noise and CCIR Requirements Based on Radiated Power at ISM Band (2.4 - 2.5 GHz) Edges.	6-4
7-1	Cathode and Anode Diameter Dimensions for Magnetrons Operating at 20 Kilovolts and a B/B_o Ratio of 7 with Different Number of Space Charges.	7-22
7-2	Estimated Mass of Packaged Magnetron Including Cooling, Amplitude Control, Phase Control and Power Conditioning Function.	7-27
7-3	Projected Electrical Characteristics of the Magnetron Package.	7-29
7-4	Projected Mechanical Characteristics of the Magnetron Package.	7-31
8-1	Harmonic Levels in SPS System Based Upon (1) Harmonic Measurements on Output of Microwave Oven Magnetron, (2) Filter Rejection, and (3) Radiating Antenna Pattern for Harmonics	8-7
11-1	Breakdown of Costs for SPS Magnetron Package	11-2

SATELLITE POWER SYSTEM (SPS) MAGNETRON TUBE ASSESSMENT STUDY

0. EXECUTIVE SUMMARY

0.1 INTRODUCTION

The objectives of this study were two fold: first, to extend the data base with respect to the magnetron directional amplifier and its operating parameters that are pertinent to its application in the solar power satellite; secondly, on the basis of the resulting extended data base to outline the design of a magnetron that would meet the requirements of the SPS application and then to define a technology program that would result in its development.

The incentive for this study was the favorable findings from previous studies* that indicated the potential of the magnetron directional amplifier for the SPS application. Included in these findings were exceptionally high signal to noise ratio and potentially very long life based upon a low operating temperature of the carburized thoriated tungsten cathode. When these findings were added to the already confirmed observations of the high efficiency of the device and its mechanical and electrical simplicity, it seemed desirable to support the additional effort reported upon here to extend the data base further and to help resolve some of the emerging technical and system interface issues.

The following material will summarize the considerable accomplishments of this study and conclude with the remaining things that need to be investigated or demonstrated to provide high confidence that the magnetron directional amplifier will meet all of the requirements of the SPS system. It is important to bear in mind that the ultimate objective is to define the system and that investigating the interactions between the system and the microwave generator may well lead to modifications of previous

*Briefing Document by Raytheon, "Crossed-Field Directional Amplifier for Use in the Solar Power Satellite," to NASA/JSC and NASA/MSFC (September 1978) and to D.O.E. and NASA (December 1978).

W.C. Brown, "Microwave Beamed Power Technology Improvement" Final Report, JPL Contract No. 955104, May 1980. Raytheon Report PT-5613.

R.M. Dickinson, "Beamed Microwave Power Transmitting and Receiving Subsystems Radiation Characteristics" JPL Publication 80-11, June 15, 1980.

system and tube configurations. In particular, it would be premature to start the development of the SPS space tube until all of these interactions and their importance are understood.

It should be pointed out that any portions of this study that involved experimental data made use of the microwave oven magnetron that is readily available for test. However, the proposed magnetron design for the SPS is a close scale of the microwave oven magnetron and resembles it closely physically and electrically.

0.2 SUMMARY OF ACCOMPLISHMENTS

0.2.1 Demonstration of Phase and Amplitude Tracking Capability of the Magnetron Directional Amplifier

At a presentation given to both DOE and NASA officials in December 1978 on the magnetron directional amplifier, it was agreed that an issue that needed prompt resolving was whether the phase and amplitude of the microwave output from the magnetron directional amplifier could be made to follow accurately and simultaneously phase and amplitude references. That this could be made to happen with straightforward engineering procedures was adequately demonstrated during the study. The experimental arrangement involved an assembly of the magnetron directional amplifier, in which the conventional microwave oven magnetron was used, with a slotted waveguide antenna array together with the required sensors, phase and amplitude comparators, amplifiers, and the actuating devices in the feedback control loops. The actuator to control the amplitude of the output was a buck-boost coil that added to or subtracted from the residual magnetic field supplied by permanent magnets. The actuator to control the phase of the output was a motor-driven mechanical phase shifter inserted between the drive signal and the magnetron directional amplifier to compensate for the phase shift in the magnetron directional amplifier that is caused by various environmental and operational factors. The experimental equipment demonstrated phase tracking to within + and -1 degree and output amplitude tracking to within + and -3%, both of which are well within the requirements of the SPS system. Typical power gain of the amplifier was 100 (20 dB) and typical power output was 600-1200 watts.

0.2.2 Development of Concept to Greatly Expand the Range of Power Over which the Magnetron Directional Amplifier can Operate

In general the range of current, voltage, and DC power input over which a magnetron directional amplifier will operate without retuning the magnetron is proportional to the one-half power of the level of microwave drive. To avoid this undesirable tradeoff between range of operational power and amplifier gain, the magnetron may be designed with a tuning element whose position and therefore influence upon the natural resonant frequency of the tube is actuated by a solenoid excited by the output of the operational amplifier in the feedback loop of the phase control system. Since both the tuning element and the actuating coil in the solenoid are supported on a compliant member there are no mechanical sliding contacts. Further the response time of the sytem should be only a few milliseconds, a response time more than adequate for any disturbance of the microwave power system. The "voice coil" tuning principle has a precedent in the 6177 CW magnetron that is used in an altimeter application. This new concept, although straightforward, remains to be demonstrated as a phase control means in the magnetron directional amplifier.

0.2.3 The Use of the Amplitude Control Feature of the Magnetron to Greatly Simplify Power Conditioning Design and Procedures in the SPS

An investigation was made of combining the amplitude control afforded by the buck-boost coil with a logic control center to provide overall control of the SPS system from the utility interface at the earth receiving station. It was found that the arrangement would have the desirable features of: (1) the system could be operated at maximum overall system efficiency, (2) there would be very fast response time to a need for a change in power level, and (3) there would be no need for conventional conditioning of the power between the photovoltaic array and the microwave generator that is necessary with other approaches.

0.2.4 The Preliminary Design for the Overall Architecture of the Power Module, Subarray and Transmitting Antenna

The investigation of the many interfaces between the microwave generator and other parts of the system resulted in a new architecture that integrates the magnetron and magnetron directional amplifier into the subarray. One of the attractive features of the use of the magnetron directional amplifier in the architecture is a reduction in the estimate of the mass of the transmitting antenna in the SPS reference design by a factor of two. The estimated cost is reduced by essentially the same factor.

0.2.5 Demonstration of Magnetron Starting Using the Amplitude Control System

The amplitude control feedback loop with small modification was used to control the starting of the microwave oven magnetron in the magnetron directional amplifier and to prevent the radiation of spurious signals during the starting operation. While the magnetron filament is being heated for a period of about 5 seconds, an additional DC reference signal is applied to the input of the operational amplifier which results in boosting the magnetic field to the point where anode current cannot be drawn at the applied anode voltage even though the cathode is hot enough to supply emission. When the cathode filament is sufficiently heated the additional input to the operational amplifier is removed and normal operating conditions are then reached in about three milliseconds. The external source of filament power is also removed.

0.2.6 Study of Sources of Auxiliary Power

Auxiliary DC power is needed for the phase and amplitude control circuitry, and either DC or AC power is needed to initially heat the cathode filaments when the system is placed into operation. These needs for auxiliary power require low voltage so that a complicated DC - AC - DC power conditioning process to obtain the auxiliary low-voltage from the 20 kilovolt output of the solar cell array would be required. The results of the study suggest a different approach in which the auxiliary DC power

is derived directly from microwave power by rectifying it with Schottky barrier diodes made with Gallium Arsenide material. For the auxiliary DC power required for the control circuits for phase and amplitude tracking, the technology is immediately available from the diodes that have been successfully developed for the rectenna. For the higher power and lower voltage required for the magnetron filaments, the study suggests the use of impedance transformation at the microwave level with many special diodes operated in parallel to produce the necessary current. An advantage to this approach is that each subarray develops its own auxiliary power.

0.2.7 Study of the Microwave Drive Chain in the Subarray

With the use of the tuning element in the magnetron as discussed in 0.2.2 a sufficiently high value of gain in each magnetron directional amplifier may be obtained so that a single additional magnetron directional amplifier of identical design may be used as the driver for all the other magnetron directional amplifiers in a subarray of substantial size, for example, one containing 256 magnetrons. This common driver could then in turn be driven by a solid state source with approximately 30 watts of output.

The report describes a start-up scenario in which the only power that is brought into the subarray is the main 20 kilovolt bus. The very small amount of power that is initially needed to activate the startup procedure is supplied by three small batteries. In the event the battery source is not practical, the small power levels do have to be provided from external sources.

0.2.8 Mathematical Modeling and Computerized Study of the Design of the Pyrolytic Graphite Radiating Fin; Discussion of Brazing Techniques and Cost of Fabrication

This activity resulted in a design graph from which may be found the minimum mass of a radiating fin on which are placed the constraints of quantity of heat to be radiated and the maximum allowable operating temperature at the inner diameter of the radiator. A simplifying constraint is that all fins have the same

outer diameter which is determined by the spacing of radiating slots in the slotted waveguide radiator. It is found that the pyrographite cooling fin accounts for about 35% of the total mass of the magnetron.

An approach to the bonding of the pyrographite fin to the copper anode with high temperature brazing techniques that have been used successfully in similar applications is discussed. Discussed also are the present facilities available for the production of pyrographite and the investment necessary to produce large quantities of fins for SPS use.

0.2.9 Magnetic Circuit Study

The purpose of the magnetic circuit study was to narrow down the range of expected mass of the magnetic circuit for the SPS tube by analytical and experimental techniques. The design was based upon the requirement of 2700 gauss across a gap of 1.75 cm between poles. The assumption was made that samarium cobalt with an energy product of 24,000,000 would be available in the time period when production would take place. To validate this assumption, orders are now being taken by some magnet manufacturers for material with 22,000,000 energy product and it is understood that 28,000,000 has now been achieved in the laboratory. In our experimental study a material with 14,000,000 energy product was used. This arrangement gave a measured value of 2070 gauss in the tube interaction area. This measurement is consistent with a value of 2700 gauss if 24,000,000 energy product material had been used. The analytical procedure based upon the use of a well established and proven algorithm gave values of field very close to those found experimentally.

The measured mass of the experimental magntic circuit was 266 grams, inclusive of the permanent magnet mass but not of the mass of the buck boost coil.

0.2.10 Outline of the Design of a Magnetron Package with Power Generation, Radiative Cooling, Phase Control and Power Conditioning Functions

The study that was made of the interaction between the system requirements and the tube design indicated that the tube package should contain in addition to the power generation, cooling and amplitude control functions, the functions of the phase control actuator and system power conditioning. The latter two functions would generally be supplied elsehwere in the system; the first, in the form of a phase shifter and the latter in the form of relatively complex power conditioning equipment. Our study indicated that great savings in overall system mass, system cost, and system development time could be achieved if all the functions could be incorporated into the tube package.

It is believed that all of these functions have been successfully incorporated into the conceptual design of a tube that would be reasonable to develop and place into production. The tube design that includes all of these functions has a calculated mass of 1018 grams. It is believed that there is a 90% probability that the mass of the tube that results from the proposed tube development program will lie between 850 grams and 1500 grams. The largest potential growth factor in the mass of the tube is the growth in mass of the buck boost coil to meet exceptionally wide variations in the voltage current characteristic of the solar photovoltaic array. If the buck boost coil is used only to compensate for variations between tubes and variations with life of the tube the 90% probability mass would lie between 850 and 1150 grams.

The power output of the tube design is 3.2 kilowatts for an assumed overall efficiency of 85% and 5.0 kilowatts for an assumed overall efficiency of 90%.

0.2.11 Projection of the Electrical and Mechanical Characteristic of the Magnetron Package

These are given in tabular form in the report, and are to be used for system integration purposes.

0.2.12 Development of Equipment to Measure Higher Ratios of Signal to Broadband Noise; Examples of Exceptionally High Signal to Noise Ratios Made on the Magnetron Directional Amplifier; Significance of Measurements to the Electromagnetic Compatibility of the SPS

The determination of the residual background noise level of the magnetron directional amplifier had previously been limited by the residual noise level of the spectrum analyzer, even though a narrow band notch filter reduced the carrier level by a factor of 25 dB to prevent saturation and destruction of the analyzer by the carrier power. A task under this contract was to increase the measurement sensitivity by at least 20 dB by installing a high power notch filter for the carrier and in effect rejecting all but one part in 100,000 of the carrier signal so that all of the noise output of the microwave generator could feed directly into the spectrum analyzer.

This task was successfully completed and the sensitivity of the measurements increased considerably beyond the 20 dB specified to a figure of nearly 40 dB. The equipment can measure spectral noise density that is over 190 dB below the carrier at frequencies removed by more than 10 MHz from the carrier.

In terms of application, the equipment was used to measure the noise emission from a microwave oven magnetron that was used in a directional amplifier. The amplifier exhibited a spectral noise density (noise in a bandwidth of 1 Hz) that was 196 dB below the carrier. This is a very low level of noise that would provide a safety factor of 45 dB over the CCIR requirements even assuming the same gain for the noise as for the carrier signal in the 0.3 square meter aperture associated with each magnetron directional amplifier.

0.2.13 Harmonic Suppression by Notch Reflection Filters; Significance of Measurements to Electromagnetic Compatibility of SPS

Because of the single operating frequency of the magnetron directional amplifier and its relatively low operating power level it is possible to employ a coaxial line output from the magnetron and to place stub lines along the coaxial line to reflect

power at the harmonic frequencies. The study examined the use of this technique for the second harmonic and found that the stub filter attenuated the second harmonic by an additional 40 dB. Because the second harmonic was already below the carrier level by about 60 dB, the second harmonic level was down approximately 100 dB below the carrier. When this attenuation of the second harmonic is added to the attenuation and scattering in the slotted waveguide radiator the second harmonic level from the SPS is found to be compatible with the CCIR requirements.

0.2.13 Definition of a Technology Development Program to Develop the Magnetron Directional Amplifier for SPS Use

This study has made it possible to much more accurately define the design of the magnetron and to estimate the development effort involved in the development of a magnetron for SPS use. It is estimated that the cost of a four phase program would be approximately $4,900,000 in 1980 dollars, exclusive of facilities, to complete and would require approximately 8 years. The effort included a three year Phase IV program devoted to construction of a quantity of tubes and to life test.

In the event of a desire to speed up the development, it would be possible to perform much of the Phase III and IV development programs in parallel and thereby substantially cut down the development time.

0.3 REMAINING ISSUES

The results of the study being reported upon have significantly advanced the status of the magnetron directional amplifier (MDA) as a major contender for the Microwave generator in the SPS. However, there are a few remaining issues that need to be resolved.

These issues vary in their basic nature. Some relate to the tube directly, others relate to the magnetron's integration into a directional amplifier that is compatible

with all of the requirements imposed by a space environment and higher levels of integration, while still others defy a strict classification. These various issues are so classified, listed, and discussed in the following material. The discussion is abbreviated and not intended to cover many of the finer points of the issues or their resolution.

0.3.1 Basic Issues Related to the Magnetron

1. An understanding of the residual sources of noise in the microwave oven magnetron and how they may be controlled.

2. An understanding of the sources of inefficiency in the microwave oven magnetron and how they can be eliminated.

3. A demonstration that both high efficiency and high signal to noise ratio can be obtained while operating at a high DC input impedance level.

   Discussion of Items 1, 2 and 3: It seems logical that a satisfactory resolution of Items 1 and 2 would be a prerequisite to the demonstration of Item 3. The best opportunity to study any of these issues (1,2,3) is in the context of the microwave oven magnetron where a great deal of data has already been accumulated and where modification in tube design can be most easily made. It is recommended that studies relating to items 1 and 2 be pursued.

0.3.2 Basic Issues Related to the Form of the Magnetron Directional Amplifier (MDA) and Its Interface with the Power Bus

4. The determination of the proper passive directional device to use with the magnetron to form the Magnetron Directional Amplifier (MDA).

5. Interface of the Magnetron Directional Amplifier with the power bus. The concerns are the following: (1) parallel operation of MDA's on the same bus, involving both steady state and start conditions, (2) procedures to disconnect the magnetron from the power bus in case of a short within the tube (3) the amount of mass and power required for the buck-boost coils to accommodate the expected variation in voltage-current characteristic of the photovoltaic array.

Discussion of Items (4) and (5): MDA performance data with phase and amplitude control have been accumulated with the use of a single magnetron and a ferrite circulator device to form the MDA. This arrangement is compatible with successful starting and operating in parallel with similar MDA's on the hard 20 kV bus. Although this arrangement is suitable for terrestrial use it is not suitable for space use in its present form because ferrite circulators have not yet been developed for a high temperature environment nor is it known that they can be. This situation has led to the proposed solution of eliminating the need for a ferrite circulator by using two magnetrons with balanced output and phase in a 3 dB hybrid or similar arrangement. However, the approach brings with it complications of how to insure tube balance by control circuitry that must have phase and amplitude comparators in a high temperature environment. The interface of a dual tube MDA with the power bus is also much more complicated than the single tube MDA.

It is recommended that investigations be supported for (1) assessing the probability of developing a ferrite circulator that would meet the requirements of operation in a high temperature environment, and (2) the development of a dual-magnetron MDA that will meet all of the system and environment requirements, (3) determining the amount of mass and power required for the buck-boost coils to accommodate the expected variation in voltage-current characteristics of the photovoltaic array.

0.3.3 Basic Issues Related to Both Tube and Higher Levels of Integration

6. Demonstration of phase tracking by employing magnetron "voice coil" tuning.

Discussion of Item 6: The demonstration is principally for the purpose of gaining acceptance of the concept by that portion of the SPS community concerned with the Microwave subsystem and its ability to take over much of the power conditioning function. It is recommended that the 6177 CW magnetron that has a "voice coil" tuner in it be used for this purpose.

1.0 INTRODUCTION

The objective of this study as given in the Statement of Work is "to provide MSFC and the NASA with additional accurate and sufficient data and information to allow the SPS system study activities to evaluate the potential role of magnetrons in the SPS concept and make recommendations to management".

There are two principal tasks in this study. The first task is the "extension of the laboratory data base on the injection locked magnetron", or the magnetron directional amplifier as it is alternatively called to designate that it belongs to the larger class of crossed-field type directional amplifiers. The second task, based in part upon the first, calls for the "projection of the magnetron directional amplifier technology." An important end product to the second task is the outline of a technology development program that embraces both the magnetron tube as a separate entity, and the various interface components that are considered essential in making the magnetron directional amplifier a viable candidate to meet the severe SPS requirements of high efficiency, long life, low mass, minimal radio frequency interference operation in a high temperature environment and reasonable cost.

In carrying out these tasks it has been necessary to look at several higher levels of integration: (1) the magnetron tube is combined with a passive directional device and a control loop for tracking both a reference phase and amplitude to form the magnetron directional amplifier; (2) the magnetron directional amplifier is combined with a section of slotted waveguide radiator to form the "radiating unit"; (3) radiating units are combined to form "power modules"; (4) power modules are grouped together and combined with auxiliary power sources and an rf driver to form the subarray. Also the output amplitude of the magnetron directional amplifier is controlled by a logic and control center to provide a capability to maximize overall efficiency of the system and to permit automatic control of the SPS output to meet the requirements of the utility interface on the ground. This integration study has led to a rather definitive architecture of the power module and subarray with a great deal of detail in it as described in Section 4.0.

There were several subtasks included in an extension of the laboratory data base. These were (1) demonstration of phase and amplitude tracking capability of the magnetron directional amplifier including operating data over a broad range of power and gain; (2) magnetron starting; (3) analytical study of the pyrolytic graphite radiator and formulation of design data; (4) analytical and experimental study of the magnetic circuit leading to a specific design for the magnetron; (5) study of auxiliary DC power sources; (6) study of rf drive for the magnetron directional amplifier; (7) improvement of noise measuring techniques for detection of noise at a much lower level, and a demonstration of the equipment on two tubes; (8) an investigation of the suppression of harmonic power by means of stub filters.

The information derived from the above tasks was combined with other sources of information to design a magnetron tube package with a definite set of mechanical and electrical characteristics as described in Section 7.0 that can provide the system designer with much of the information he needs for the integration of the magnetron and the closely associated magnetron directional amplifier into a system design.

The interrelationship of the various portions of the study activity is shown in the "Activity Flow Chart" given in Figure 1-1. The end-product of the study is a final report which reports upon the various items added to the laboratory data base and which defines a technology development program to develop the magnetron directional amplifier for SPS use.

It is important that the content of this report be properly related to other activities, and important that it be understood why the study was undertaken. There will be no problem in understanding either the motivation of the study or in the application of its results by those familiar with the total background of the microwave generator in the SPS. To those not familiar with this background the study may appear to have no roots and its application uncertain. For this reason, the history of the crossed-field directional amplifier in the SPS concept leading up to the reason for the undertaking of the present study is summarized in the next section.

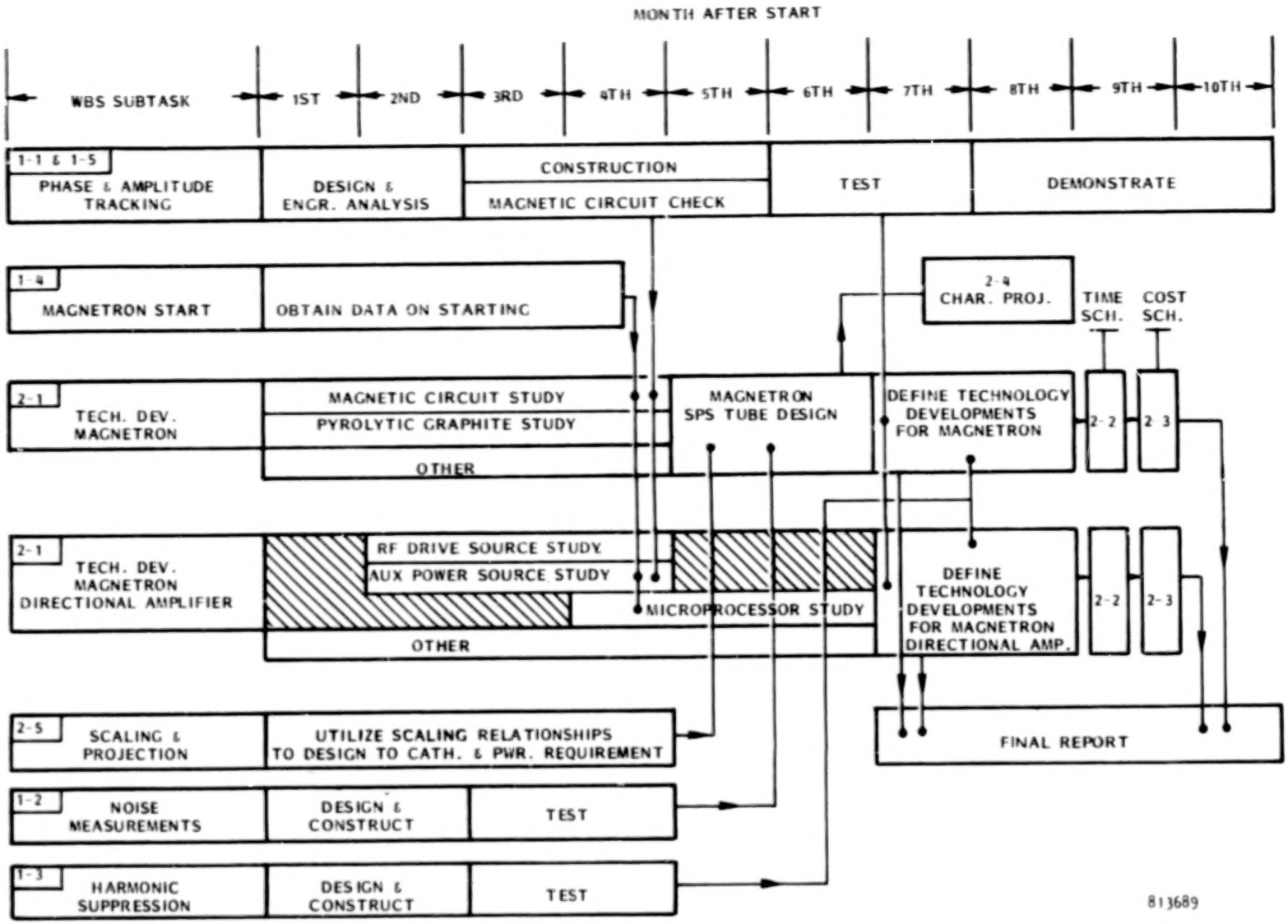

Activity Flow Chart

For those readers who are not familiar with the general properties of the crossed-field directional amplifier Appendix A has been attached to provide some level of understanding of the device.

1.1 Background Information

A proper understanding of this study needs the perspective provided by a review of what has already been done and found out with respect to the use of crossed-field devices in the SPS. The history of the approach of using crossed-field devices indicates that there were a number of "discoveries" of great importance. These discoveries have reshaped the original direction of approach in using these devices. It has been the active test and tube development efforts that have been the key to discovery, change, and progress toward the desired goal of the use of the crossed-field device in the SPS.

The earliest studies on the SPS conducted by the four-company team of A.D. Little, Raytheon, Grumman, and Textron, determined what has since been many times confirmed, i.e. disposing of the wate heat generated during DC to microwave conversion was a major problem.(1) The need for high efficiency to help solve this problem and the need for extremely long life, led to the proposal to use amplitrons which were recognized for both high efficiency and the use of a pure metal cathode operating on secondary emission which has unlimited life.(2) The amplitron development effort by Raytheon for NASA LeRC projected the optimum mass, power handling capability, efficiency, and other properties of the amplitron.(3) It turns out that the results of this study are directly applicable to the projection of a magnetron design for the SPS because of the similarities of the devices.

The amplitron had other desirable features including very low phase shift across the device and the lack of the need for a high power ferrite circulator or magic T since it contains its own directional properties. However, it has the undesirable

properties of low gain and the need for a separate radiator attached to the cathode because of the rather large amounts of electron backbombardment power needed to sustain the secondary emission process. In addition, there was great uncertainty as to the noise level of the device.

During the execution of the amplitron contract for NASA LeRC, Richard Dickinson of JPL recommended investigating the use of the microwave oven magnetron as a directional amplifier for a field demonstration of a phased array which he was proposing.[4] Although the microwave oven magnetron had had the reputation for being very noisy, the author of this report, doing some voluntary initial evaluation work for Dickinson, found it to be extremely quiet if it were run on a well filtered DC power supply and if the external power to the heater were removed.

Subsequently work performed in the first phase of the amplitron development under contract NAS 3-20374 for NASA LeRC by Raytheon proved to be disappointing from the viewpoint of obtaining emission from the pure metal platinum cathode by injection of drive power. When a thoriated tungsten helix cathode was used and heated from an external source, operation was obtained and under certain operating conditions low noise was obtained. Another finding that is of major importance in scaling to high voltage and low current to obtain long-life from primary-emitting cathodes was that very low leakage current from the interaction area could be maintained by pole pieces kept at cathode potential. However, the tube had a number of problems including less than expected efficiency and much lower power output than expected at the 8 dB gain level. These defects were attributed to poor microwave field patterns in the interaction area between cathode and anode but time and level of effort did not allow for correction of the field patterns. The program effectively terminated in June of 1978 with the decision not to carry out any technology development effort that directly involved the SPS concept. This decision effectively cancelled the original plan to continue amplitron development activity through a second phase.

In April of 1978, Raytheon begain work on a sub-contract from JPL entitled "Microwave Beam Power Technology" which was directed toward general improvements in microwave power transmission and not specifically towards the SPS application.(5) By August of 1978, enough interesting information had been obtained on low noise operation and other magnetron operating aspects to justify presentation of the data, with the approval of JPL, to JSC and MSFC by Raytheon. The Raytheon team, headed by Mr. Owen Maynard, also presented some scenarios on how the magnetron directional amplifier might fit into a subarray unit in the SPS.(6)

At the JSC presentation, JSC personnel raised the issue as to what the life of magnetron tubes might be in the SPS application. The subsequent efforts at Raytheon to answer this question led to a second important discovery.(5) It was determined that if the microwave oven magnetron is operated at anode current levels 2/3 of the normal value, the temperature of the carburized thoriated tungsten cathode is so low as to give 10 to 20 years of cathode life as established from data on the life behavior of similar cathodes in high power triodes. Further, it was noted that tubes scaled to operate at 3 to 7 kilowatts and 20 kilovolts in the SPS could have cathodes that would have over 50 years of life, as discussed in Section 7.5. Also, in space any possibility of filament sag would be eliminated by the gravity free environment.

Additional advantages are the additional increase in overall tube efficiency over that of a tube with a pure metal secondary emitting cathode and the elimination of the external cathode heat radiator that would probably be necessary for the pure metal cathode.

It was recognized that the negative aspect of the use of a heater is that it will need a source of power for a few seconds to initiate a minimum amount of emission required for starting.

In its presentation to JSC and MSFC, Raytheon also presented a package concept for the microwave tube in which the tube, its heat radiator, and section of slotted waveguide were packaged together as shown in Figure 1-2.[6] This concept was similar to that earlier proposed by JPL for its ground based phased array concept. Since then the concept for space use was given considerable substance by a novel method developed by Raytheon to accurately fabricate slotted waveguide radiators out of thin metal.[5] A large slotted waveguide radiator that follows a basic electrical design from JPL and that might be used toward the edge of the transmitting antenna and manufactured by this technique is shown in Figure 1-3.

Although the slotted waveguide unit was fabricated from 0.020" thick material it is mechanically very strong and stiff, and the indication is that the same fabrication method could be used with 0.005" thick material for fabrication of arrays for space satellite use. Without a promising approach to the fabrication of thin-walled SPS waveguides the mass had been previously estimated on the basis of 0.020" thick aluminum. In a transmitting antenna, one kilometer in diameter, the saving in mass using 0.005" material in place of 0.020" material is over 2,000,000 kilograms.

The low mass aspect of this construction is, of course, important but there are two other important aspects. One of these is that because of a combination of the poor thermal conductivity represented by the thin 0.005" thick waveguide walls and the potential use of reflective coatings to reduce transfer of heat by the radiation process, a substantial drop in temperature can be maintained between the back and front side of the slotted waveguide array. Hence, solid state components for control systems, microprocessors, etc. can be mounted on the outboard surface where the environmental temperature will be sufficiently low. The second aspect that is important is that the construction method leaves a gap of 0.50" between the waveguide walls so that this space can be used for cable runs to the solid state components mounted on the surface and possibily for the housing of some components.

Finally, the concept of mounting the individual units on supporting rails as shown in Figure 1-4 mechanically separates the waveguide sections from each other

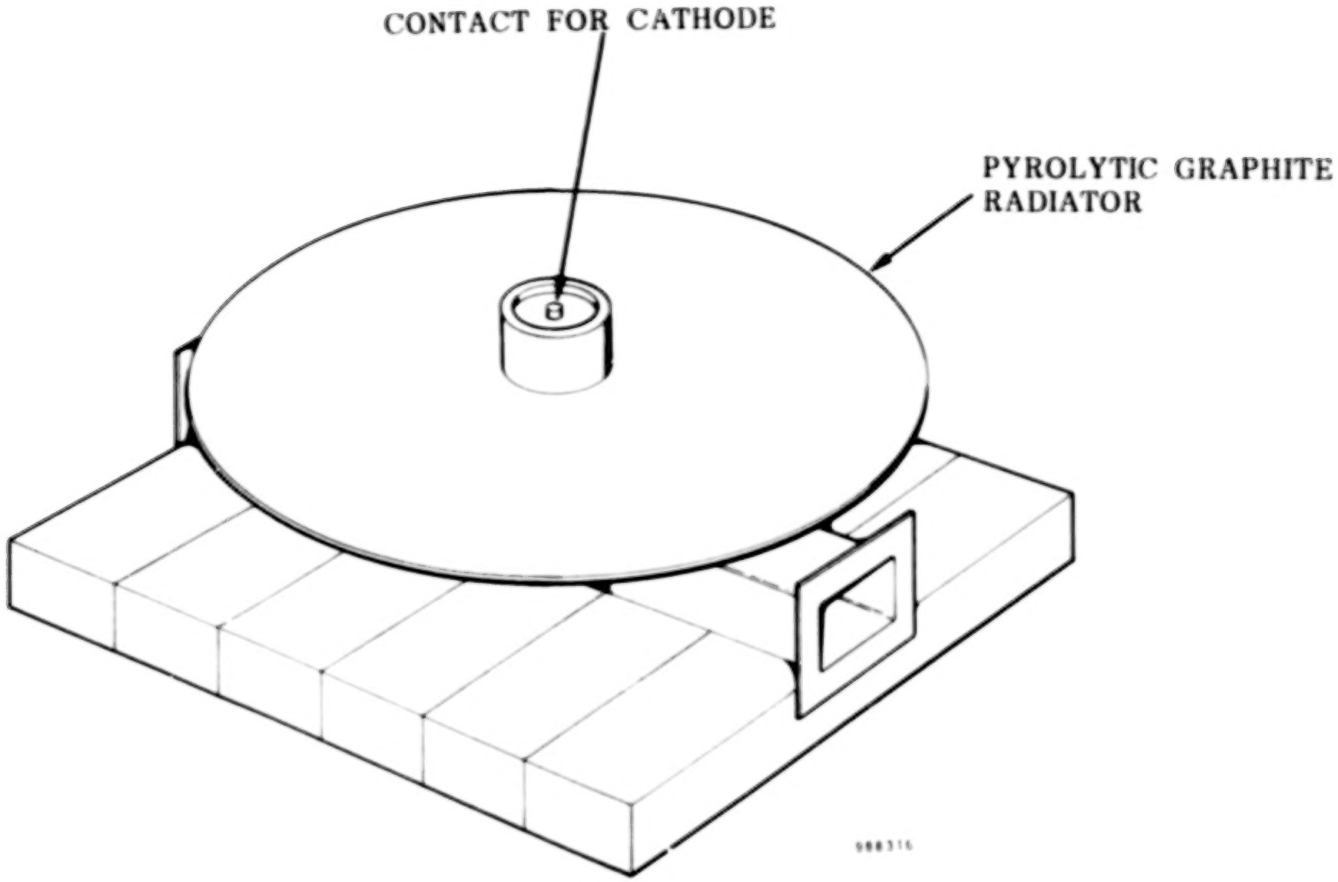

Figure 1-2. An Early Packaging Concept for Combining the Microwave Generator, its Heat Radiator, and a Section of Slotted Waveguide Radiator of Nearly the Physical Size of the Heat Radiator. In the Illustration Six Radiating Waveguides are Fed at Their Centers from a Slot in a Feed Waveguide. In the Case of the Magnetron Directional Amplifier the Feed Waveguide is Closed at Both Ends and is Fed at its Center from the Output of the Ferrite Circulator Attached to the Magnetron. Compare with Figure 4-1.

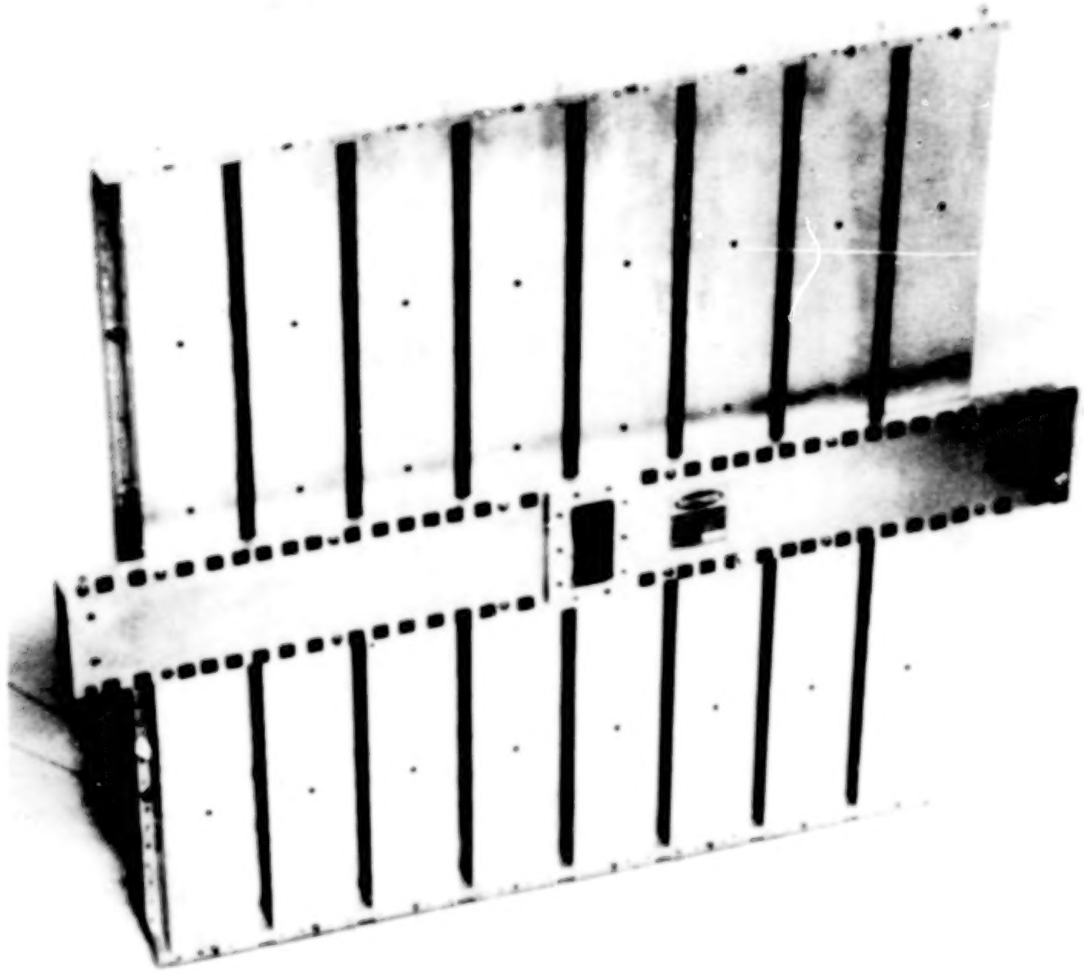

79-83304

Figure 1-3. Slotted Waveguide Radiator Made from Thin Aluminum Sheet Stock by Novel Fabrication Method Developed at Raytheon. The Fabrication Method was Applied to a JPL Electrical Design to Produce the 8 x 8 Array (Eight Waveguides with Eight Slots in Each) that is Fed from a Single Port at the Middle and which can be Coupled Directly to the Magnetron Directional Amplifier.

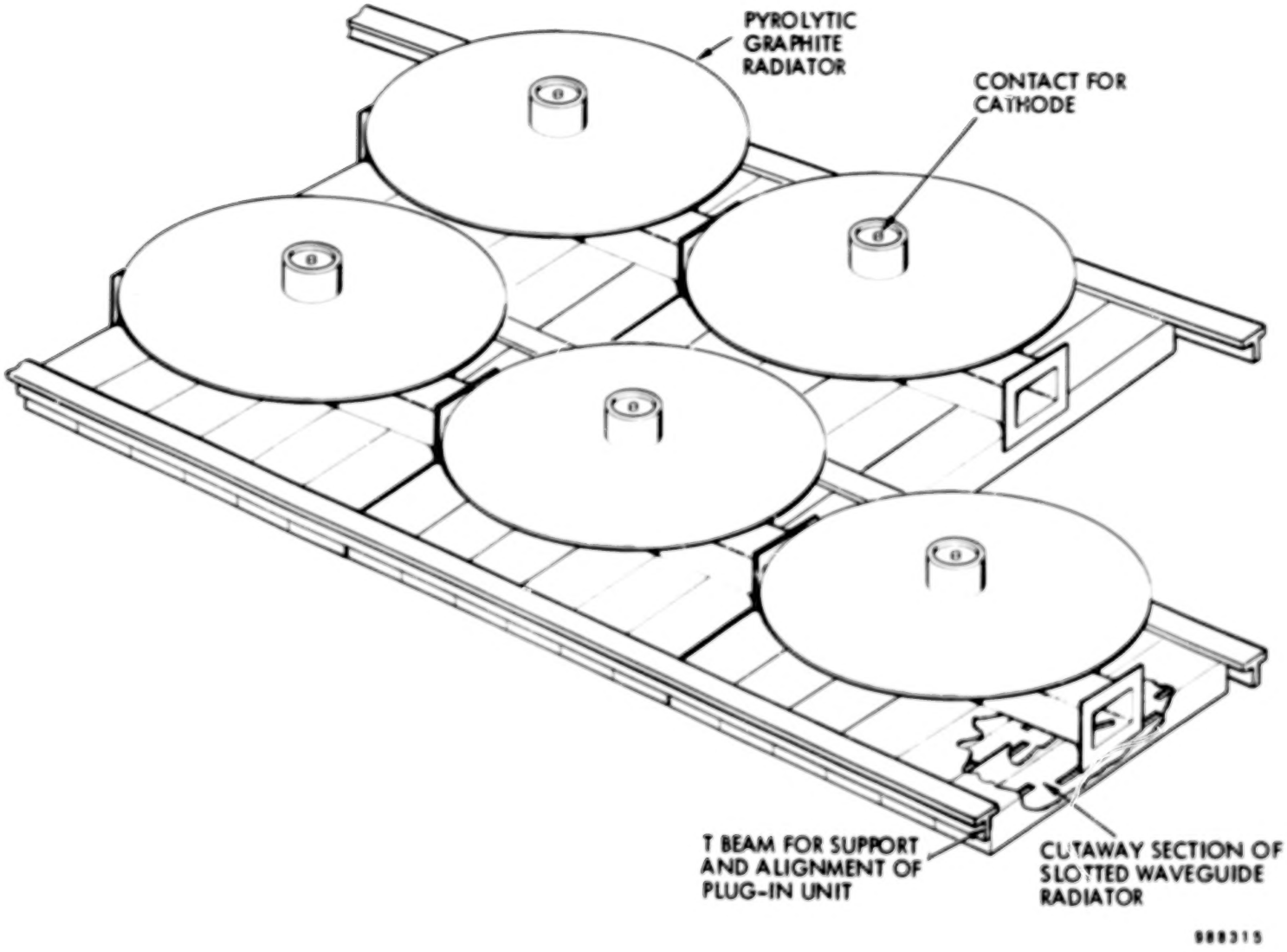

Figure 1-4. Early Concept of Assembly of Packaged Crossed-Field Generator and Slotted Waveguide Units into a Power Module. Compare with Updated Concept in Figure 4-1.

and reduces to negligible consideration the warping of the waveguide sections caused by the differences in temperature on the two faces.

One additional finding of importance was the obtaining of 82 ±1% overall efficiency from a microwave oven magnetron by operating it at a B/B_O ratio of eight.[5] As shown in Figure 1-5, the importance of this finding is not the high efficiency, but rather that the efficiency is considerably lower than theoretical and as compared with that obtained from the 8684 magnetron at 915 MHz. Hence, there is a real need to find out how to improve the efficiency of the 2.45 GHz magnetron and this should be a major element in any technology development program.

There were also some recent developments in microwave oven magnetrons that were of interest to the SPS application in confirming the high ratio of power output to mass that can be obtained from these packaged tubes. The recent Hitachi 2M106 magnetron has been built with internal permanent magnets. This tube will generate one kilowatt of power but weighs only 1.5 pounds, complete with cooling fins, and is the latest development in a reduction of mass and cost that has taken place over 20 years. Unfortunately, this tube has been removed from the market because of the high price of cobalt, a prime material in the magnet. For this and other reasons we can probably not depend upon magnetron manufacturers to continue to follow directions that parallel what is needed for the SPS.

These findings, discoveries, and developments related to the magnetron created a growing interest in the further investigation of the magnetron directional amplifier for the SPS application. One of the outstanding concerns was the phase shift through the device which varied rapidly with operating current, voltage and gain. Could that be eliminated or compensated for in some manner? Similarly, the ability of the magnetron directional amplifier to operate in parallel with other units off of the same hard voltage bus without the use of objectionable series ballasting was of concern. These two concerns were probably the principal motivation for a study to expand the data base but there was also opportunity to introduce other important study items that were listed earlier.

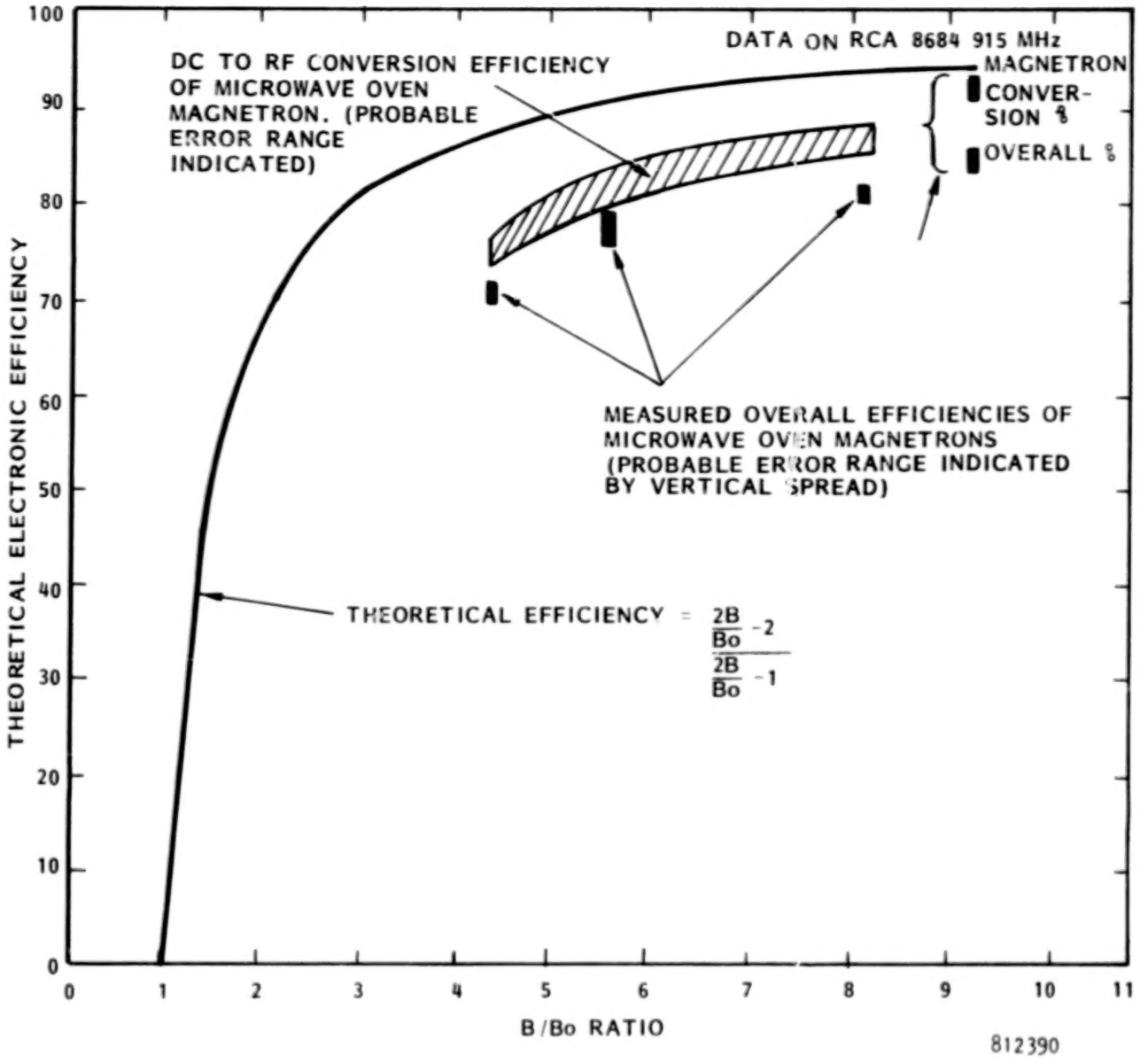
DATA ON RCA 8684 915 MHz MAGNETRON
DC TO RF CONVERSION EFFICIENCY OF MICROWAVE OVEN MAGNETRON. (PROBABLE ERROR RANGE INDICATED)
CONVER-SION %
OVERALL %
MEASURED OVERALL EFFICIENCIES OF MICROWAVE OVEN MAGNETRONS (PROBABLE ERROR RANGE INDICATED BY VERTICAL SPREAD)
THEORETICAL EFFICIENCY = 2B/Bo -2 / 2B/Bo -1
THEORETICAL ELECTRONIC EFFICIENCY
B/Bo RATIO
812390

Figure 1-5. Theoretical and Experimentally Observed Electronic Efficiencies of Conventional Microwave Oven Magnetron and 915 MHz Magnetron. Electronic Efficiency is Efficiency of Conversion of DC Power into Microwave Power. Overall Efficiency Includes Circuit Inefficiencies which can be Ascertained from Cold Test Data.

1. W.C. Brown, O.E. Maynard, "Microwave Power Transmission in the Satellite Solar Power Station System." Raytheon Report ER 72-4038, 27 January 1972.

2. "Microwave Power Transmission System Studies", NASA CR-134386, Raytheon ER 75-4368, December 1975. NASA LeRC Contract NAS 3-17835.

3. W.C. Brown, "Design, Fabrication and Testing of a Crossed Field Amplifier for Use in the Solar Power Satellite", NASA CR-159410, Raytheon PT-5228, August 1978. NASA LeRC Contract NAS 3-20374.

4. R.M. Dickinson, "Microwave Power Transmitting Phased Array Antenna Research Project Summary Report", JPL Publication 78-28, December 15, 1978.

5. W.C. Brown, "Microwave Beamed Power Technology Improvement", Final Report on JPL Contract No. 955104 Raytheon Report PT-5613, May 1980.

6. O.E. Maynard, H.R. Ward, J.T. Haley, J.M. Howell, W.C. Brown, Raytheon Briefing on Crossed Field Directional Amplifiers for Use in the Solar Power Satellite, September 1978.

2.0 PHASE AND AMPLITUDE TRACKING DEVELOPMENT AND DEMONSTRATION

2.1 Introduction and Summary of Results

The output phase of any microwave generator in the SPS, regardless of kind, must be carefully controlled in order that it not appreciably impact the overall phase budget of the subarray which must include many other factors. Open ended control for the magnetron directional amplifier and klystron is not feasible and probably only marginally feasible for the amplitron. For the magnetron directional amplifier and klystron this control must utilize a low level phase reference at the output, a comparator circuit to compare the phase of the generator output with the reference phase and to generate an error signal, and a feedback loop to make a compensating phase adjustment at the input.

The control of the output amplitude in the face of many factors that tend to change that amplitude is also essential for generating an efficient microwave beam. In the case of a crossed-field device the output amplitude can be controlled to a fixed desired value by another control loop which makes use of small electromagnets that can be used to boost or buck the residual field provided by permanent magnets.

The amount of power required to compensate for expected variations in the permanent-magnet field with temperature and life, and minor changes in the dimensions of the tube with life are very small. With additional power, but still reasonable in the context of power dissipation from other causes, this arrangement can also adjust the operating voltage of the microwave generator array to correspond to the most efficient operating point of the solar photovoltaic array. This would be very difficult by any other means of power conditioning because the output of the solar cell array is DC and the direct transformation from one DC voltage to another is not possible without resistive losses. Indirect methods such as transformation to high frequency AC, then an AC voltage change by transformers, and then back to DC again by rectification would appear to be highly impractical in this application where huge power, very low mass requirements, and difficulty of dissipating the inevitable losses in the transformation process prevail.

Another factor of importance is that the efficiency of the magnetron is impacted to only a minor degree by reasonable variations in the applied voltage. It can therefore accommodate itself to the changing voltage characteristics of the solar photo voltaic array while its efficiency variation would be only two or three percent.

The overall schematic for the combined phase and amplitude control of the magnetron directional amplifier is shown in Figure 2-1. Also shown is how this control can be related to the overall power absorption by the solar cell array. A central computer establishes the most efficient operating point (maximum power output) of the solar cell array and then adjusts the reference power output of the banks of magnetron directional amplifiers, making certain of course not to err on the side of asking for more power than is available from the array.

A test bed was constructed for the purposes of taking data and for demonstrating the performance of the array to MSFC's contractor, Rockwell International, who had the responsibility for the study of the integration of the magnetron into the overall SPS system. The assembly that was demonstrated is shown in Figure 2-2. In this demonstration the microwave power generated by the magnetron directional amplifier was fed into the slotted waveguide array which in turn radiated the power into a glass-foam load that was well matched to space and absorbed nearly all of the power.

It was also possible to interchange the slotted waveguide array with a well matched water load which enabled accurate measurement of power output to be made. The measurements that were made during the study are presented in considerable detail in Section 2.2. The general performance may be summarized by noting that the output phase of the radiated power followed a reference phase to within ± 1 degree, and that the amplitude followed the reference amplitude within $\pm 3\%$ over a very wide operating range of both current and voltage. The performance may be considered as successfully meeting the objectives of the study.

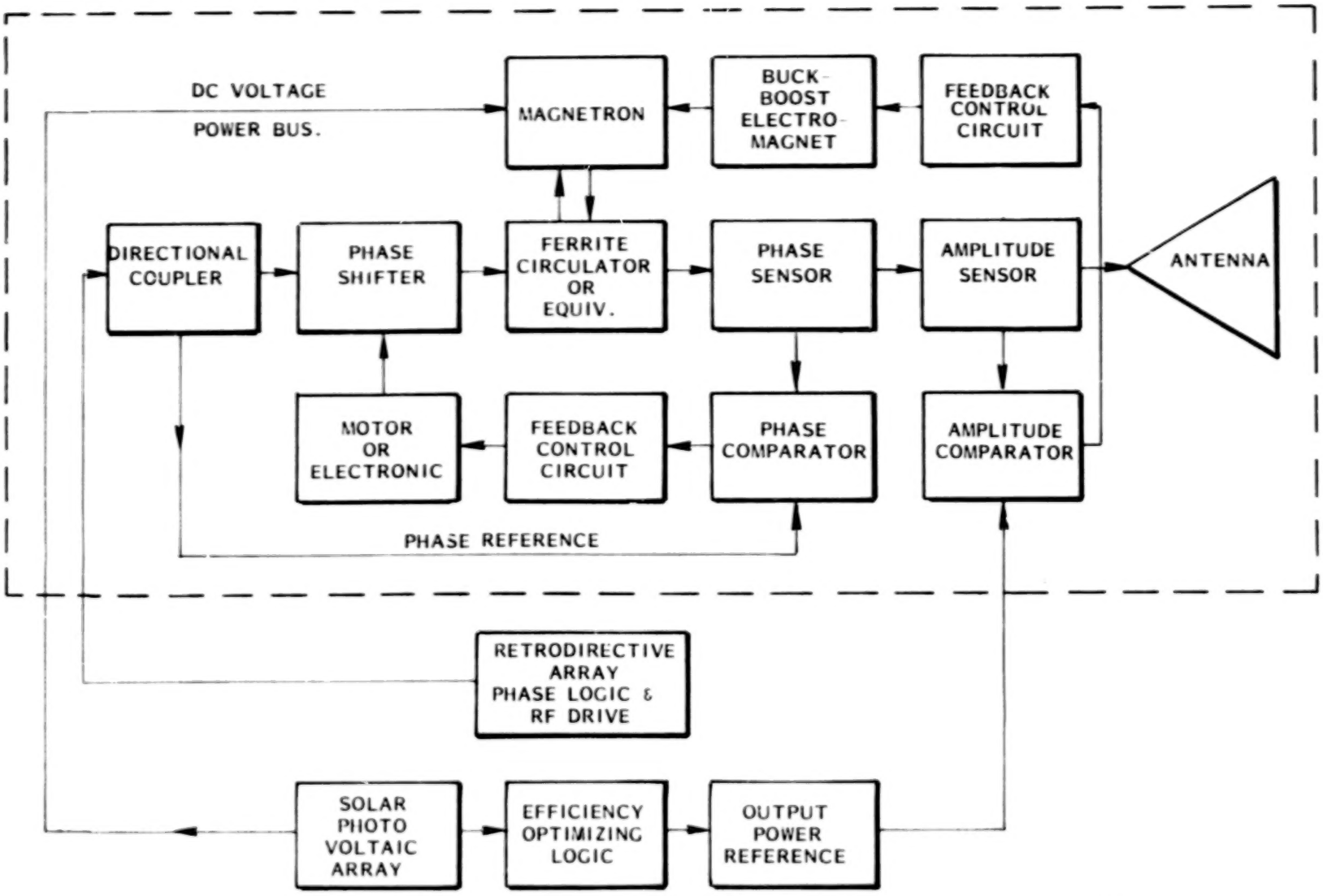

Figure 2-1. Schematic Diagram of Phase and Amplitude Control of Output of Magnetron Directional Amplifier. The Proposed Packaged Unit is Enclosed in Dotted Line. Relationship to SPS Overall System is Indicated Outside of Dotted Line.

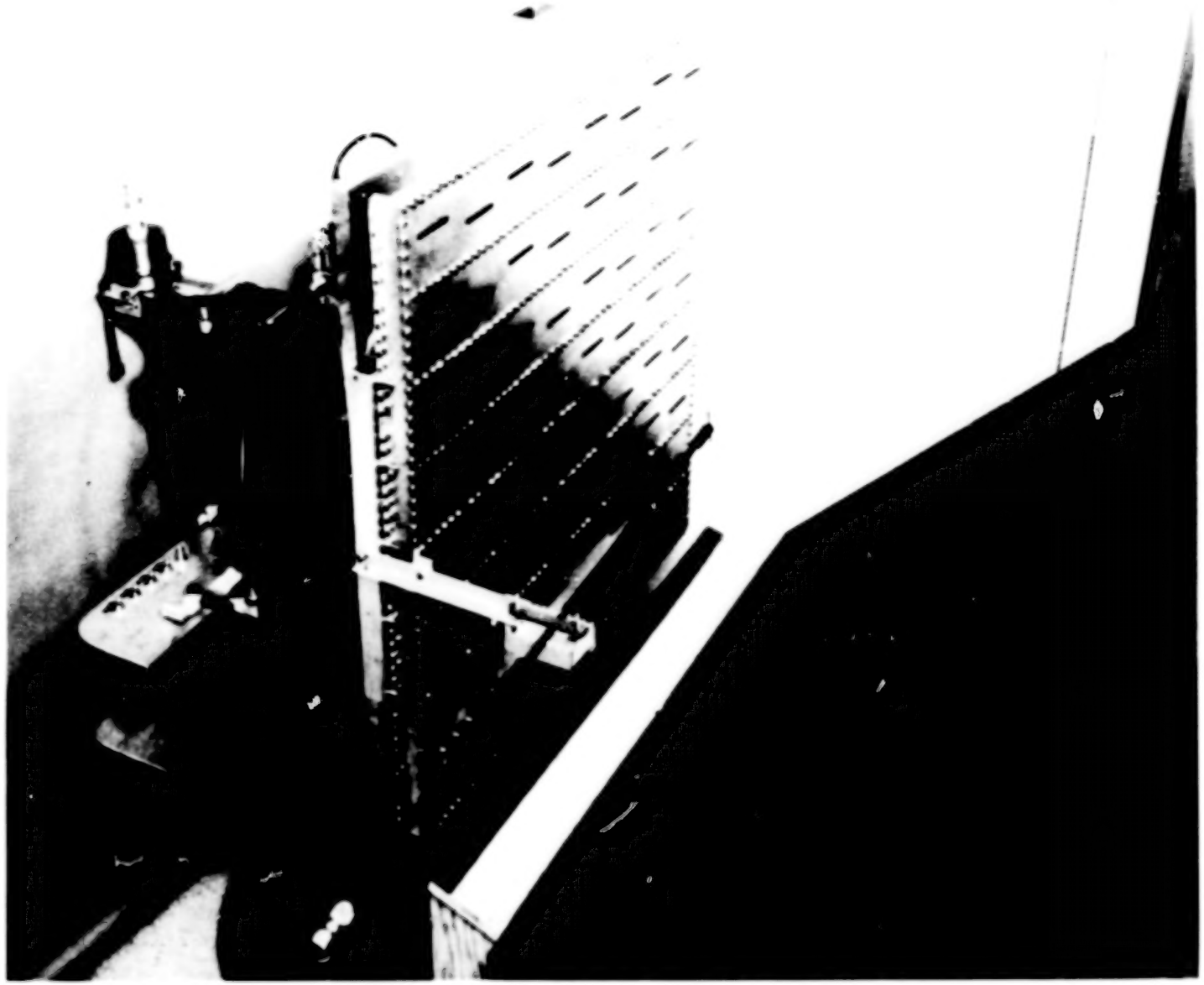

80-1041B

Figure 2-2. Photograph of Test Bed for Phase and Amplitude Tracking Demonstration.

The remainder of this introduction will be devoted to the organization of the rest of Section 2.0. In part 2.2, a review of the performance results will be set forth. Section 2.3 deals with the physical set up and circuit details, feedback loops, etc. Part 2.4 reviews the theoretically predicted behavior of the amplitude control loop and compares the predicted with experimentally observed results. Section 2.5 addresses the status of phase control analysis; 2.6 documents circuitry, and 2.7 discusses a new concept for achieving phase control over a very large operating range of current and voltage by retuning the magnetron.

The reader is referred to Section 9.0 which deals with the application of amplitude control to maximizing system efficiency and interfacing with the electric utility load.

Finally it should be noted that the amplitude control feature of the magnetron directional amplifier is of great importance in starting the magnetron, as will be discussed in Section 3.0.

2.2 Phase and Amplitude Tracking Data

The test arrangement for the magnetron directional amplifier is shown in Figure 2-3 which will be recognized as a modification of the schematic of Figure 2-1. With respect to the phase references, the external phase reference is the phase of the microwave drive source. The internal phase reference that is required for the internal phase control loop is obtained by coupling off some of the drive power through a directional coupler. The amplitude reference is an adjustable DC voltage which is calibrated in terms of microwave power output by noting the DC power output of the amplitude sensor at various power output levels as measured by the waterload.

The microwave drive source may be either a 10 watt TWT amplifier which is driven by a frequency-swept oscillator, or power which is coupled from a low-noise magnetron oscillator. In the latter case there is some limited frequency adjustment and the power output may be varied from zero to 50 watts, the upper limit being

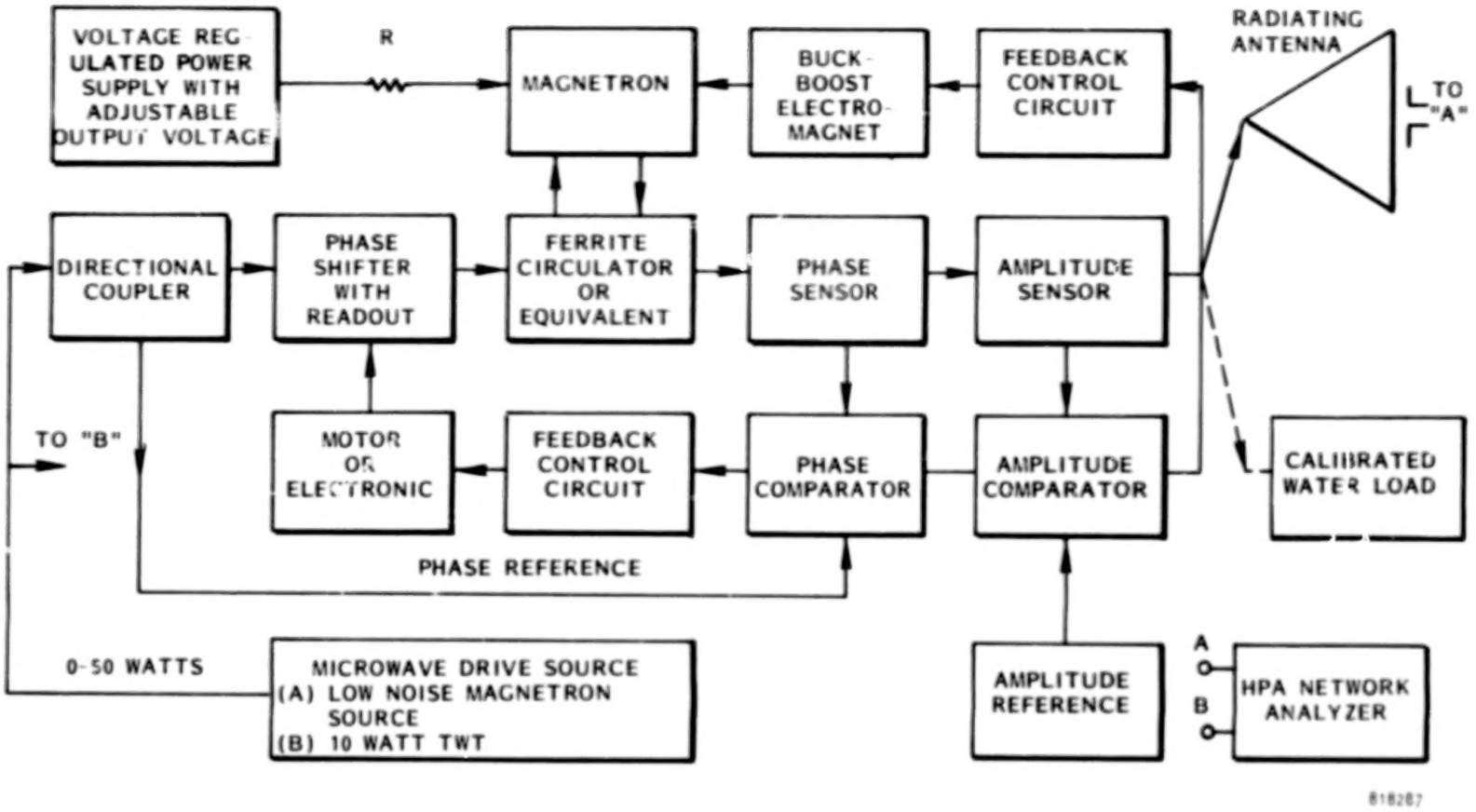

Figure 2-3. Test Arrangement for Evaluating the Magnetron Directional Amplifier with Phase and Amplitude Tracking Feature.

imposed by the power handling capability of the microwave cables or other power transmission arrangement. The major reason for using the magnetron driver is its very low noise level as compared to the output of the TWT.

The power supply source is a voltage regulated power supply which simulates the hard voltage bus in the SPS whose potential is unaffected by the power drawn from it by a single tube. A resistance R is inserted between the power supply and the magnetron directional amplifier. Most of the data was taken with a value of 100 ohms for R, although some was taken with 800 ohms, a value of resistance that more closely simulates that of the total solar photovotaic array when the complete bank of magnetrons is simulated by one magnetron.

The power dissipated in the 100 ohm resistor represents about 1% of the DC power input at an anode current of 313 milliamperes, which is a representative operating value for the microwave oven magnetron. The same resistance when used with the intended magnetron design for the SPS would represent only about 0.3% loss. The use of a 100 ohm resistor will allow for the resistance of a fuse which will be used to disconnect the SPS magnetron from the high voltage bus in case of an internal short in the tube. In this sense, the magnetron with a series fuse can be regarded as analagous to the incandescent lamp which is self fused.

Of course, if the fuse blows for any reason the magnetron cannot function again until the fuse is replaced. However, there should be no reason for a short in the tube unless there should be "whisker" growth, a phenomena which is common in all classes of tubes but whose importance in this application cannot be assessed without experimental data on actual operating tubes. If there should be this problem, then the 100 ohms will also allow for the DC resistance that would be inherent in an inductor which could also be inserted in series with the fuse and which would allow the whisker to be vaporized with a transient flow of current of a modest value which would not cause the fuse to blow. The mass of the whisker which is very small would be very much smaller, probably by a factor of a thousand, than the mass of the fuse so that even the simplest kind of fuse would have a "slow-blow" response to the extinction of a whisker.

The first data, presented in Figure 2-4, shows the variation of output phase as sensed by the dipole probe (see Figures 2-2 and 2-3) with respect to the reference phase while the power output is held nearly constant over a very wide range of applied voltage from the voltage regulated power supply. As the data indicates, the output phase variation is held constant to within $\pm 1^{o}$ while the phase shift through the magnetron directional amplifier itself is 110^{o} as read from the readout on the phase shifter which compensates for the phase shift in the magnetron directional amplifier. The microwave drive level for this set of data was 10 watts while the nominal power output was 700 watts, giving an rf gain of 18.5 dB.

The format of the data in Figures 2-5 to 2-7 is different. Here the coordinates, familiar to those who use magnetrons, are voltage on the vertical scale and current on the horizontal scale. The data is taken by setting the output reference and then noting the anode current, power output, and phase shift across the magnetron directional amplifier as the voltage output of the voltage stabilized power supply is varied. During the taking of this data the output phase tracking error as read from the calibrated voltage output of the phase comparator circuit was within $\pm 1^{o}$.

The test conditions for Figures 2-5 to 2-7 differ in the level of microwave drive that was applied. With higher drive a considerably larger range of operation in terms of anode current is obtained. Figure 2-5 is for 10 watts of drive, 2-6 is for 50 watts of drive, while 2-7 is for only 2.5 watts of drive. This behavior is consistent with the data taken on the magnetron directional amplifier without amplitude control as shown in Appendix B.

In Figures 2-5 to 2-7 the current-voltage relationships that result from a specific setting of the amplitude control reference are almost contours of constant power output as well. The power output levels at the "edge of locking" points (EL on the graphs) are within $\pm 3\%$ of the power called for by the amplitude control.

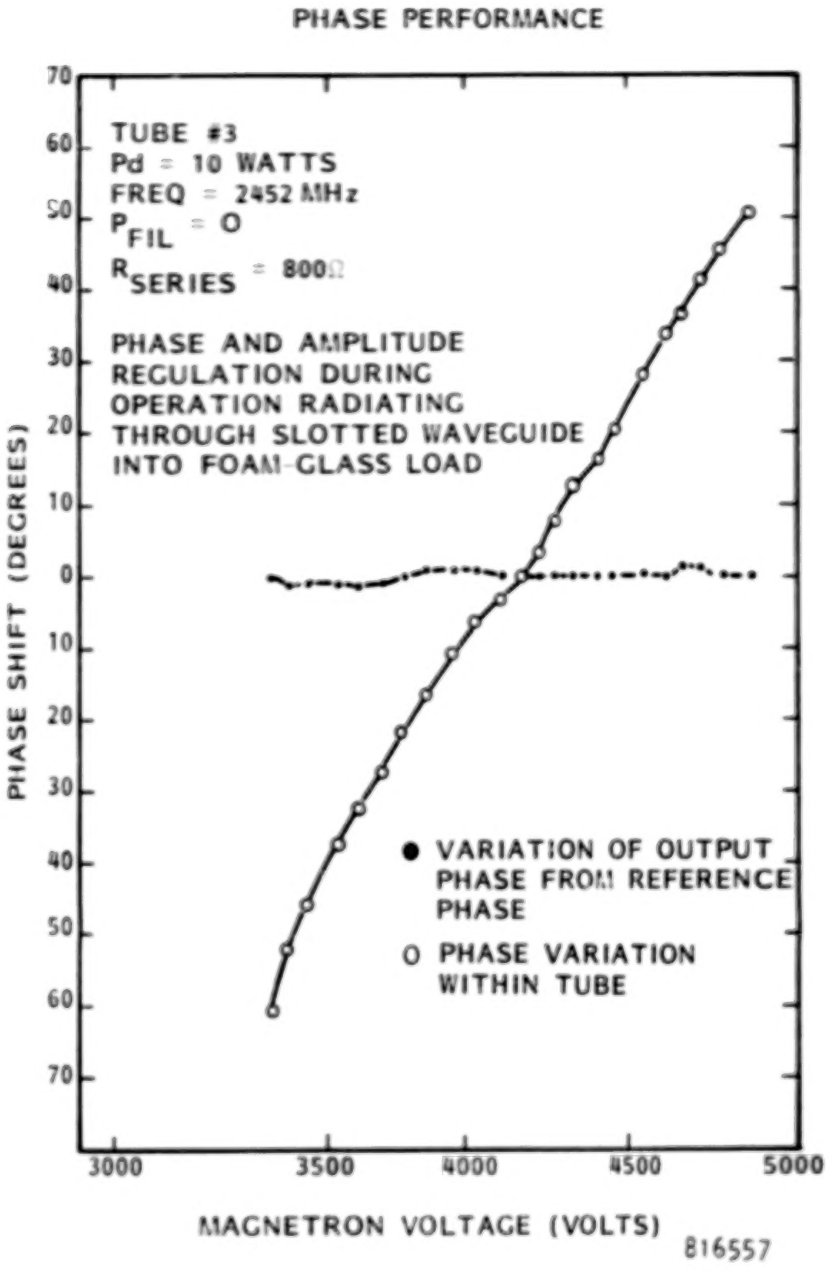

Figure 2-4. Phase Tracking of Output Phase to Reference Phase and Phase Shift through Magnetron Directional Amplifier as Function of Anode Voltage Level. Amplitude of Microwave Output is Held Constant.

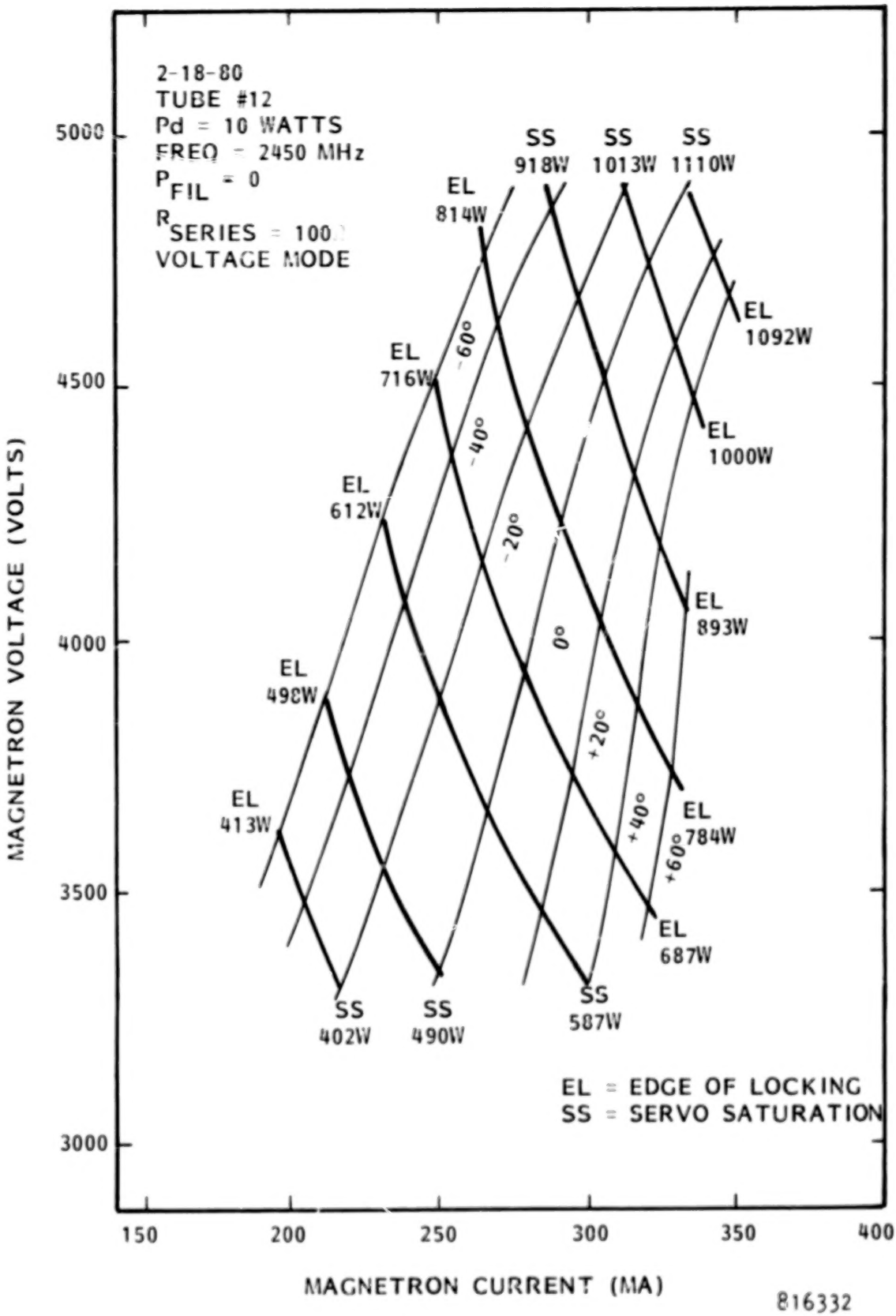

Figure 2-5. Phase and Amplitude Tracking Data with Series Resistance Reduced to 100 ohms to Simulate Operation Across a Hard Voltage Bus-10 Watts of Drive.

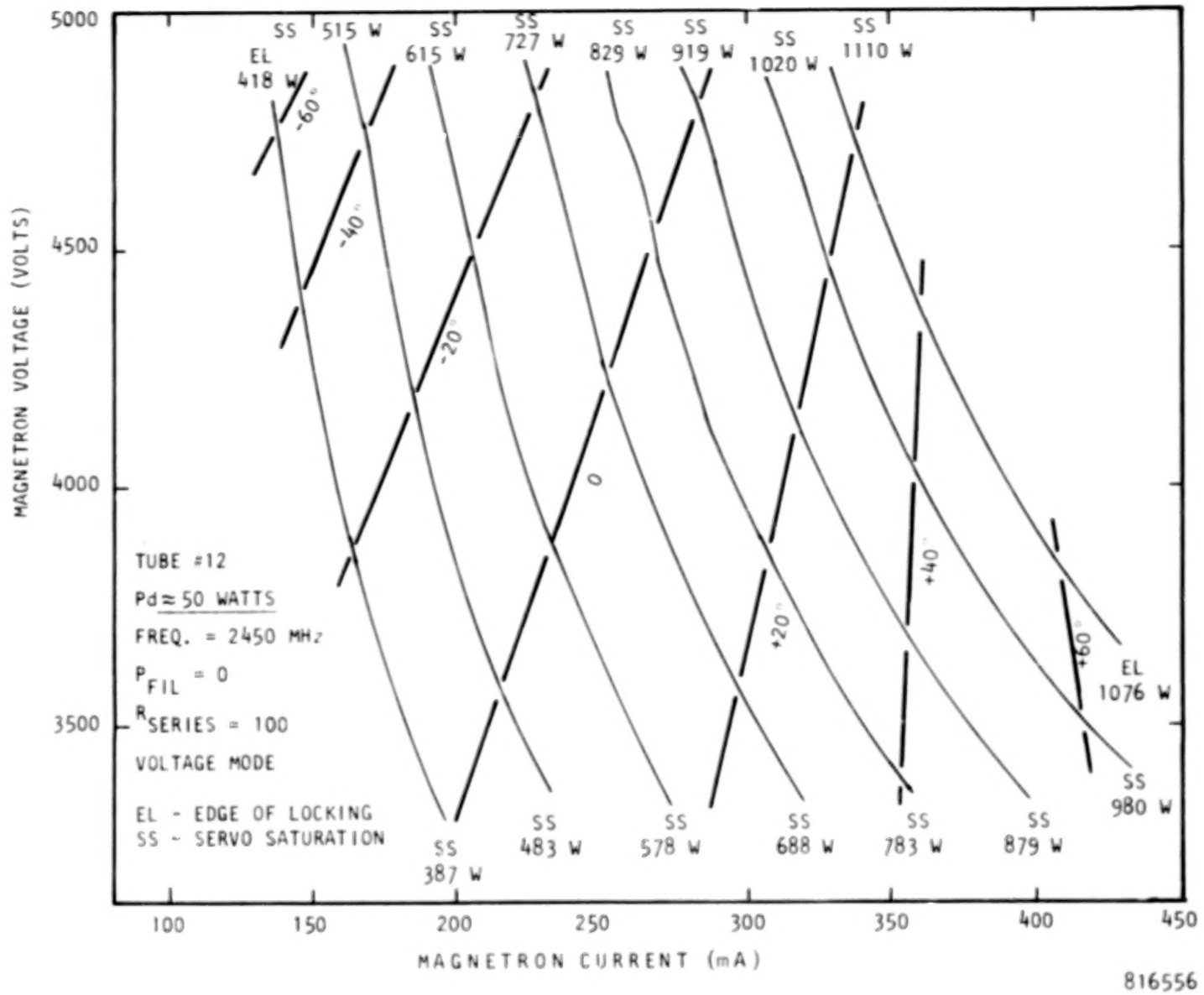

Figure 2-6. Phase and Amplitude Tracking Data with 50 Watts of Drive.

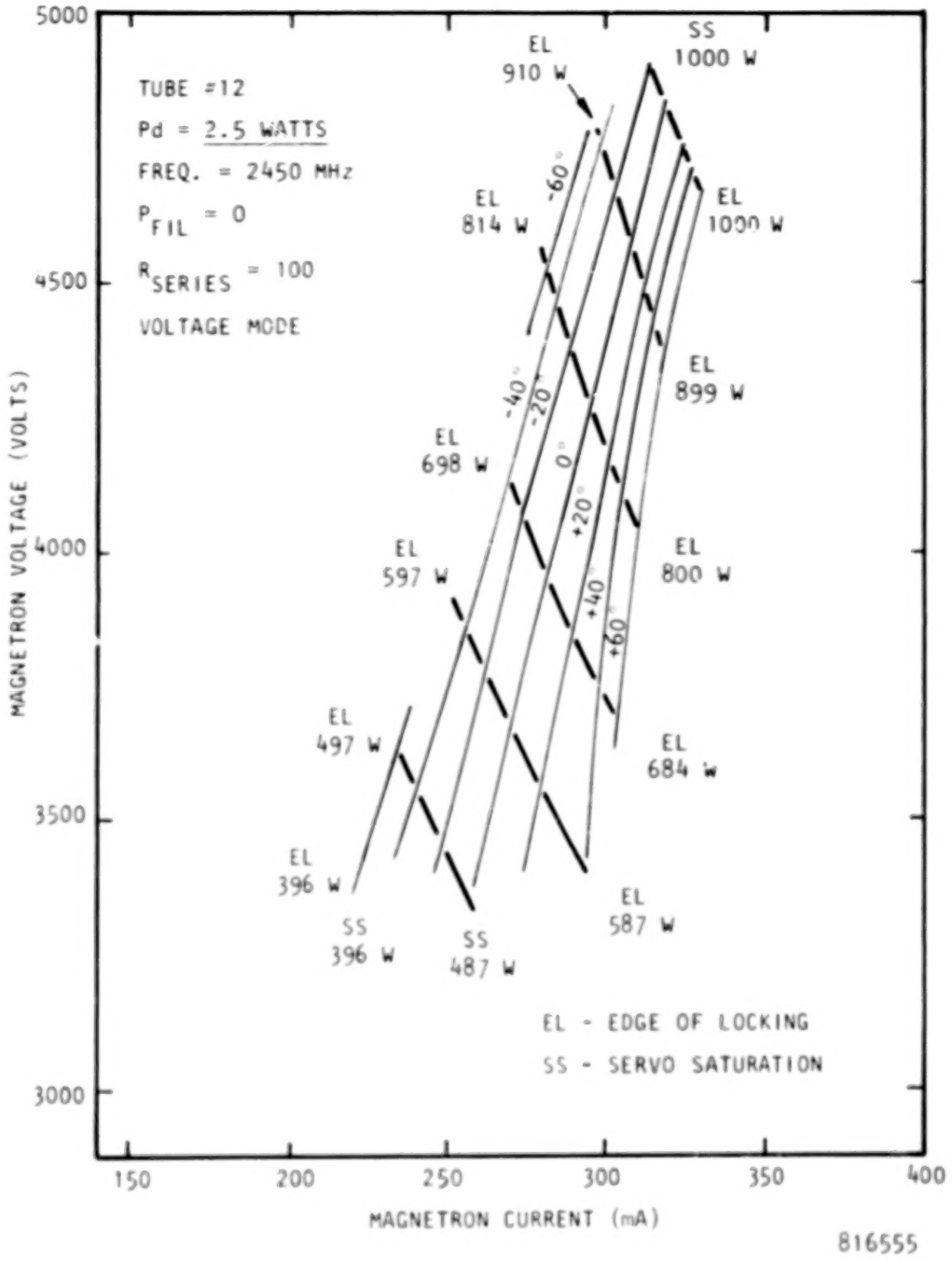

Figure 2-7. Phase and Amplitude Tracking Data with 2.5 Watts of Drive.

The voltage current relationships in Figures 2-5 and 2-7 are quite different from those shown in the figures in Appendix B, where the voltage-current relationship that results from setting the magnetic field at a specific value is essentially a horizontal line.

It would have been possible to plot contours of constant efficiency on the graphs as well but they would make the graphs more difficult to read. The efficiency at any point can be estimated with good accuracy by extrapolating the power output data to that point and then dividing that value by the product of the DC input current and DC input voltage.

Additional data with respect to signal to noise level was obtained with the set-up shown in Figure 2-3 using the low noise magnetron oscillator drive source. As anticipated, the data was the same as when the magnetron directional amplifier was operated without the phase and amplitude tracking loops.

2.3 Description of the Demonstration Test Bed, the Integration of the Magnetron with the Buck-Boost Coil, and Other Supporting Data

This section will contain some of the more detailed information on the construction of the demonstration test bed, a description of the integration of the magnetron with the buck boost coil, the relationship between the operating voltage of the magnetron and the current and power in the buck-boost coil, a description of the microwave sensors and comparators, and circuit diagrams for the feedback amplifiers.

2.3.1 Physical Description of the Demonstration Test Bed

One view of the test bed for Phase and Amplitude Tracking Demonstration and data taking was shown in Figure 2-2. Figure 2-8 is a view from the back of the unit. Figure 2-8 will be used in conjunction with the circuit schematics of Figures 2-1 and 2-3 to describe the physical arrangement of the test bed.

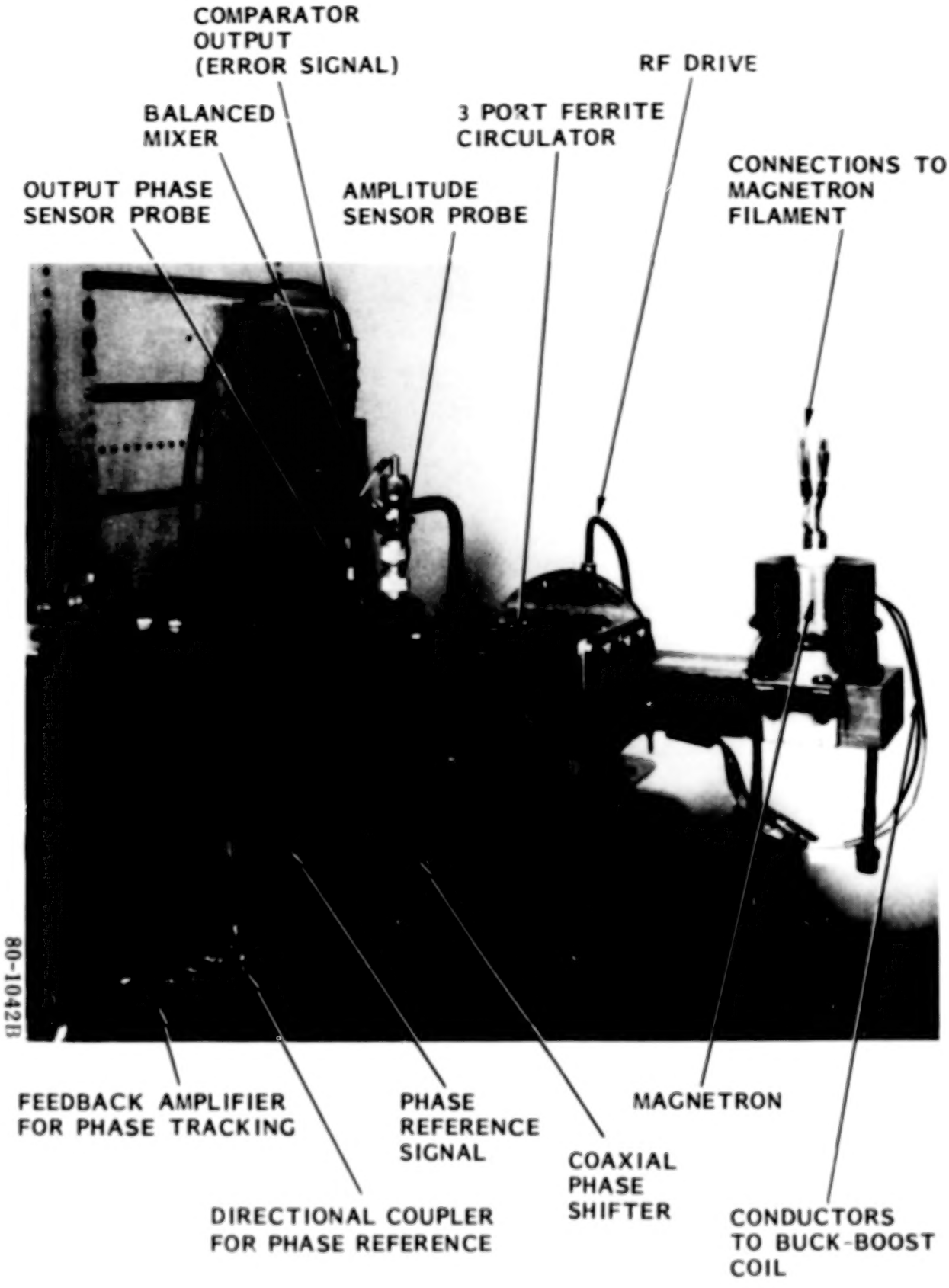

Figure 2-8. Overall View of Phase and Amplitude Control Circuits on Test Bed.

As shown in Figure 2-8 the waveguide attached to the magnetron is connected to a three port ferrite circulator that is a low cost unit used in commercial microwave ovens. Shown on the further side of the circulator is the cable terminal for the rf drive input. The other terminal of the cable is attached to the output of the coaxial mechanical phase shifter shown in the middle foreground. The external rf drive is fed to the other terminal of the phase shifter through a directional coupler from which a small sample of the rf drive is removed and used as the phase reference. The phase reference is then fed into one input port of the balanced crystal mixer. The other input port is attached to the loop-type directional coupler probe shown next to the 1 inch x 6 inch vertical slab that supports the structure. The output of the crystal mixer is fed into the amplifier shown in the extreme left foreground. The output of the amplifier is fed into the small DC motor shown mounted on the mechanical coaxial phase shifter that completes the phase tracking portion of the test bed.

The amplitude of the output is sampled by the second loop-type directional coupler probe shown next to the ferrite circulator. The crystal rectified output of the rf sample is sent by cable to the other feedback amplifier (out of the picture on the extreme lower left) where it is compared with a voltage reference. The amplified output is fed by cable to the two input leads to the buck boost coil to complete the amplitude tracking portion of the test bed.

2.3.2 Description of the Magnetron with Buck Boost Coil; Buck Boost Coil Characteristics

Figure 2-9 is a close up view of the magnetron with buck boost coil and magnetic return shell of the solenoidal type. Figure 2-10 is an exploded view of the assembly. As shown in Figure 2-10 it consists of (1) an ordinary microwave oven magnetron from which the cooling fins and ceramic permanent magnets have been removed, (2) the solenoid coil which is the source of the buck-boost magnetic field, (3) the top and bottom portions of the return part of the magnetic circuit made from cold-rolled steel, and (4) two samarium cobalt magnets placed inside of the two ends of the steel shell. These magnets supply the permanent portion of the magnetic field in the cathode-anode interaction area of the magnetron.

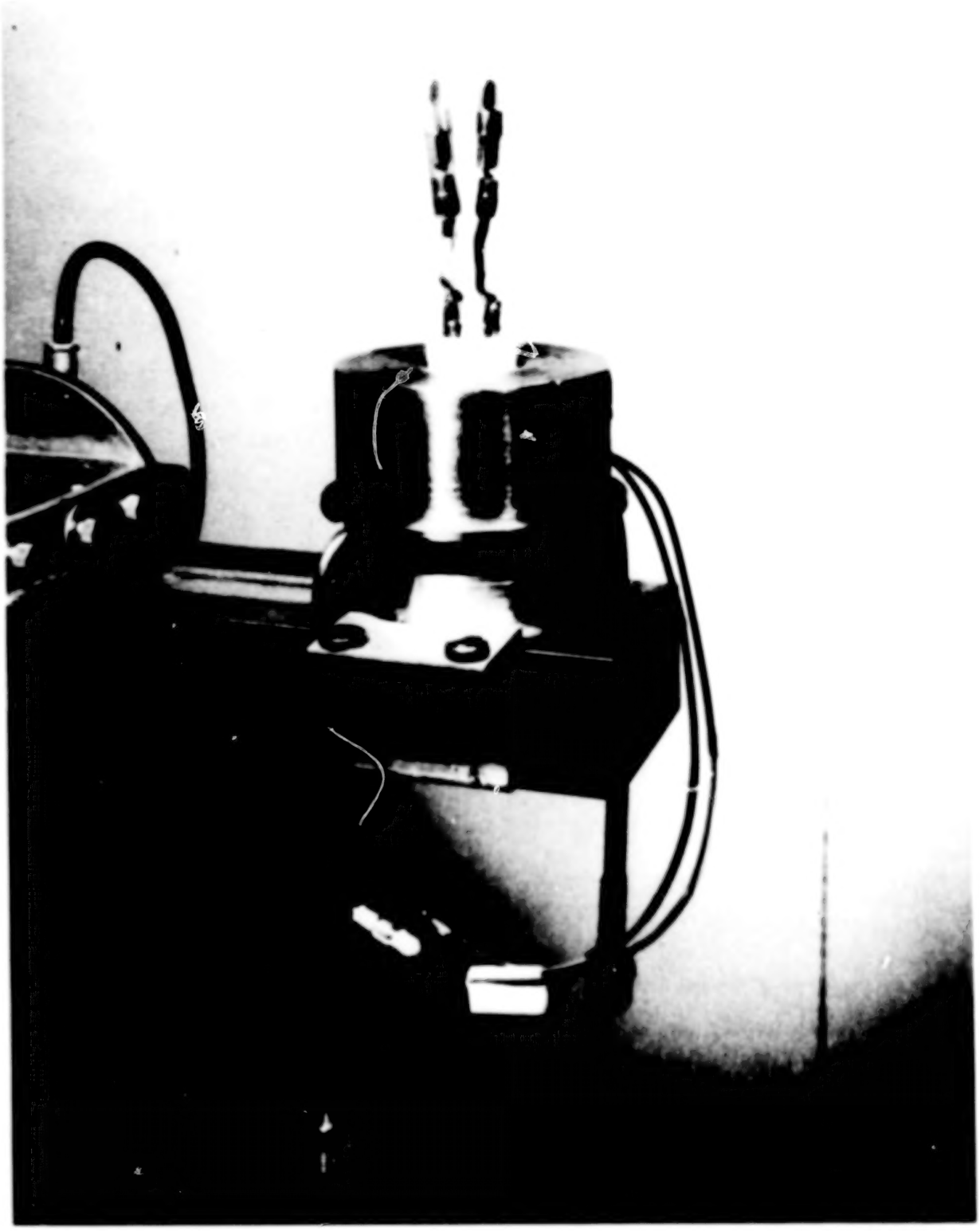

80-1037B

Figure 2-9. Closeup View of Magnetron with Buck-Boost Coil Fitted to Waveguide in Phase and Amplitude Tracking Test Bed.

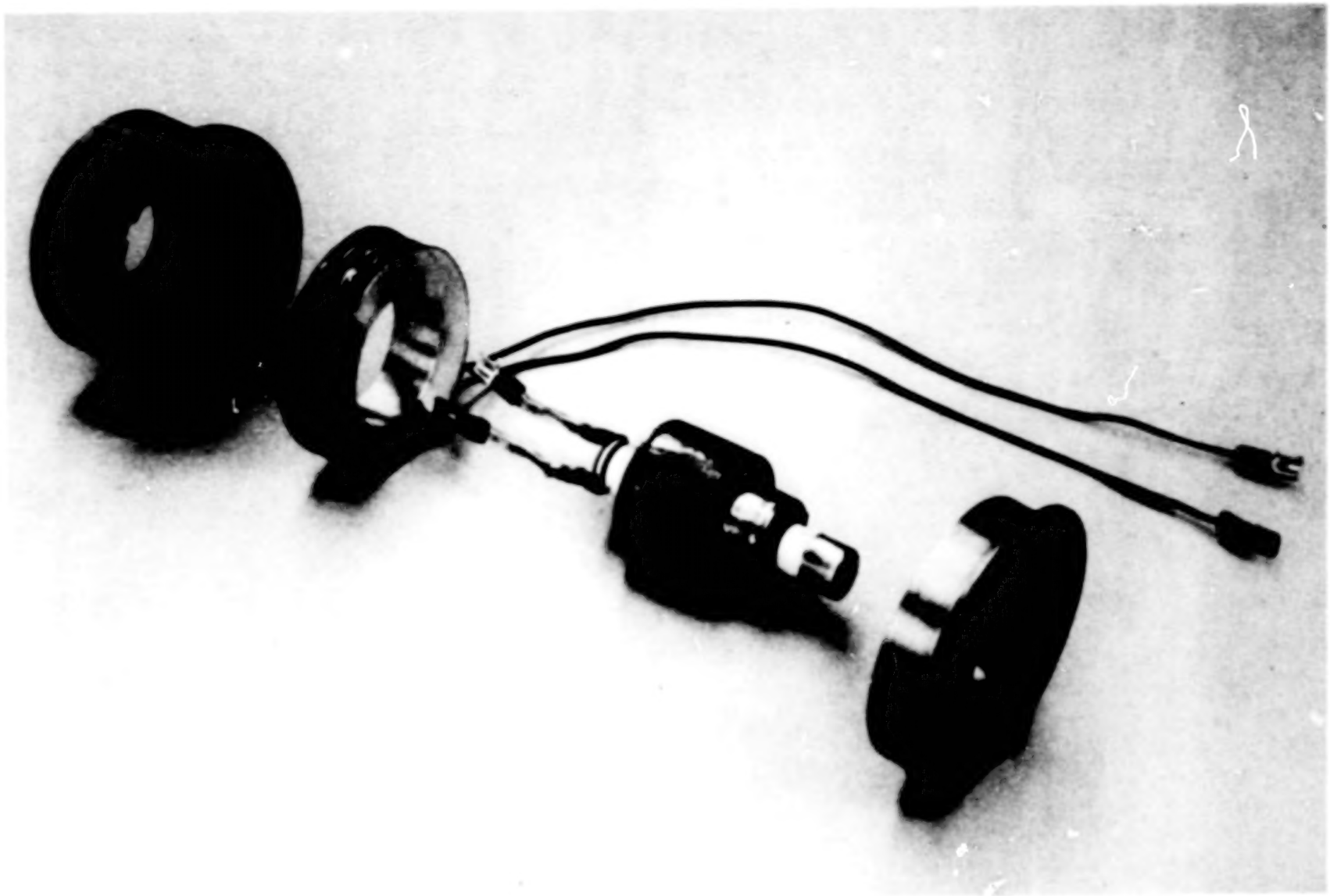

Figure 2-10. Modification of microwave oven magnetron showing (1) magnetron stripped of cooling fins and ceramic magnets (2) buck-boost coil (3) cold-rolled steel shell, and (4) samarium cobalt magnets (inside ends of each portion of shell).

It should be noted that the assembly shown in Figure 2-10 is the second arrangement that was used. It was much superior in performance to the first arrangement shown in Figure 2-11, and much closer to the design that is anticipated for use in the SPS tube itself. In fact, the second arrangement was carried to the point where the pyrographite radiator was simulated by the use of a water cooled copper band that was clamped around the tube. However, this arrangement did not prove to be practical and for final use in the demonstration test bed a special solenoid coil was made up whose appearance resembled that shown in Figure 2-11 but which had an inside diameter about 1/16 inch larger than the outside diameter of the tube to allow for a sheet of cooling water to flow around the anode. The solenoid was applied to the anode with the use of "O" rings at either end to contain the water flow. (See Figure 6-6 for use of solenoid in noise measurements.)

The operating voltage of the magnetron as a function of the current through the "buck boost" coil is shown in Figure 2-12. Also shown in Figure 2-12 is the power in the buck-boost coil as a function of the current in the coil. It is seen that less than 3 watts of power are required to change the operating voltage by $\pm$10%. Ten watts of power into the buck boost coil will change the operating voltage by $\pm$22%.

It is difficult to estimate from this data the amount of power that will effect the same percentage change in the operating voltage of the magnetron designed for the SPS. The reasons for this are explained in Section 7.0. More analytical and experimental data will be needed.

2.3.3 Description of the Sensors, Comparators, and Other Components in the Phase and Amplitude Feedback Control

2.3.3.1 Components in the Phase Control Loop

The phase comparator was an ANAREN 70116 balanced mixer. Its characteristics as determined experimentally are shown in Figure 2-13. Figure 2-13a

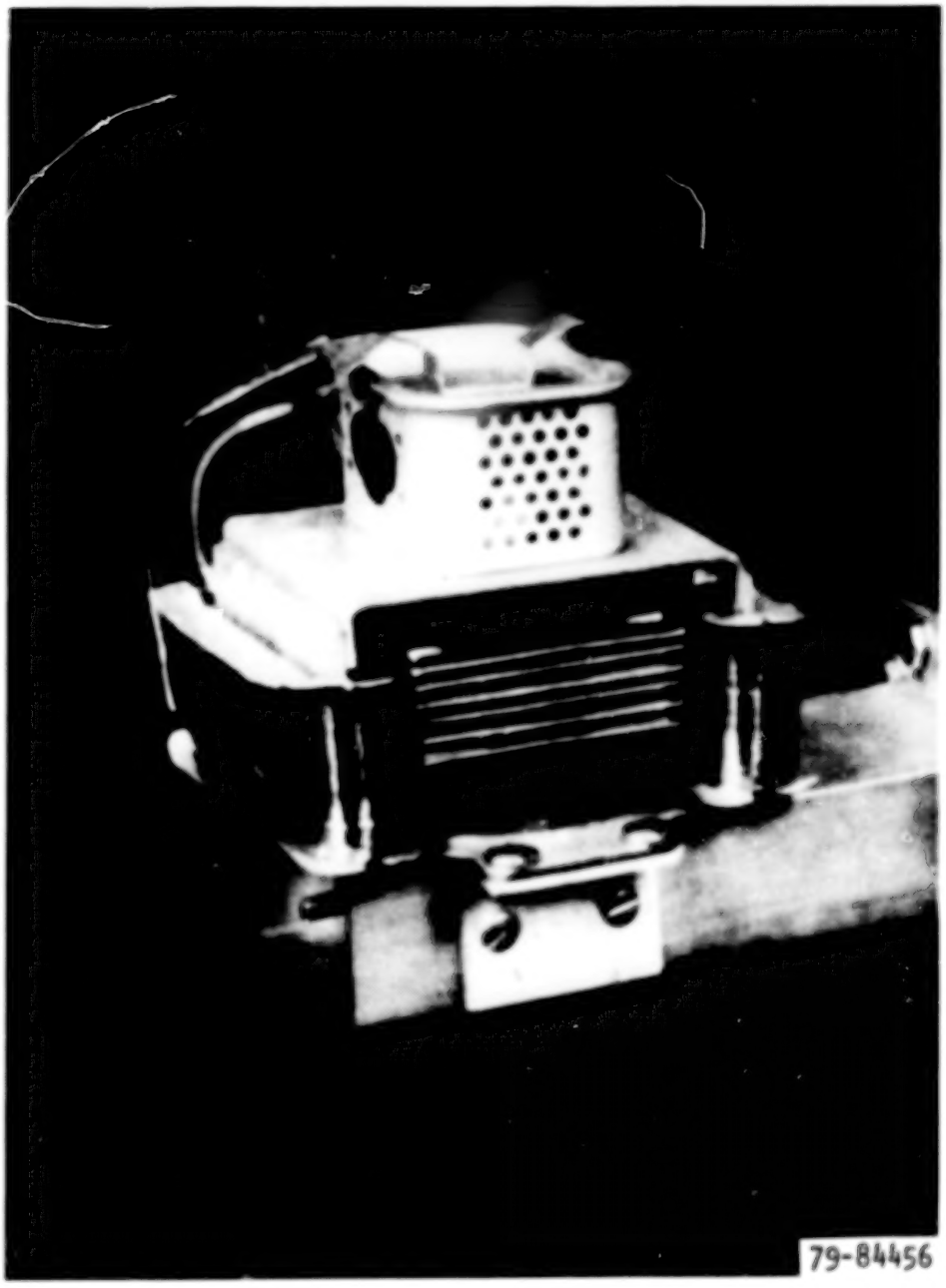

Figure 2-11. Conventional microwave oven magnetron whose magnetic circuit has been modified by the addition of coils which can be used to buck or boost the residual magnetic field established by permanent magnets of the original packaged tube.

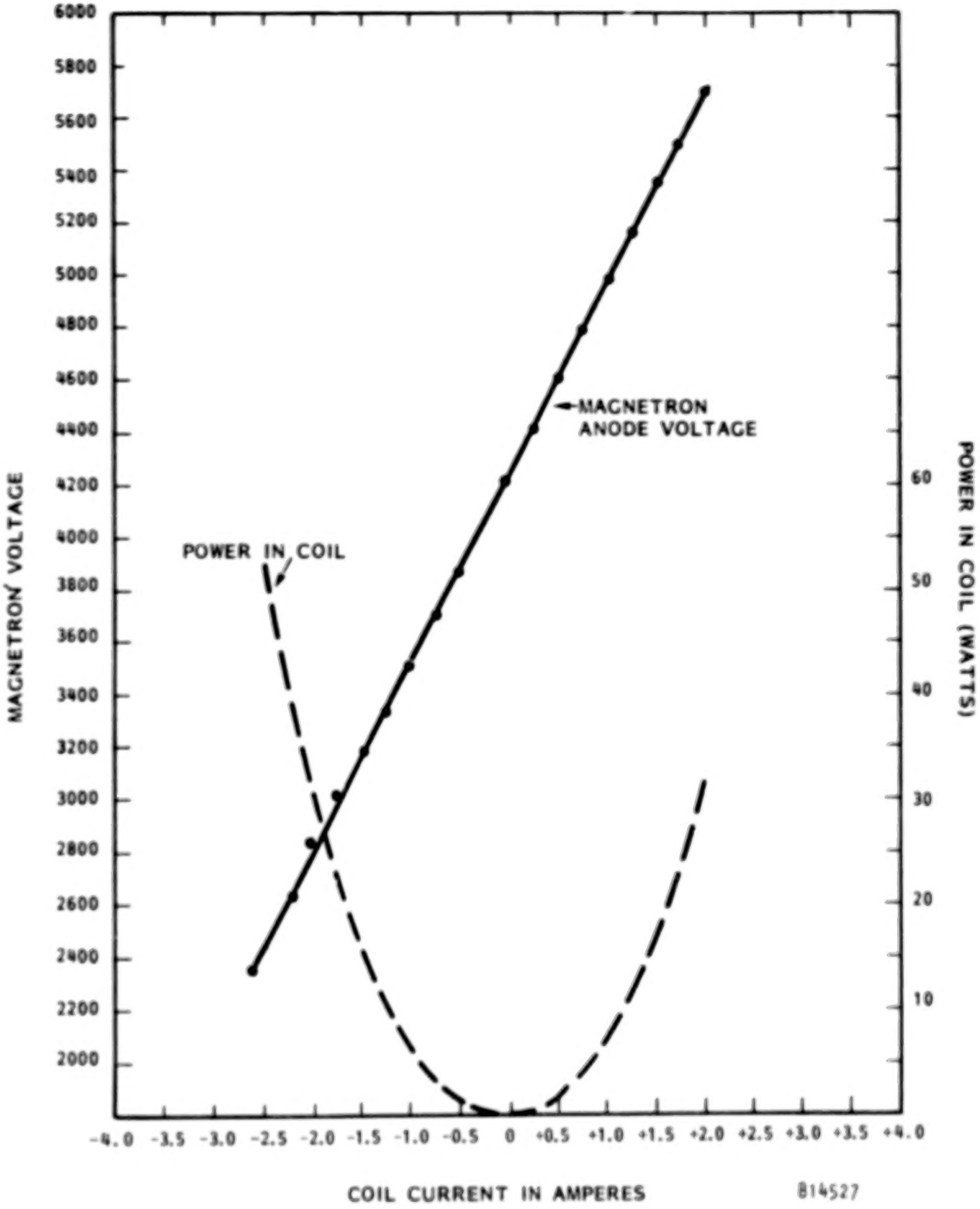

Figure 2-12. Magnetron anode voltage and power dissipated in buck-boost coil as function of current in buck-boost coil. The relationship of anode voltage to coil current is very linear as shown.

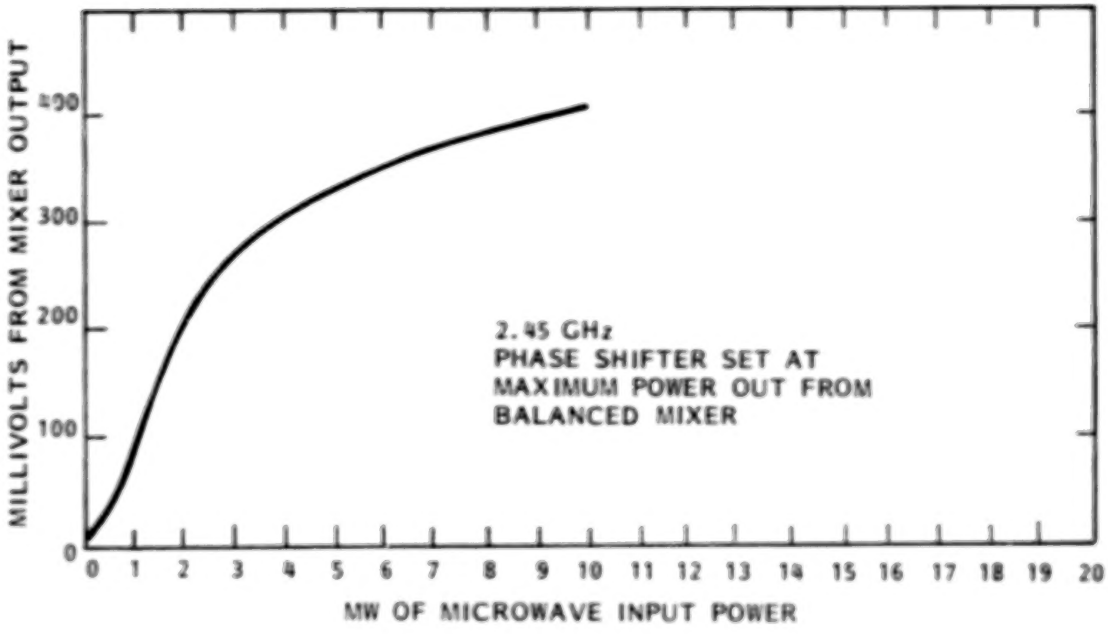

Figure 2-13a.

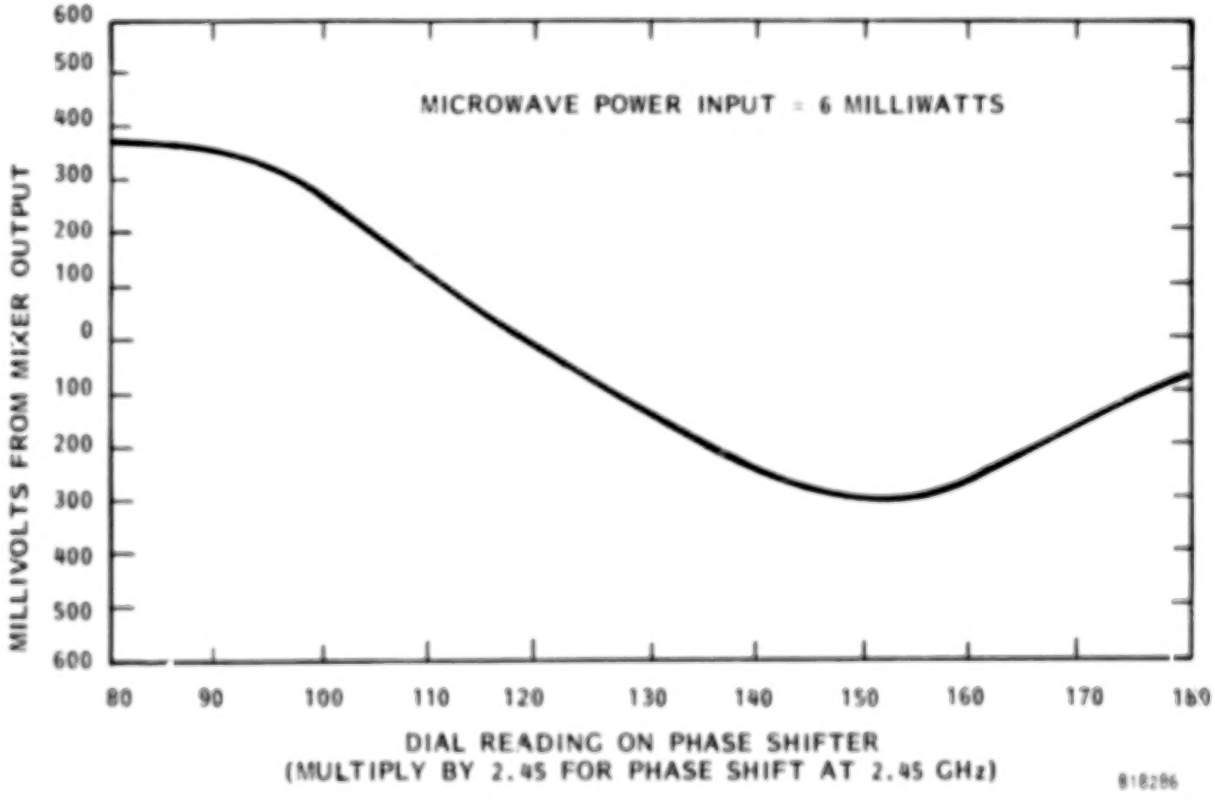

Figure 2-13b.

Figure 2-13a & b. Characteristics of ANAREN 70116 Crystal Mixer at 2.45 GHz.

shows the power output from the balanced mixer as a function of signal level with the two inputs out of phase with each other, the condition for maximum power output. It was concluded that an input power level of 6 milliwatts would be a satisfactory operating level. At this input power level the DC voltage output from the balanced mixer as a function of the setting of a phase shifter which was inserted into one of the two inputs is given in Figure 2-13b.

The balanced mixer in this application is operated around the null point. The null point is insensitive to a difference in amplitude of the two inputs as long as their amplitudes are within a factor of two.

The phase shifter and control element in the phase control loop was a NARDA model 3752. This is a coaxial phase shifter selected because of its high power handling capability and its direct readout of phase. It was driven by a small DC servo motor through a set of gears. Maximum DC power into the motor is one watt.

Of course, such a phase shifter is not suitable for use in the SPS, but the objective of this study was to demonstrate that the phase of the output of the magnetron directional amplifier could track a reference phase. In the SPS a much faster acting phase shifter and one that has no sliding contacts of any kind will be necessary. Such phase shifters are discussed in Section 2.7.

2.3.3.2 Components in the Amplitude Control Loop

In the case of the amplitude control loop the comparator is merely the summation of two DC input voltages in an operational amplifier input. One of these DC input voltages is the reference voltage and the other DC input voltage is the rectified power output from the crystal in the microwave power output sensor. A nominal value for these voltages is one volt and the input impedance level is 2000 ohms so that the power represented by them is negligible.

The control element in the amplitude control loop is the buck-boost coil that has been previously described in Section 2.3.2. It has an inductance of 16 millihenries when inserted into the magnetic circuit and its DC resistance is 5.6 ohms.

2.4 Analysis of the Microwave Power Amplitude Control System

There are two different aspects of the microwave power amplitude control system that are represented by two different inputs to the control system. The first input is the control or reference input. The power output is expected to increase or decrease to closely follow a change in the control input. The second input is a change in the voltage that is applied to the magnetron. Such a change is a disturbance to the system and it is desired that the power output remain relatively unperturbed by such a disturbance.

From a control circuit point of view, the system appears with the quantities in Laplace Transform Notation:

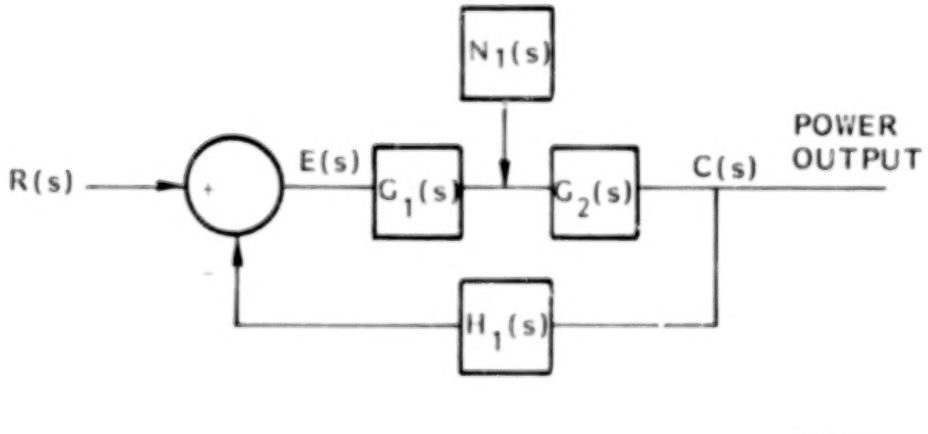

816330

The two items of major interest are the response of the output C (s) to the control signal R (s) and to the disturbing signal N_1 (s). These ratios are expressed as

$$\frac{C\ (s)}{R\ (s)} = \frac{G_1\ (s)\ G_2\ (s)}{1 + H_1\ (s)\ G_1\ (s)\ G_2\ (s)} \tag{1}$$

$$\frac{C\ (s)}{N_1\ (s)} = \frac{G_2\ (s)}{1 + H_1\ (s)\ G_1\ (s)\ G_2\ (s)} \tag{2}$$

G_1 (s) is the transfer function identified with the gain in the operational amplifier, the current flow through the buck-boost coil, and the subsequent change in the operating voltage of the magnetron.

G_2 (s) is identified with the electrical resistance between the DC power bus and the tube, the resulting current flow in the magnetron, and the resulting change in power output.

H_1 (s) is identified with the transducer that converts the microwave power output to a voltage that can be compared with the reference input R (s) which is also a voltage. It may be a crystal, thermistor, or other device.

G_1 (s) is given as the ratio of the change in operating voltage of the magnetron to the error signal E (s) which is in the form of a voltage.

$$G_1\ (s) = \frac{k_1\ k_2}{R_1 + sL}, \text{ where} \tag{3}$$

k_1 = voltage gain of amplifier

k_2 = Ratio of change in operating voltage of magnetron to current through the buck-boost coil

R_1 = resistance of buck-boost coil

L = inductance of buck-boost coil

G_2 (s) is given as the ratio of the microwave power output to the voltage difference between the DC power source and the operating voltage of the magnetron

$$G_2(s) = \frac{k_3}{R_2}, \quad \text{where} \tag{4}$$

R_2 = resistance interposed between the DC power supply and the magnetron and

k_3 = the ratio of microwave power output to current flow in the magnetron

If we substitute these values into Equation 1, we obtain:

$$\frac{C(s)}{R(s)} = \frac{\frac{k_1 k_2 k_3}{R_2 (R_1 + sL)}}{1 + \frac{H_1(s) k_1 k_2 k_3}{R_2 (R_1 + sL)}}$$

from which

$$\frac{C(s)}{R(s)} = \frac{k_1 k_2 k_3}{R_2 (R_1 + sL) + H_1(s) k_1 k_2 k_3} \tag{5}$$

However, we wish this in the form

$$\frac{C(s)}{R(s)} = \frac{K_1}{1 + T_a s} \tag{6}$$

and in this form

$$K_1 = \frac{k_1 k_2 k_3}{R_1 R_2 + H_1(s) k_1 k_2 k_3} \tag{7}$$

and

$$T_a = \frac{R_2 L}{R_1 R_2 + H_1(s) k_1 k_2 k_3} \tag{8}$$

If we substitute the values for the constants that are fixed by the buck-boost coil, the magnetron characteristics, and the power sensor we obtain:

k_2 = 700 (volts per ampere)

k_3 = 2000 (watts per ampere)

R_1 = 5.6 ohms

L = 0.016 henries

$H_i(s) = \frac{1}{600}$ (volts per watt of output)

and find that K_1 from (7)

$$K_1 = \frac{1.4 \times 10^6 k_1}{5.6 R_2 + 2333 k_1} \tag{9}$$

and T_a from (8)

$$T_a = \frac{0.016 R_2}{5.6 R_2 + 2333 k_1} \tag{10}$$

If we divide the numerator and denominator of equation (6) by T_a, we have

$$\frac{C(s)}{R(s)} = \frac{K_1}{T_a} \left[\frac{1}{S + \frac{1}{T_a}} \right] \tag{11}$$

If R (s) is a unit step function

$$C(s) = \frac{K_1}{T_a} \frac{1}{s} \left[\frac{1}{S + \frac{1}{T_a}} \right] \tag{12}$$

and the transform of this into the time domain gives:

$$e(t) = K_1 \left(1 - e^{-\frac{t}{T_a}}\right) \tag{13}$$

and from (9) and (10)

$$e(t) = \frac{1.4 \times 10^6 \, k_1}{5.6 \, R_2 + 2333 \, k_1} \left[1 - e^{-\left(\frac{5.6 \, R_2 + 2333 \, k_1}{0.016 \, R_2}\right)t}\right] \tag{14}$$

(14) is the time response to the step application of one volt of reference (or control) potential.

If values for $K_1 = 150$, and $R_2 = 800$ are inserted into equation 14

$$e(t) = 592 \left[1 - e^{-(350 + 27339)t}\right] \text{ watts} \tag{15}$$

Several things may be observed from equations (14) and (15). The transient response for an inductive coil with resistance to a step function is $e^{-Rt/L}$ or in this case e^{-350t}. This is the first term in the exponential. Thus, equations (14) and (15) show that the system has a far faster time response than the coil itself. Since k_1 is typically 150 and R_2 is in the range of 150 to 1500 we see that the response time is from 50 to 500 times as fast.

Further, we see that this time response will remain the same if the ratio $\frac{k_1}{R_2}$ is kept constant.

The steady state response is given by the multiplying factor in (14). If $R_2 = 0$, then $e(t) = 600$, - that is, one volt of reference voltage will produce 600 watts of power. If $R_2 = 800$, and $k_1 = 180$, $C_t = 592$. So there is a slight error resulting from the finite value of R_2. The error is less if $R_2 = 100$ ohms, by a factor of eight.

Now, let us examine the response of the system to a change in the DC voltage applied as given by (2), putting in the value of the constants for k_2, k_3, and H_1 (s) as we do so.

$$\frac{C\ (s)}{N\ (s)} = \frac{2000\ (R_1 + sL)}{SLR_2 + R_1\ R_2 + k_1\ 2333} \tag{16}$$

Making use of the final value theorem,

$$\lim_{s \to 0} sF\ (s) = \lim_{t \to \infty} f\ (t)$$

$$e\ (t)_{ss} = \frac{2000\ R_1}{R_1\ R_2 + k_1\ 2333} \tag{17}$$

Equation (16) is for a 1 volt change in anode potential. For R_2 = 800 ohms and k_1 = 150, $e\ (t)_{ss}$ = 0.0316 watts. A 1000 volt change in plate voltage would result in a 31.6 watt change in output. That is about what is experimentally observed.

The transient response to a change in anode voltage will be different than the response to a change in control voltage because of the addition of the zero in the numerator. If we insert values for the constants in (16) of R_1 = 5.6, L = 0.016, R_2 = 800 and k_1 = 150, we obtain

$$\frac{C\ (s)}{N\ (s)} = \frac{2.5\ (S + 350)}{(s + 27694)} \tag{18}$$

and for a unit step function

$$C\ (s) = \frac{2.5\ (s + 350)}{s\ (s + 27694)} \tag{19}$$

When this expression is transformed back to the time domain

$$C(t) = 0.0315 + 2.468e^{-27694t} \qquad (20)$$

Expression (20) indicates a very large but highly damped response to a change in voltage. A change of voltage of only one volt produces an initial change of 2.5 watts. A reduction of the series resistance R_2 from 800 ohms to 100 ohms would increase the impact of a one-volt change to 20 watts.

From an operational point of view in the SPS there should be no reason for sharp transients in applied DC voltage to the operating magnetron. As indicated in Section 2.2, the DC voltage is first applied to the bus before the magnetron is started. Main circuit breakers could open while the tubes are operating but this would automatically cause the tubes to be incapable of drawing any current within two or three seconds at most because the filament automatically cools off. Closing the main circuit breakers again after seconds would require going through the start-up process again. Thus, the circuit breakers would cause no problem unless they chattered.

Aside from the main circuit breaker function, it is difficult to imagine any scenario other than a comparatively slow ramp type change in applied voltage. And as equation (20) indicates, the response time of the control system is extremely fast and would have no difficulty in coping with such ramp applications of voltage.

It may be interesting to observe what happens when a sinusoidal perturbation of voltage is applied. Normally, the resulting variation in power output would be $\frac{V\ k_3\ \sin\ wt}{(R_2)}$. If $k_3 = 2000$, and $R_2 = 800$ ohms, each volt would produce a peak-to-peak change of 5 watts in output power.

In equation (18), if N (s) = V sin wt, then C (s) in equation (19) becomes

$$C(s) = \frac{w}{(s^2 + w^2)} \quad \frac{2.5\ (s + 350)}{(s + 27694)} \qquad (21)$$

where the first term $w/(s^2 + w^2)$ is the Laplacian of sin wt.

If w = 377, the time response transform of (21) is

$$f(t) = 0.045 \sin (377t + 135^{O}) + 0.033e^{-27694t}$$

Thus, the 5 watt peak-to-peak power ripple has been reduced by the ratio of 5 to 0.09 or 55.

If w = 3770 or ten times greater, then

$$f(t) = 0.325 \sin (3770t - 1.76^{O}) + 0.033e^{-27694t}$$

so that the reduction in power ripple is only 7.9.

It appears that the transient response of the present arrangement is fast enough for the SPS application and that the steady state error is also sufficiently low. It therefore does not appear necessary at this time to consider compensation of either the lead or lag type. But both could be added with negligible increase in mass.

2.5 Analysis of the Microwave Power Phase Control System

No analysis of the phase control system was made because it was not considered immediately applicable to the SPS as was the case for the amplitude control system. It was known a priori that the feedback control loop requirements were undemanding and that the arrangement that was used would operate stably. This will continue to be the case even for a fast acting phase shifter without friction contacts that would be needed for the SPS. However, in the event that such a phase shifter is developed then a thorough analysis of its characteristics would be considered necessary.

2.6 Documentation of the Electronic Circuits in the Amplifiers for Phase and Amplitude Control Circuitry

The state-of-the-art in solid state operational amplifiers and high power linear amplifiers has changed very rapidly in recent times and so it is possible to house all of the needed amplifier circuitry into a small volume. In the case of the amplifier for the phase control loop all of the active amplifiers and nearly all of the other circuit components were contained within the K08A envelope which is the same size as the T03 package. The device that was used was the LH0021.

The-state-of-the-art was advancing so rapdily that by the time the contract was completed it would have been possible to put the amplifier for the amplitude control system, which is more demanding from a power point of view, into the same size package.

For documentation purposes, the circuitry that was used for the amplifier in the phase control circuit is shown in Figure 2-14. The circuitry that was used for the amplitude control system is shown in Figure 2-15.

In conclusion, it should be noted that gallium arsenide microwave circuits are advancing rapidly and it should soon be possible to put the balanced mixer on a small chip. Eventually it may be possible to combine the microwave comparator

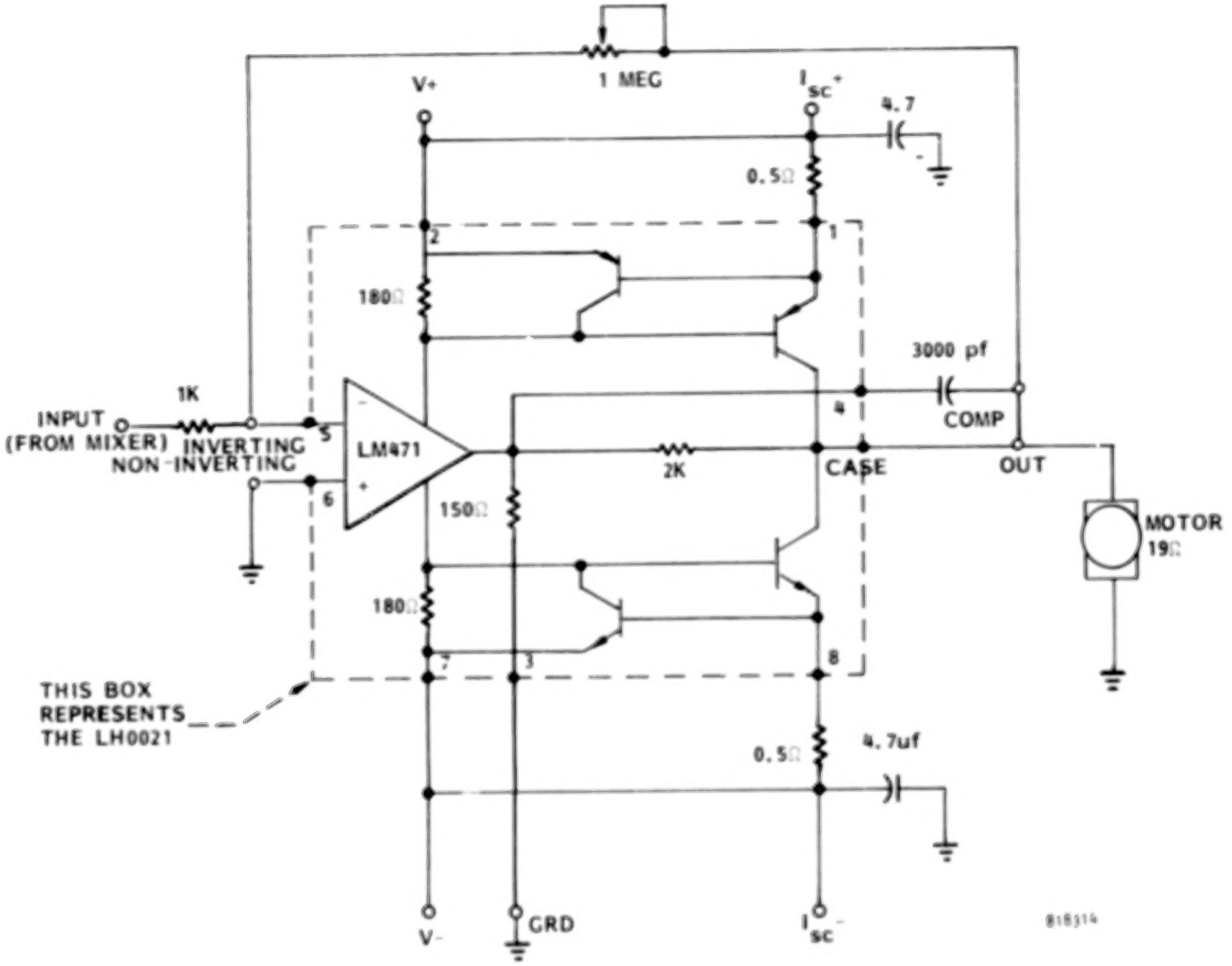

Figure 2-14. Schematic Diagram of Amplifier in Phase Tracking Feedback Loop.

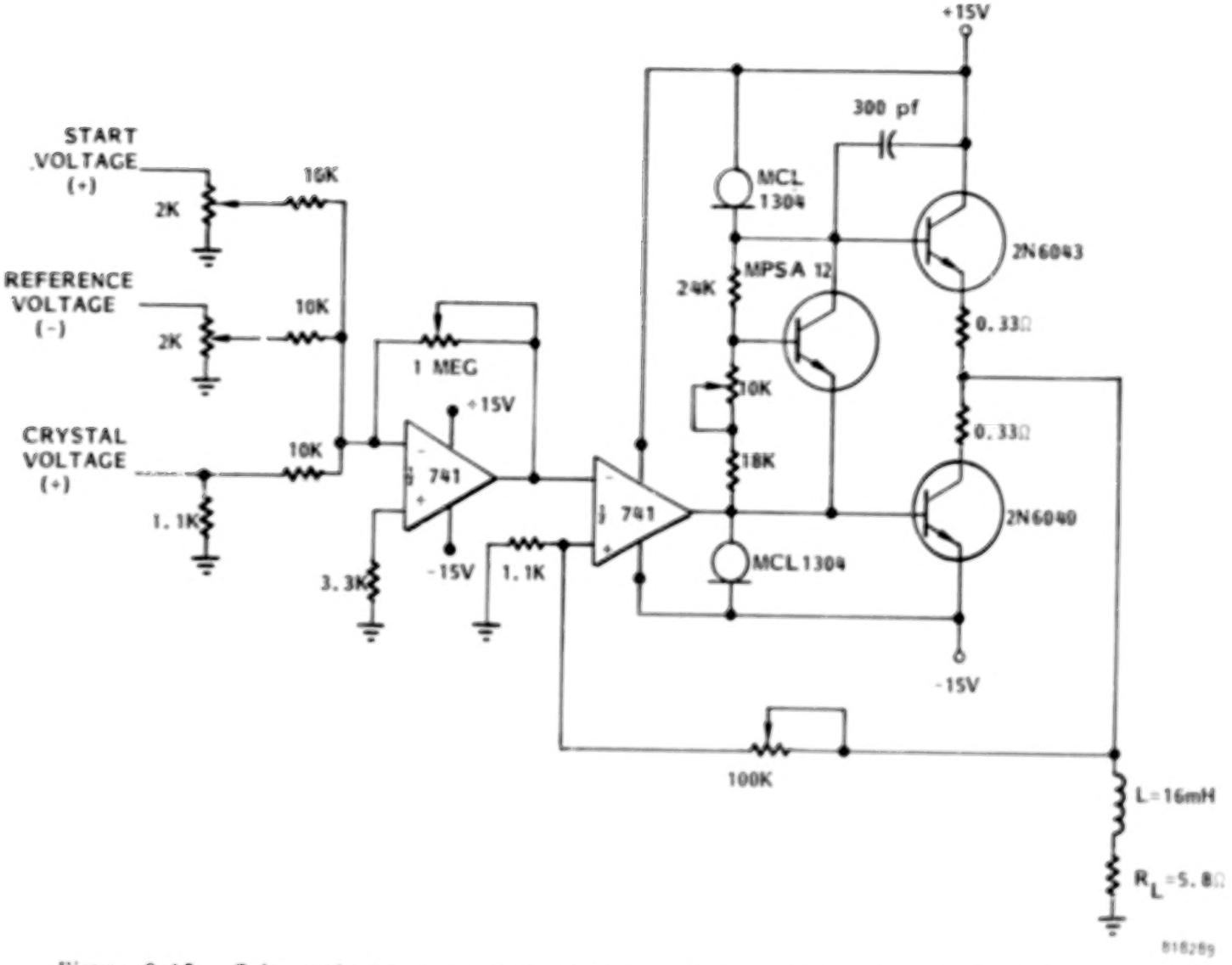

Figure 2-15. Schematic Diagram of Amplifier in Amplitude Tracking Feedback Loop.

and the DC power amplifier on the same chip. Certainly gallium arsenide will be the choice material for both the amplifier and the sensor because of its capability to operate at the required temperatures in the SPS.

2.7 Suggested Approach for a Phase Shift Device in the SPS Architecture

One of the conclusions that can be rapidly reached from an examination of the data in Figures 2-5 to 2-7 is the dependency of the range of current over which the magnetron directional amplifier can be operated upon the level of rf drive. This dependency, of course, is not a discovery and the range of operation can be theoretically predicted rather accurately from a knowledge of the "pushing" and "pulling" characteristics of the tube. The magnetron characteristic that dominates in controlling the current operating range is the pushing characteristic of the tube which is expressed as the ratio of the change in the free-running (undriven) frequency of the tube to the change in anode current. This pushing is inversely proportional to the loaded Q, so if the loaded Q is reduced to increase the frequency range over which locking will occur, the two results cancel each other out and the current operating range remains approximately the same.

Fortunately, there appears to be an arrangement in which the operating range can be greatly expanded while still retaining the same gain level. At the same time it will be possible to eliminate the sliding friction of a mechanical device and to shorten the time response of the phase control system to about one millisecond. In this context, the reader is reminded that the coaxial phase shifter used in the current investigation of phase control was chosen as the best approach to a demonstration of a phase tracking system because of its low cost, shelf availability, and power handling capability.

The proposed arrangement would compensate the frequency change in the tube for any reason with a tuner that would automatically make a compensating adjustment as part of the phase control system. The same basic feedback arrangement

that is presently used to drive a motor that positions a phase shifter can be used to drive a "voice coil" arrangement that will tune either an external cavity attached to the tube or a tuner within the tube itself. Such a feedback system can be made very stiff and responsive so that it would not be affected by any mechanical vibrations that might take place in the transmitting antenna. A schematic for the control arrangement is compared with that of the present arrangement in Figure 2-16.

The motion of the mechanical tuner would avoid any mechanical friction by the use of spring compliance support. Fatigue should not be a problem because it would rarely move more than a very small fraction of its total allowed movement. It should also be possible to design it to operate at 300°C and thereby eliminate the problem of attempting to use solid-state phase shifters which would have to be mounted elsewhere than close to the tube.

The power and mass requirements for such a tuner is not expected to be large. It is expected that the mass can be held down with the use of samarium cobalt to no more than 30 grams, while the maximum power consumption is expected to be in the range of one to two watts. If only a small amount of tuning is required the power consumption would be a small fraction of a watt. However, the design must be for the maximum power consumption expected.

It was not possible to do any work on the actual design and construction of such a tuner under this contract, but such activity is included in the technology-development program to be defined and recommended under this study in Section 10.0.

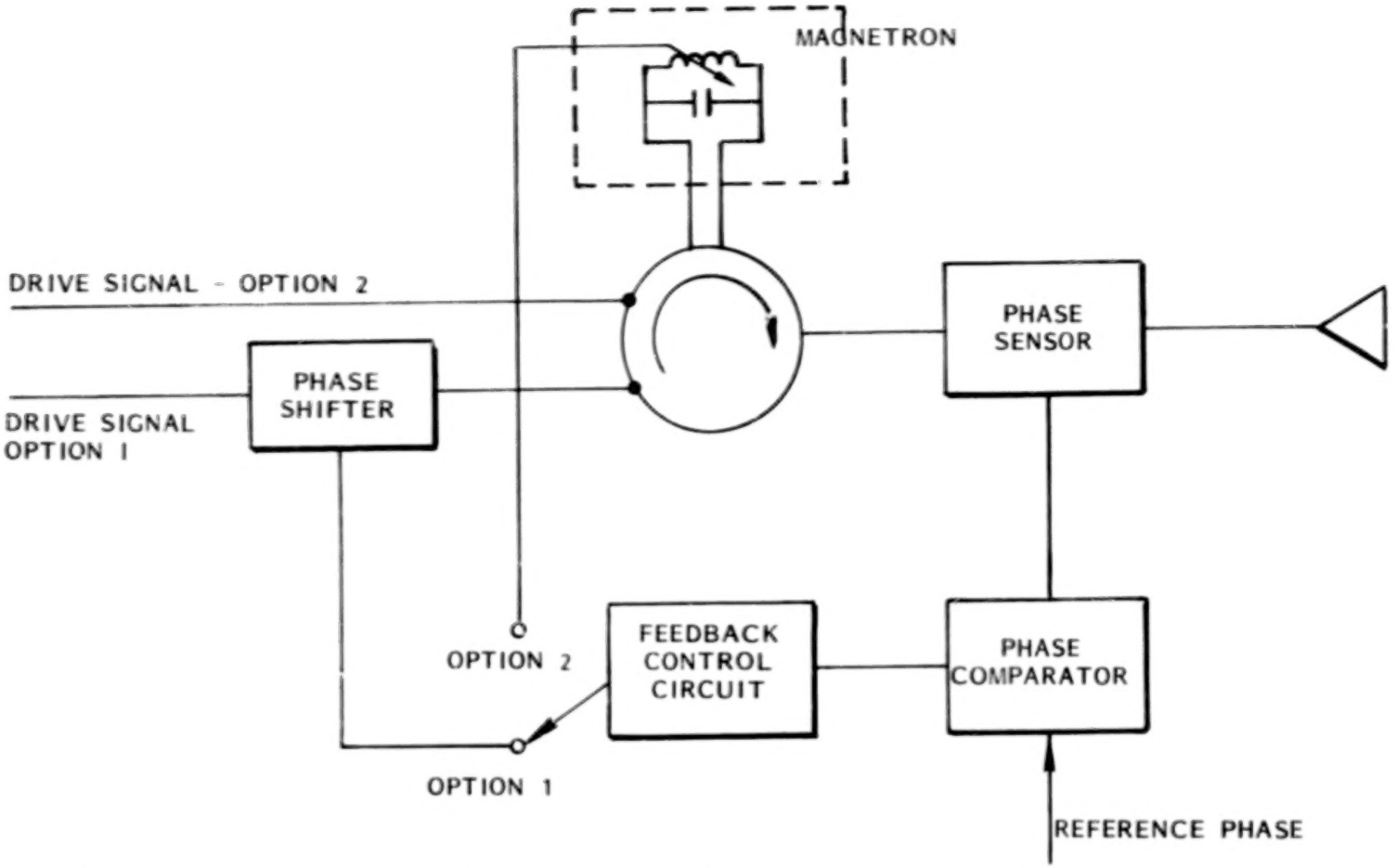

OPTION 1 IS CONVENTIONAL APPROACH ALREADY EXPERIMENTALLY DEMONSTRATED

OPTION 2 IS IMPROVED CONCEPT UTILIZING "VOICE COIL" INDUCTIVE TUNING OF MAGNETRON

818315

Figure 2-16. A Comparison of Present Phase Control Arrangement with Proposed Magnetron Tuning Which Provides Fast, Frictionless, Response and Broad Operating Range.

3.0 MAGNETRON STARTING

For application in the SPS satellite transmitter the magnetron has a desirable characteristic in that during normal operation the filament of the tube is heated indirectly by backbombardment and so it does not require an external source of heater power during normal operation. However, it does require external power for about five seconds to heat up the filament during start-up operations. Because bringing the power level of the SPS up to full power output may require several minutes for other reasons, it is reasonable to think of using a single filament power supply to sequentially start a relatively large number of tubes. This will be discussed further in Section 5.2. In this section we will review experimental data that was obtained in starting a single magnetron.

The starting sequence that was used and that is exactly analogous to that proposed for the SPS transmitter was as follows:

(1) The DC voltage is applied to the magnetron which has a cold cathode and cannot be started in that condition.

(2) The magnetic field on the tube is elevated by an artificial reference voltage to a value that will not allow the tube to draw anode current and start when the filament is turned on and heated.

(3) The filament power supply is then turned on to heat up the filament. About five seconds is required.

(4) The filament and artificial reference voltage are then turned off and simultaneously the reference voltage that controls the steady state amplitude of the microwave power output is applied.

(5) The resulting transient period is of the order of a few milliseconds.

In carrying out the mechanics of the starting sequence, the summing aspect of the input to the operational amplifier is utilized. Referring to Figure 2-15, a "start" voltage is applied to one of the inputs to the operational amplifier. This is of the same sign as the crystal voltage and is much greater than the reference voltage. The system therefore, thinks it is operating at a very high power level and so it adjusts the magnetic field higher to reduce the power output. Of course it is driven into saturation at the magnetic field corresponding to saturation.

The removal of the "start" voltage after the filament is warmed up then confronts the control system with the fact that there is really no crystal voltage and no microwave power output so the control system now drives itself as rapidly as possible in the direction of reduced magnetic field.

In the experimental evaluation of the starting sequence it was determined that a minimum of four seconds is needed to heat the filament and that a relatively high heat input is needed to provide enough cathode primary emission to allow the tube to immediately jump to the power level dictated by the reference voltage.

The transient start-up is timewise characterized as follows: (1) first, a period when the magnetic field is being reduced as rapidly as possible but current flow change is limited by the applied voltage which in turn is limited by amplifier saturation; this is typically 3 milliseconds, (2) then current starts to flow and the time constant of the control system should become effective, (3) however, the source impedance in the voltage-regulated power supply that is being used experimentally is not zero for a transient start. The storage capacity of the capacitance in the output of the power supply is only 0.8 joules or 0.8 watt-seconds. The rapid discharge of energy forces the control circuit to change the magnetic field to an even lower value until the electronic regulation system of the regulated power supply becomes effective.

It follows, therefore, that what is seen experimentally is a combination of the time constants of the power supply and of the amplitude control system.

Figure 3-1 shows a number of transient starts with both the phase and amplitude control circuits active. Time zero on the horizontal time scale corresponds to turn-on of the active servo and turn-off of external heater supply. The delay time before current is drawn is about 2 milliseconds for an operating voltage of 3900 volts, and slightly over 3 milliseconds for an operating voltage of 3650 volts, reflecting the time required for the servo amplifier saturated at nine volts of output voltage to change the magnetic field enough to start magnetron current flow (bottom photograph is for the lower operating voltage).

The faster rise time in the center photograph may be attributed to the higher heater power and higher temperature cathode. The "ringing" in the center photograph is probably a characteristic of the voltage regulated power supply.

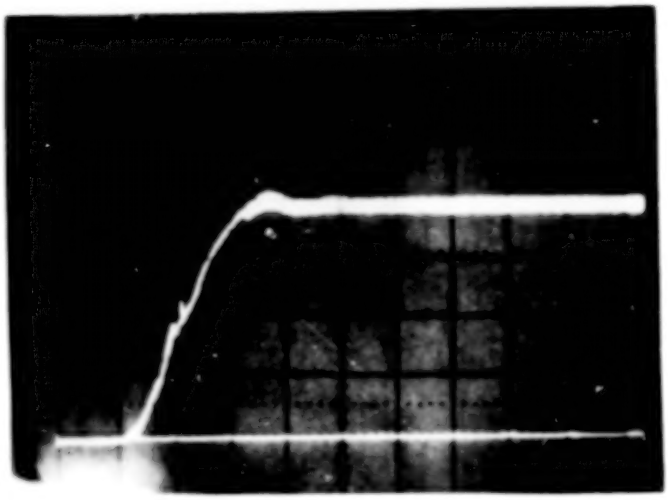

OPERATING DATA

Tube #12 in directionzl amplifier circuit driven with 10 watts at 2453 MHz.

Filament E_f = 3.7 V, I_f = 13.5 A for 5 sec.

Operate conditions: E_b = 3900 volts, I_b = 300 mA, I_f = 0

Buck-boost coil saturated at 1.37 A initially.

Time scale of photo- 2 mV,/div.

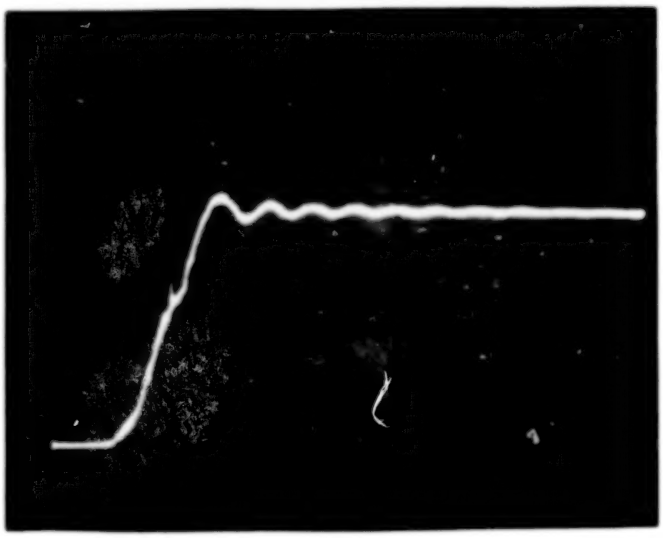

Tube #12 in directional amplifier circuit driven with 10 watts at 2453 MHz.

Filament E_f = 4.5 V, I_f = 15.5 A for 5 sec.

Operate conditions: E_b = 3900 volts I_b = 300 mA, I_f = 0

Buck-boost coil saturated at 1.37 A initially.

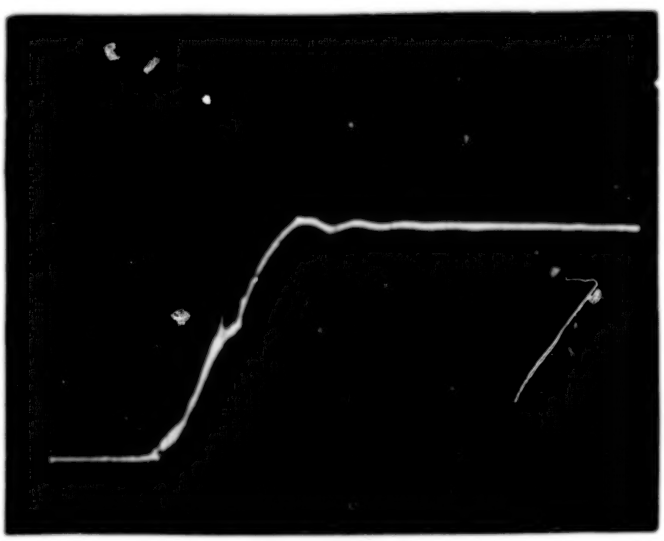

Tube #12 in directional amplifier circuit driven with 10 watts at 2453 MHz.

Filament E_f = 4.5 V, I_f = 15.5 A for 5 sec.

Operate conditions: E_b = 3650 volts, I_b = 330 mA, I_f = 0

Buck-boost coil saturated at 1.37 A initially.

Figure 3-1. Transient Starting Behavior of Magnetron Directional Amplifier.

4.0 CONCEPT OF THE POWER MODULE AND ITS INTERFACE WITH THE REST OF THE SATELLITE

4.1 Definition of the Power Module and Its Interface with the Subarray

To determine how the magnetron directional amplifier fits into the rest of the system it is necessary to provide realistic models of the higher levels of integration. In this section we will discuss the concept and design of the power module and its various interfaces with the rest of the microwave power transmission system and the satellite.

Figure 4-1 shows two power modules side by side. The relationship of the power module to the subarray is shown in Figure 4-2. The power modules as shown in both figures consist of four radiating units, each of which consists of two magnetrons, a "Magic T" or equivalent structure and a section of slotted waveguide array. The present concept is to have the width of the power module only two radiating units wide and the length made up of enough radiating units to equal half the width of the array. In subsequent discussion it will be evident that the power module is "hard wired" and should be considered as a plug-in entity to be taken out for repair and replacement if necessary.

Some perception of the physical appearance of the subarray shown in schematic form in Figure 4-2 may be obtained if certain assumptions are made as to the size of the subarray and the size of the radiating unit. The size of the radiating unit (two magnetrons and corresponding section of slotted waveguide) is determined by the physical dimensions of the slotted waveguide array. As discussed in Section 7.2 the size and mass of the pyrolytic graphite radiator is quantized in large steps by the number of waveguide slots that are associated with each radiator. It turns out that this size for the present radiating unit is 77.48 cm (30.5") by 36.83 cm (14.5"). Subsequent designs, if made, will not depart substantially from these dimensions.

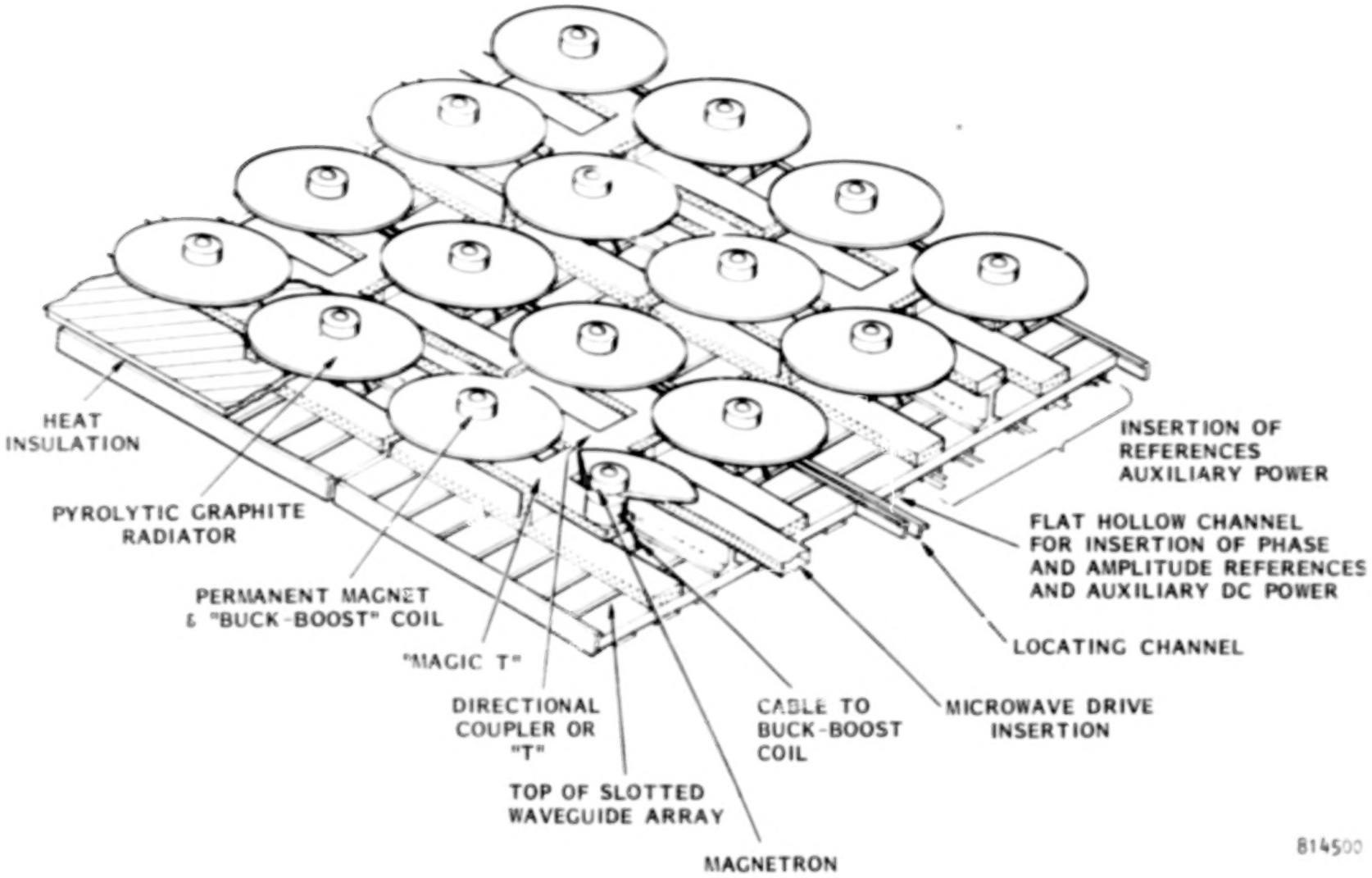

Figure 4-1. Assembly Architecture for the Magnetron Directional Amplifier in the Antenna Subarray. Two Power Modules are Shown. Microwave Drive and all References and Auxiliary Power are Inserted from the "Backbone" of the Subarray. The Array has Two Distinct Temperature Zones. The Top is Used to Radiate the Heat. The Bottom is Used for Mounting of Solid State Components.

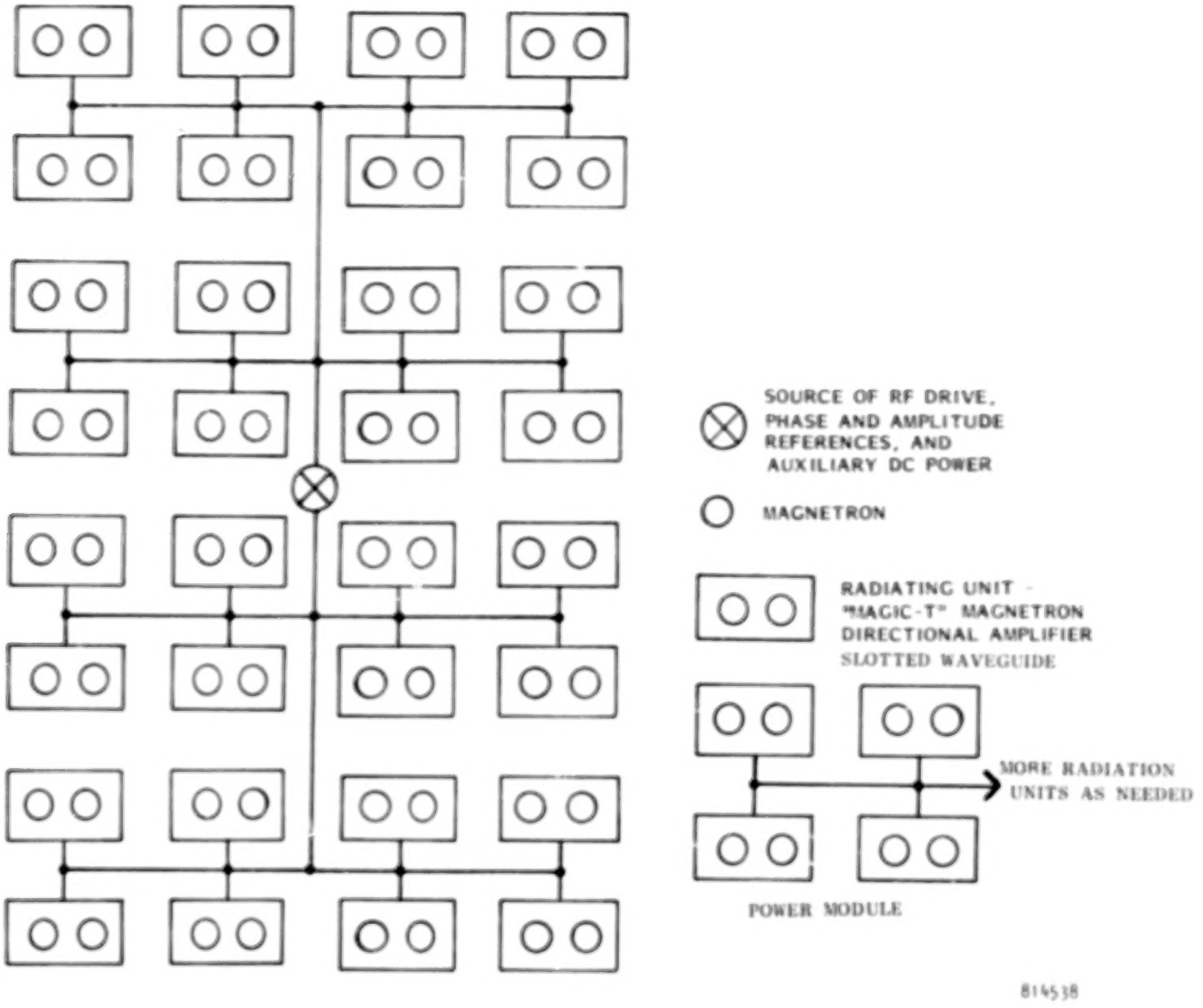
SOURCE OF RF DRIVE, PHASE AND AMPLITUDE REFERENCES, AND AUXILIARY DC POWER
MAGNETRON
RADIATING UNIT - "MAGIC-T" MAGNETRON DIRECTIONAL AMPLIFIER SLOTTED WAVEGUIDE
MORE RADIATION UNITS AS NEEDED
POWER MODULE
814538

Figure 4-2. Schematic of Subarray Made from Power Modules.

While the size of the radiating unit is uniquely quantized by slotted waveguide radiator considerations the choice of the size of the subarray itself is impacted by many different considerations. Ten meters square was considered at one time, largely because of the exagerrated expected cost of the phase control electronics at that time. A size as small as two meters square has also been considered to fit the scenario of only one high power klystron assigned to each subarray.

The size that we will arbitrarily select for the subarray that is composed of magnetron directional amplifiers is one that fits the scenario of a single rf driver for all of the magnetrons that are contained within the subarray. The size then depends upon the gain of each magnetron directional amplifier. If we assume a gain value of 24 dB, then a driver with the same power output as each magnetron directional amplifier in the array will drive an array of 256 magnetrons, 128 radiating elements, and 16 power modules. The resulting array size, as shown in Figure 4-3, is 4.64 meters by 4.41 meters (15.22 feet x 14.47 feet). As shown in Figure 4-3, the single magnetron directional amplifier that operates as a driver is supported far enough above the back of the subarray that it does not seriously impact the radiation of heat from the pyrographite cooling fins of the other magnetrons. At the same time a reflecting shield is used on the bottom side to prevent the absorption of heat by the driver directional amplifier. The cooling fins on the drive have essentially the same opportunity to radiate heat into space as the cooling fins on the other magnetrons.

There are many other scenarios as the size of the subarray. There is no reason why larger arrays and the use of intermediate amplifiers could not be considered. It is the author's judgment, however, that the trend will be toward smaller sizes and therefore towards simplicity in the driver arrangement.

It has been stated that the number of tubes that can be handled by one driver will depend upon the value of gain that is practical. It will be recalled that the quality of the output of the magnetron directional amplifier is unaffected by the gain but that the operating range in voltage and current becomes restrictive as the gain is increased if the tube is not retuned. Presumably this would not be the case if the tube were automatically retuned by the phase control systems as discussed in Section 2.7.

TABLE OF CONTENTS

Section			Page	
0		EXECUTIVE SUMMARY	0-1	1/B2
1.0		INTRODUCTION	1-1	1/B14
	1.1	Background Information	1-4	1/C4
2.0		PHASE AND AMPLITUDE TRACKING DEVELOPMENT AND DEMONSTRATION	2-1	1/D3
	2.1	Introduction and Summary of Results	2-1	1/D3
	2.2	Phase and Amplitude Tracking Data	2-5	1/D9
	2.3	Description of the Demonstration Test Bed, the Integration of the Magnetron with the Buck-Boost Coil, and Other Supporting Data	2-13	1/E5
	2.3.1	Physical Description of the Demonstration Test Bed	2-13	1/E5
	2.3.2	Description of the Magnetron with Buck-Boost Coil; Buck-Boost Coil Characteristics	2-15	1/E7
	2.3.3	Description of the Sensors, Comparators, and Other Components in the Phase and Amplitude Feedback Control	2-18	1/E11
	2.4	Analysis of the Microwave Power Amplitude Control System	2-23	1/F2
	2.5	Analysis of the Microwave Power Phase Control System	2-31	1/F10
	2.6	Documentation of the Electronic Circuits in the Amplifier for Phase and Amplitude Control Circuitry	2-31	1/F10
	2.7	Suggested Approach for a Phase Shift Device in the SPS Architecture	2-34	1/G1
3.0		MAGNETRON STARTING	3-1	1/G5
4.0		CONCEPT OF THE POWER MODULE AND ITS INTERFACE WITH THE REST OF THE SATELLITE	4-1	1/G9
	4.1	Definition of the Power Module and Its Interface with the Subarray	4-1	1/G9
	4.2	Interface of the Power Module with the Thermal Environment and with the Auxiliary DC Power Sources	4-6	2/A6
5.0		AUXILIARY POWER SOURCE STUDY	5-1	2/A13
	5.1	Introduction	5-1	2/A13
	5.2	Application of Microwave-to-DC Power Conversion as a Source of Auxiliary Power	5-3	2/B3
	5.3	Scenario of Start-Up Procedure in Subarray that Supplies its Own Auxiliary Power	5-10	2/B13

TABLE OF CONTENTS (Continued)

Section			Page
6.0		NOISE MEASUREMENTS	6-1 2/C6
	6.1	Introduction and Summary	6-1 2/C6
	6.2	Description of the High Sensitivity Noise Measuring Equipment	6-6 2/C13
	6.3	Description of the First Magnetron Configuration Tested	6-6 2/C13
	6.4	Results from the Magnetron Directional Amplifier Using the Raytheon QKH2000 #13	6-13 2/D9
	6.5	Description of and Test Results from the Second Magnetron Configuration	6-15 2/D11
7.0		DESIGN OF THE SPS MAGNETRON	7-1 2/E5
	7.1	Introduction	7-1 2/E5
	7.2	Study of Pyrographite Heat Radiator Design and Its Manufacture and Cost	7-5 2/E9
	7.2.1	Heat Radiator Design	7-5 2/E9
	7.2.2	Bonding Pyrolytic Graphite to the Magnetron Anode	7-11 2/F3
	7.2.3	The Manufacture of Pyrolytic Graphite and Its Fabrication into Radiators	7-12 2/F4
	7.3	Magnetic Circuit Study	7-15 2/F9
	7.4	Design of Interaction Areas of Magnetron	7-19 2/F13
	7.5	Design of Cathode for Long Life	7-23 2/G4
	7.6	Mechanical Design of the Magnetron	7-24 2/G5
	7.7	Projection of the Characteristics of the Magnetron Package	7-26 2/G7
8.0		HARMONIC SUPPRESSION BY COAXIAL STUB FILTERS	8-1 3/A7
9.0		THE USE OF THE AMPLITUDE CONTROL FEATURE IN THE MAGNETRON DIRECTIONAL AMPLIFIER TO OPTIMIZE THE OVERALL SYSTEM EFFICIENCY AND TO PROVIDE DIRECT CONTROL OF SPS SYSTEM DC POWER OUTPUT BY THE ELECTRIC UTILITY	9-1 3/B6
	9.1	Experimental Verification with a Simulated Voltage-Current Characteristic of the Solar Cell Array	9-6 3/B11

TABLE OF CONTENTS (Continued)

Section			Page	
10.0		DEFINITION OF TECHNOLOGY DEVELOPMENTS FOR THE MAGNETRON PACKAGE AND MAGNETRON DIRECTIONAL AMPLIFIER	10-1	3/B14
	10.1	Introduction	10-1	3/B14
	10.2	Unresolved Issues and Additional Investigations	10-2	3/C1
	10.3	The Proposed Development Program for the Magnetron Package	10-5	3/C4
	10.4	The Proposed Development Program for the Magnetron Directional Amplifier	10-5	3/C4
11.0		ESTIMATED MAGNETRON PACKAGE PRODUCTION COSTS	11-1	3/C10
APPENDIX A		THEORY OF OPERATION OF THE MAGNETRON DIRECTIONAL AMPLIFIER	A-1	3/C13
APPENDIX B		DATA COMPARISON	B-1	3/C14

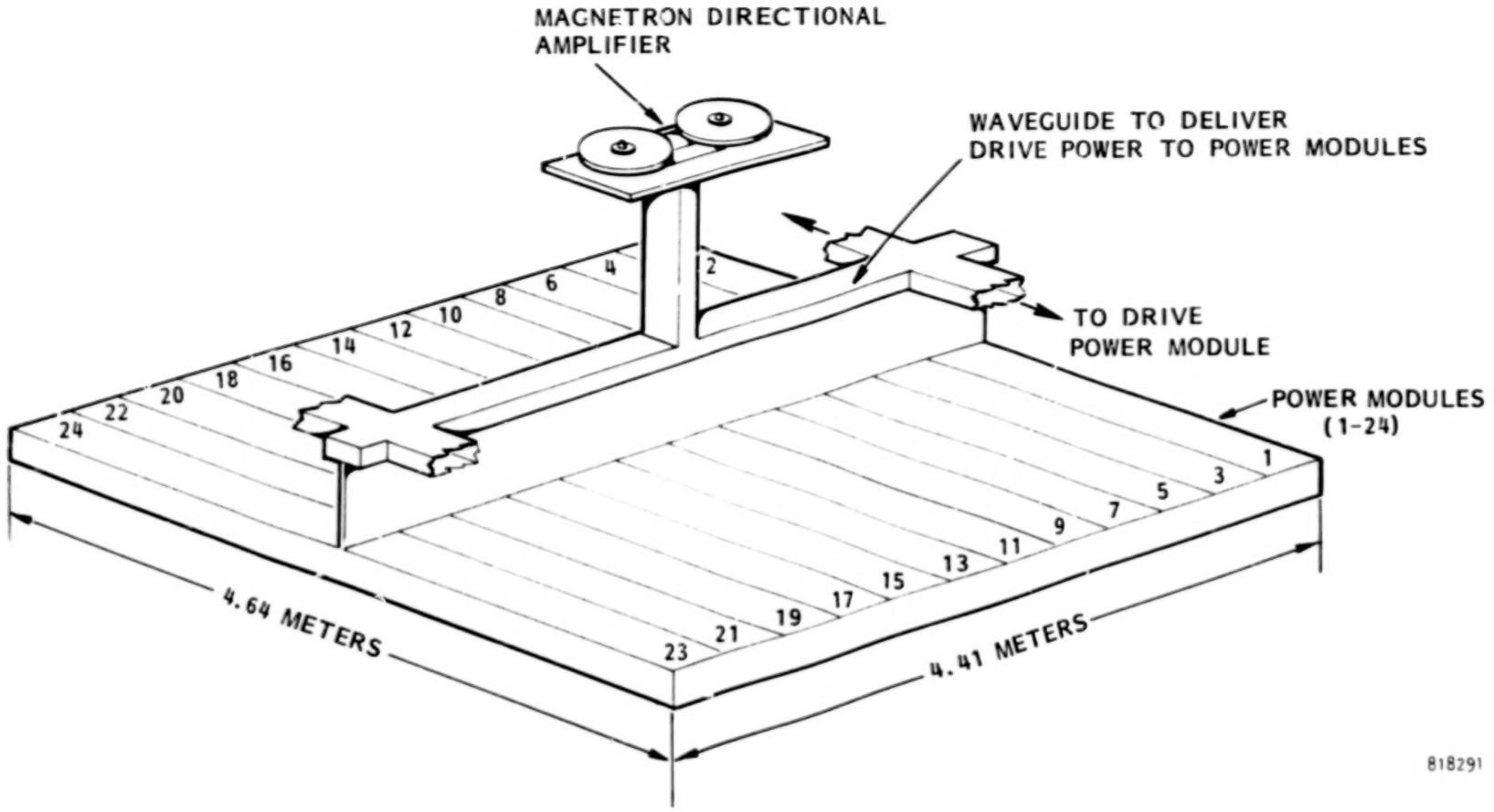

Figure 4-3. Simplified Layout of Subarray Using Assumption that One Microwave Drive Source will Drive all of the Power Modules in the Array.

The microwave schematic of the subarray that follows this scenario is shown in Figure 4-4. It is very simple. The source of the low level drive is assumed to be a solid state amplifier that can be flush mounted either on one of the slotted waveguide arrays or possibly on a very small section at the center of the array which is dedicated to cooling the solid state amplifier and does not radiate microwaves. The start up procedures for the rf drive is discussed in Section 5.3.

4.2 Interface of the Power Module with the Thermal Environment and with the Auxiliary DC Power Sources

Returning to the power module itself it is desired to better define the thermal and electrical interfaces represented in the architectural design of Figure 4-1. Figure 4-5 shows the thermal interfaces while Figure 4-6 shows the electrical interface.

The thermal design of the power module architecture is of overriding importance. On the one hand it is necessary to get rid of the power dissipated in the microwave generators at as high a temperature as possible to take advantage of the fact that the quantity of heat radiated is proportional to the fourth power of the absolute temperature. In this area, however, no solid state devices can be used. Because it is imperative to use solid state devices in a number of areas as microwave power detectors and as elements in the phase and amplitude control circuits, it is reasonable to use the cooler surface of the slotted waveguide radiator to mount and cool these devices. This surface can be kept at a temperature between 100° and 150°C by placing lightweight reflective type insulation between the upper and lower half of the architecture. Figure 4-5 indicates the approximate levels of heat radiation as a function of temperature and whether the sun is incident upon the surface.

Figure 4-1 shows spaces between the individual waveguides in the slotted waveguide radiating array. These slots are 1/2 inch wide and provide space to mount solid state assemblies which can be conductively cooled by the surface plate. They are also useful for cable runs to the magnetrons and elsewhere.

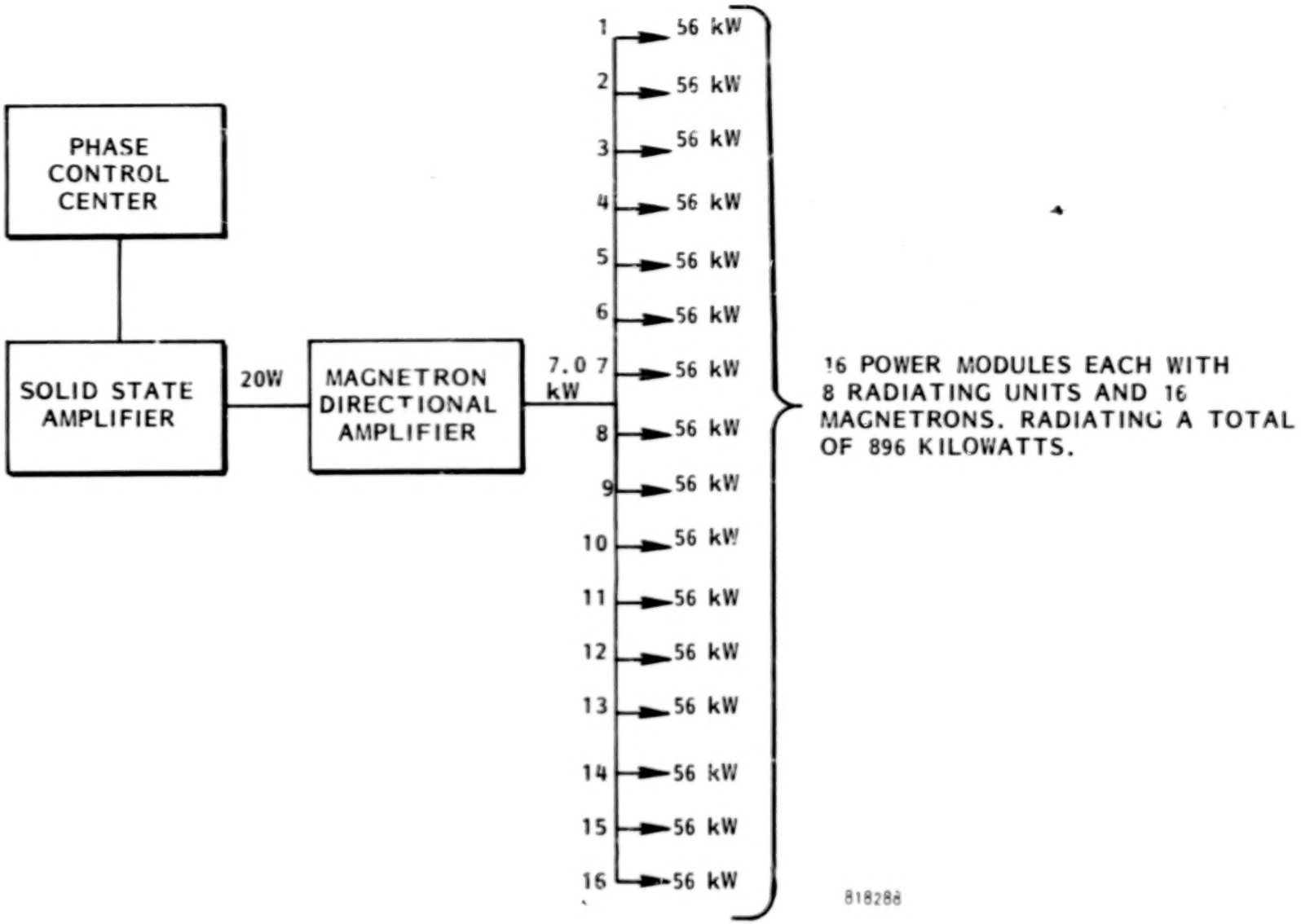

Figure 4-4. Schematic Diagram of Microwave Circuit for One Subarray.

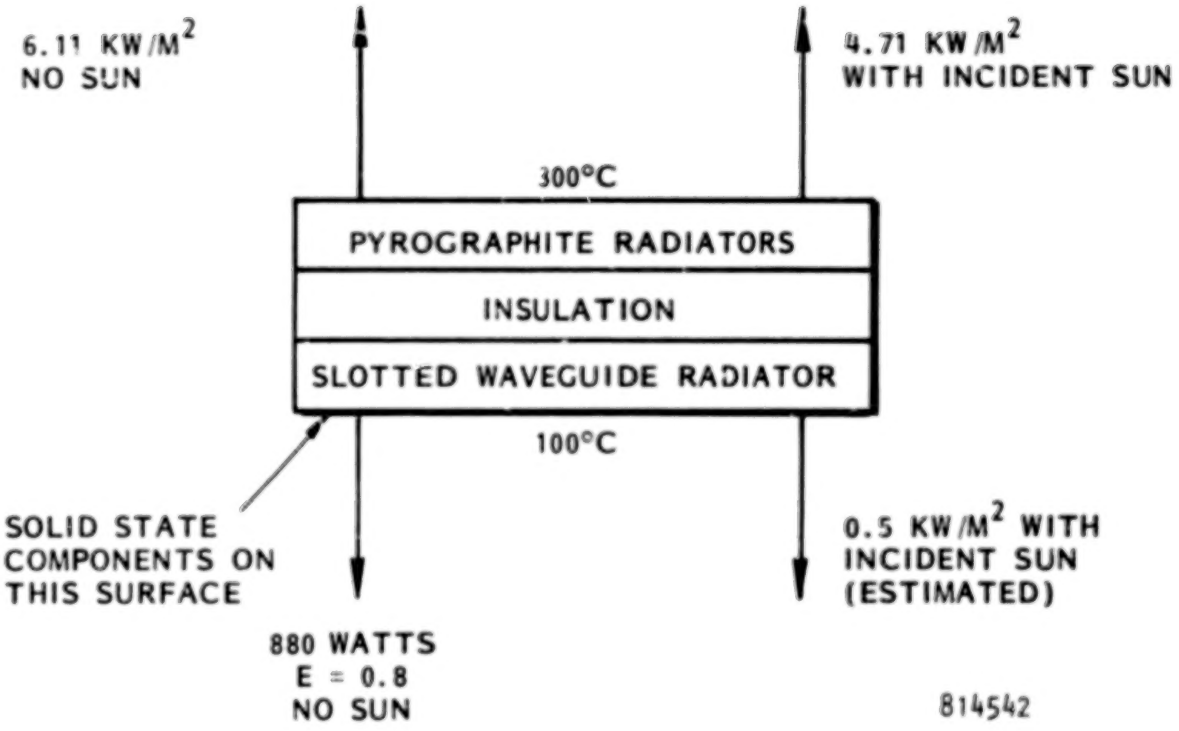

Figure 4-5. Thermal Interfaces in Power Module.

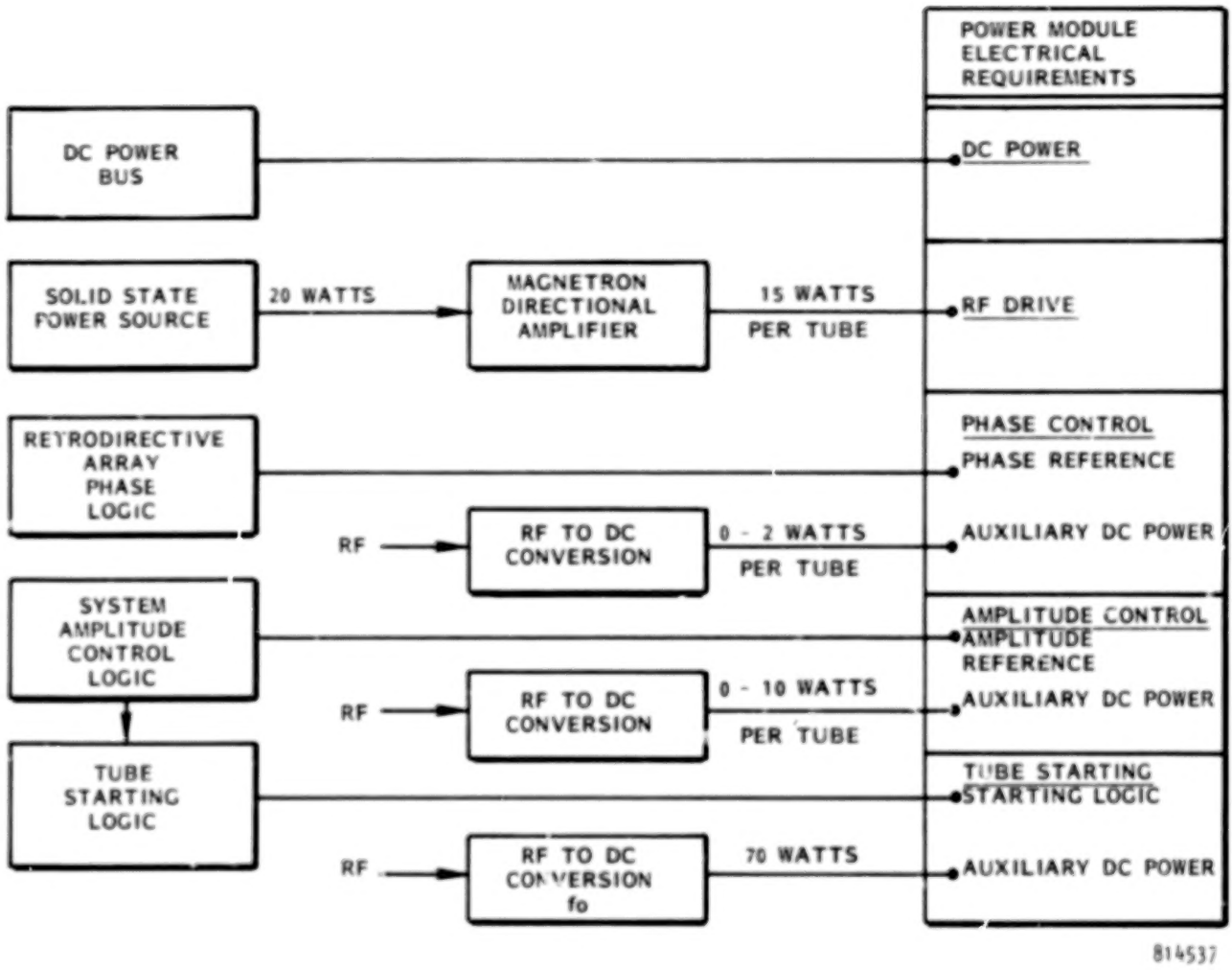

Figure 4-6. Electrical Input Interface with Subarray Showing Use of RF to DC Conversion for Auxiliary DC Power.

An important feature of the architecture shown in Figure 4-1 is that the longest waveguide dimensions are sufficiently short to reduce to negligible proportion the bending distortion that takes place because of a substantial difference in temperature between the top and bottom of the waveguides. This is true even for aluminum, which has a high coefficient of expansion. The following expression has been developed to evaluate the extent of the bending.

$$\text{Maximum depth of the concave curvature } D = \frac{d}{K\ (T_1 - T_2)} \left\{ 1 - \cos \left(\frac{\ell k\ (T_1 - T_2)}{2d} \right) \right\}$$

where
- d = distance between top and bottom of waveguide
- k = coefficient of expansion of the waveguide with temperature
- ℓ = length of waveguide section
- T_1 = temperature of top of waveguide
- T_2 = temperature of bottom of waveguide (slotted section)

This expression indicates that for a reasonable temperature difference of 50°C between the top and bottom of an aluminum waveguide 3.5 cm high that the depth of the curvature is only 0.066 cm for 15.5 inch length of waveguide in one dimension and 0.132 cm for 31.0 inch length in the other direction. The 0.066 cm dimension corresponds to 1.94 electrical degrees while the 0.132 cm dimension corresponds to 3.88 electrical degrees. The scattering caused by such small deviations, if of an rms nature, would be less than 0.5%. Of course the deviations would be ordered rather than random. On the other hand the method by which the slotted waveguide sections are made would permit predistorting the long dimension so that at normal operating temperatures there would be little or no distortion, leaving only the distortion from the shorter dimension.

The electrical interfaces with the architecture of Figure 4-1 are shown in Figure 4-6. There are essentially six electrical interfaces. The first of these is with the DC power bus. Because of the constant output amplitude feature of the magnetron directional amplifier, the individually fused tubes are essentially connected

directly to the solar cell array, dispensing with any power conditioning except for main bus circuit breakers. For a further discussion of the fusing arrangement for the tubes consult section 2.3.

The second interface with the power module is the rf drive. This has already been discussed in considerable detail.

The third interface is with the phase reference needed for phase control. The phase reference is distributed by coaxial line or strip line to the slotted waveguide section of each package consisting of magnetron directional amplifier and slotted waveguide. The phase reference for each subarray would appear to be of a spider form that is laid over the face of the slotted array. It would be so designed and so constructed that it would provide an accurate phase reference over the entire subarray. At the input to each power module (two magnetron directional amplifiers wide and any length) provision would be made for a disconnect in order to remove the entire power module for servicing, should that be necessary. Auxiliary DC power would be required for the feedback control system that keeps the phase of the output of the magnetron directional amplifier tracking the phase reference. The recommendation here is to obtain that DC power by rf to DC conversion, utilizing an auxiliary magnetron for that purpose. One auxiliary tube would probably suffice not only for the auxiliary power needed for phase control but for all other auxiliary power that is needed.

The matter of auxiliary power and how it may be obtained is discussed in Section 5.0.

5.0 AUXILIARY POWER SOURCE STUDY

5.1 Introduction

Auxiliary DC power is continuously needed for amplitude tracking and phase tracking feedback loops in the magnetron directional amplifier. Short term AC or DC power is needed to heat the filament to start the magnetrons. Auxiliary power is also needed to supply power to the phase control center and low level microwave drive sources in the subarray. Table 5-1 shows the tentative power and voltage levels required for these various functions at the unit magnetron level as well as for the scenario of a subarray with 16 power modules, 128 radiating units, and 256 magnetrons. Maximum power requirements at the unit level for the amplitude tracking is expected to be about 10 watts per magnetron, maximum power for phase tracking is expected to be about two watts. The starting power requirement per magnetron is expected to be about seventy watts but the tubes may be started in sequence from a common source of power to ease the total power requirement for this purpose.

The traditional manner in which these powers and voltages would be obtained would be by DC to DC voltage transformation, in which the DC is first converted from 20 kilovolts of DC to high frequency AC and then reduced to the required voltages through an AC transformer where it is again rectified and filtered back to low-ripple DC power. This method has several shortcomings. A principle one is the very large voltage transformation ratio that is required, making it difficult to get the low voltages required in a single step of AC voltage transformation. Another objection is that there will be serious cooling problems associated with the large power conditioning units that will be used for reasons of increasing the efficiency and reducing the specific mass (mass per unit of power delivered).

It is therefore proposed that a different approach be used, recognizing that except for initial startup ample amounts of microwave power are available as a source of "prime" power, and that it has already been amply demonstrated by the "rectenna" principle that microwave power can be efficiently converted into DC power at high power levels.[1-10]

BLANK PAGE

BLANK PAGE

TABLE 5-1. AUXILIARY POWER IN SUBARRAY*

Subarray Item Needing Auxiliary Power	Auxiliary Power Requirement	Continuous or Intermittent	Power Requirement Max.	Power Requirement Min.	AC or DC	Voltage Requirements	Potential Source of Prime Power**
Power Module	Amplitude Control	Continuous	10	0	DC	+20 -20	Bled from MDA* Driver to Start. Self Supplying After
	Phase Control	Continuous	2	0	DC	+20 -20	
	Magnetron Start	Starting 5 Sec.	70		DC or AC	5	Dedicated MDA*
MDA* RF Driver for Power Module	Amplitude Control	Continuous	10	0	DC	+20 -20	Battery to Start
	Phase Control	Continuous	2	0	DC	+20 -20	Self Supplying After
	Magnetron Start	Starting 5 Sec.	70		DC or AC	5	Battery
Solid State RF Driver	Power to Operate	Continuous	30	30	DC	+30	Battery to Start Bled from MDA* Driver
Dedicated MDA* for Auxiliary Power	Amplitude Control	Continuous	10	0	DC	+20 -20	Battery to Start
	Phase Control	Continuous	2	0	DC	+20 -20	Self Supplying After
	Magnetron Start	Starting 5 Sec.	70	0	DC or AC	5	Battery
Phase Control Center	Power to Operate	Continuous	100	100	DC	+30	Battery to Start Bled from MDA After

*MDA Means Magnetron Directional Amplifier

5.2 Application of Microwave-to-DC Power Conversion as a Source of Auxiliary Power

A rectenna element constructed in the manner in which it is normally used is shown in Figure 5-1.[7] This is a balanced configuration which provides six watts of DC power output easily with an efficiency well over 85%. Moreover, much data has been taken on an unbalanced version of this rectenna element in which a ground plane was used for one side of the device as shown in Figure 5-2[7]. In this arrangement the efficiencies were equally high and the heat sink of the diode may be in direct contact with a large heat sink. It would appear that this arrangement is almost directly applicable to obtaining the four watts required for the phase control system of two tubes in the radiating unit and approaching what would be required for the amplitude control system. Of course two such devices would be required - one to supply the plus 20 volts and the other to supply minus 20 volts to the servo amplifier.

The source of power for the transient external heating of the filament may also be obtained in this manner although in this case a considerable amount of device development may be desirable to optimize the efficiency, and decrease the mass of the heat sink needed to absorb the heat generated during the transient startup. The low impedance level of the filament combined with the need for relatively large amounts of power makes the microwave to DC power source of special interest whose investigation from a design point of view seems worthwhile. A proposed design is pursued in the following material.

The impedance level of the filament will be considerably less than one ohm so that an impedance transformation at the microwave level will be necessary in the design. Such an impedance transformation can be easily accomplished. Figures 5-3a and 5-3b show an approach to the design of such a device. As the exploded view of Figure 5-4 shows the impedance transformation consists of a quarter-wavelength section of coaxial transmission line with a characteristic impedance of 4 ohms. A

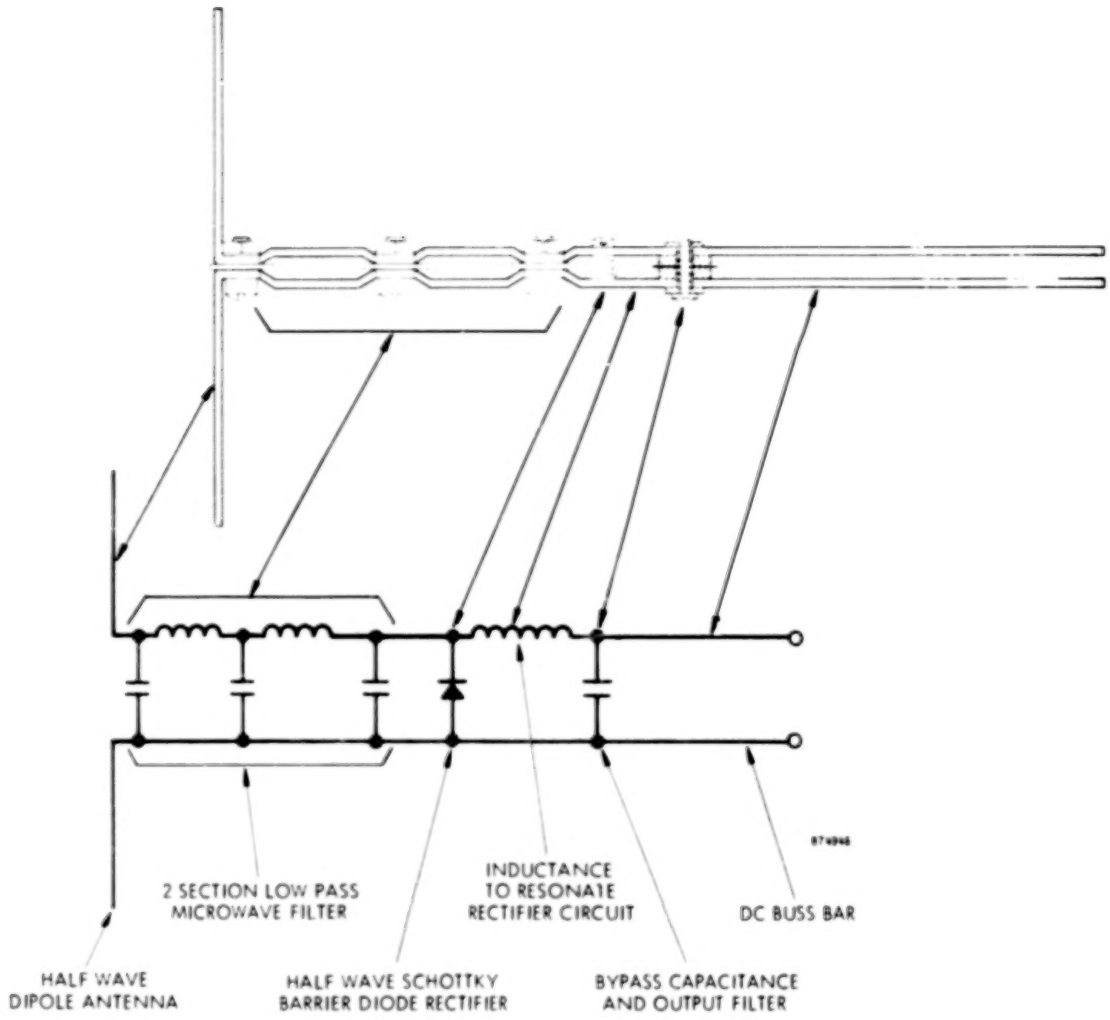

Figure 5-1. Cross Section and Schematic of Rectenna Element that Efficiently Converts Microwave Power into DC Power.

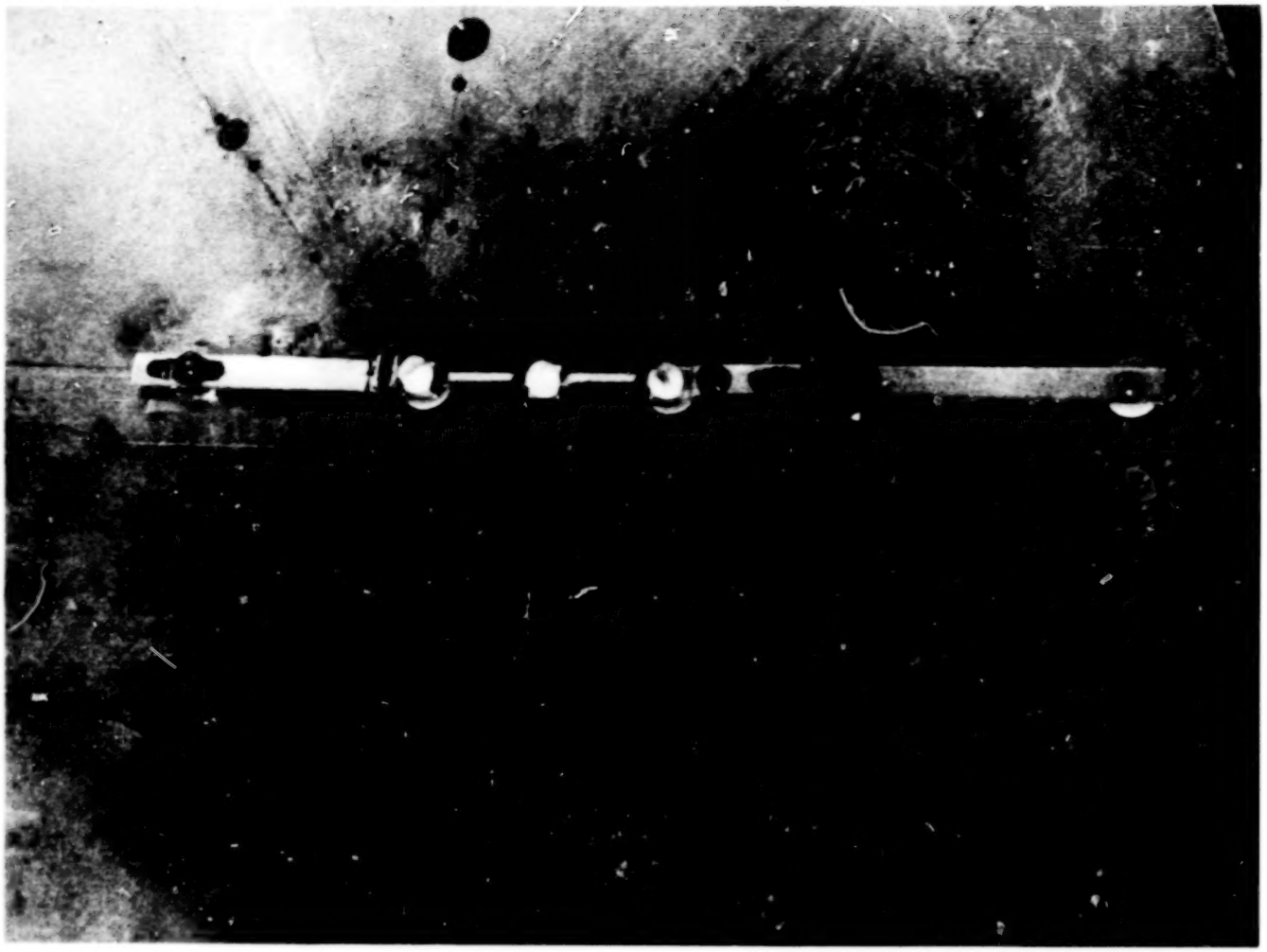

75-75955

Figure 5-2. Close-Up View of the "Split" Rectenna Element Mounted on the Ground-Plane. Diode is Cooled by Intimate Contact with Ground Plane.

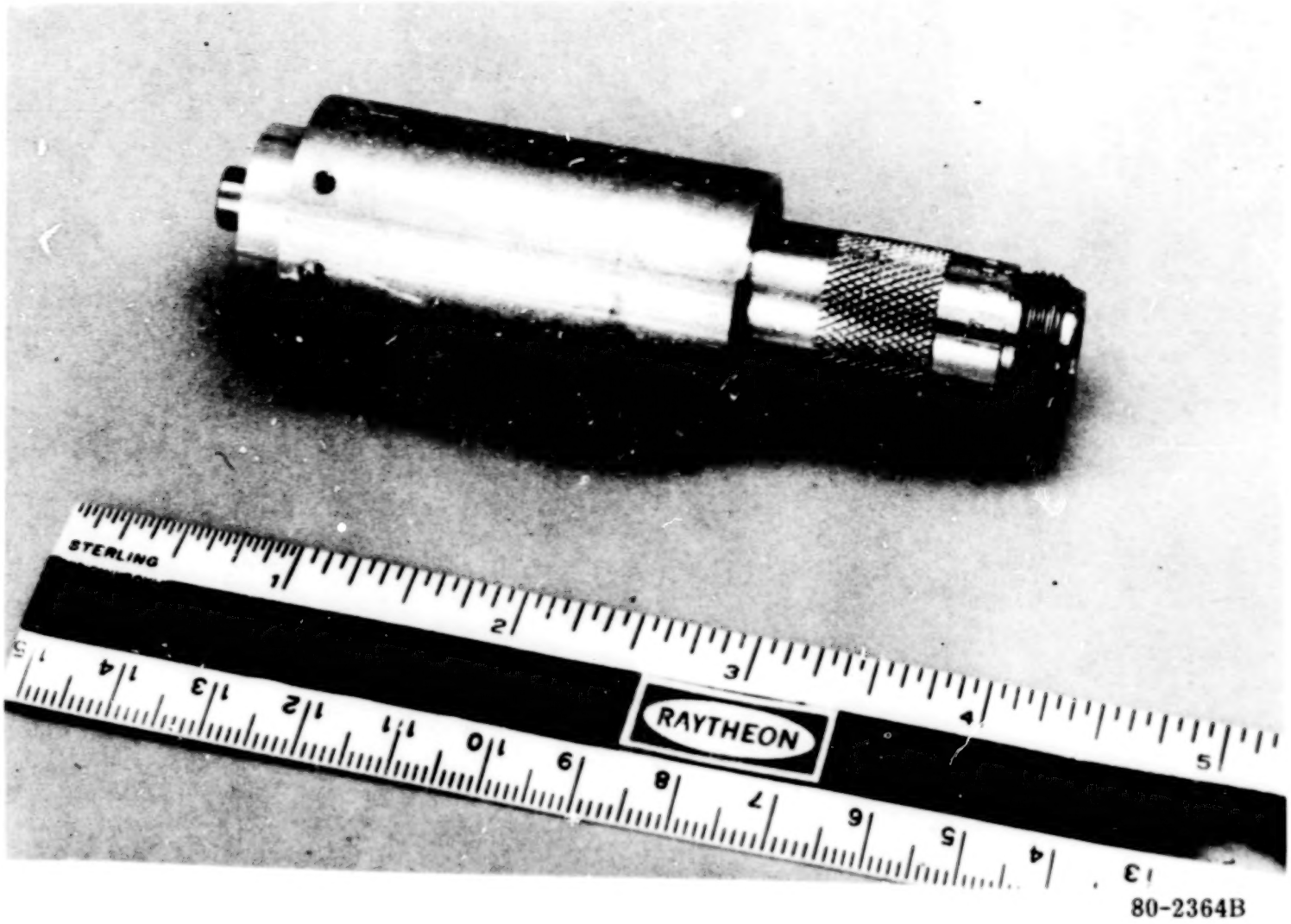

Figure 5-3a. Figure 5-3a Shows an Assembled Model of a Proposed Microwave-to-DC Source of Power for Transient Starting of Magnetrons.

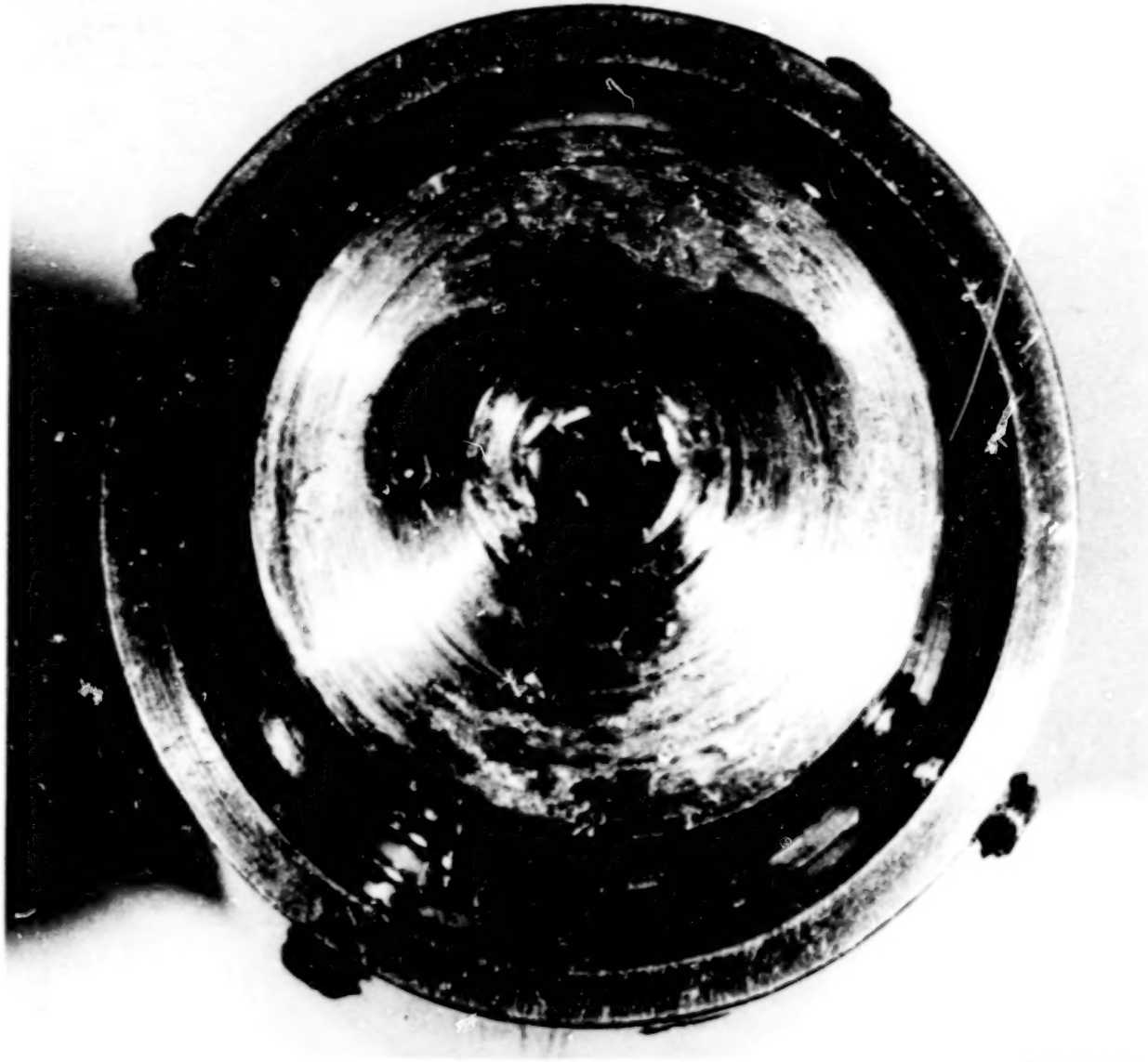

80-23643

Figure 5-3b. Indicates How Diodes of Existing Design Could be Efficiently Used.

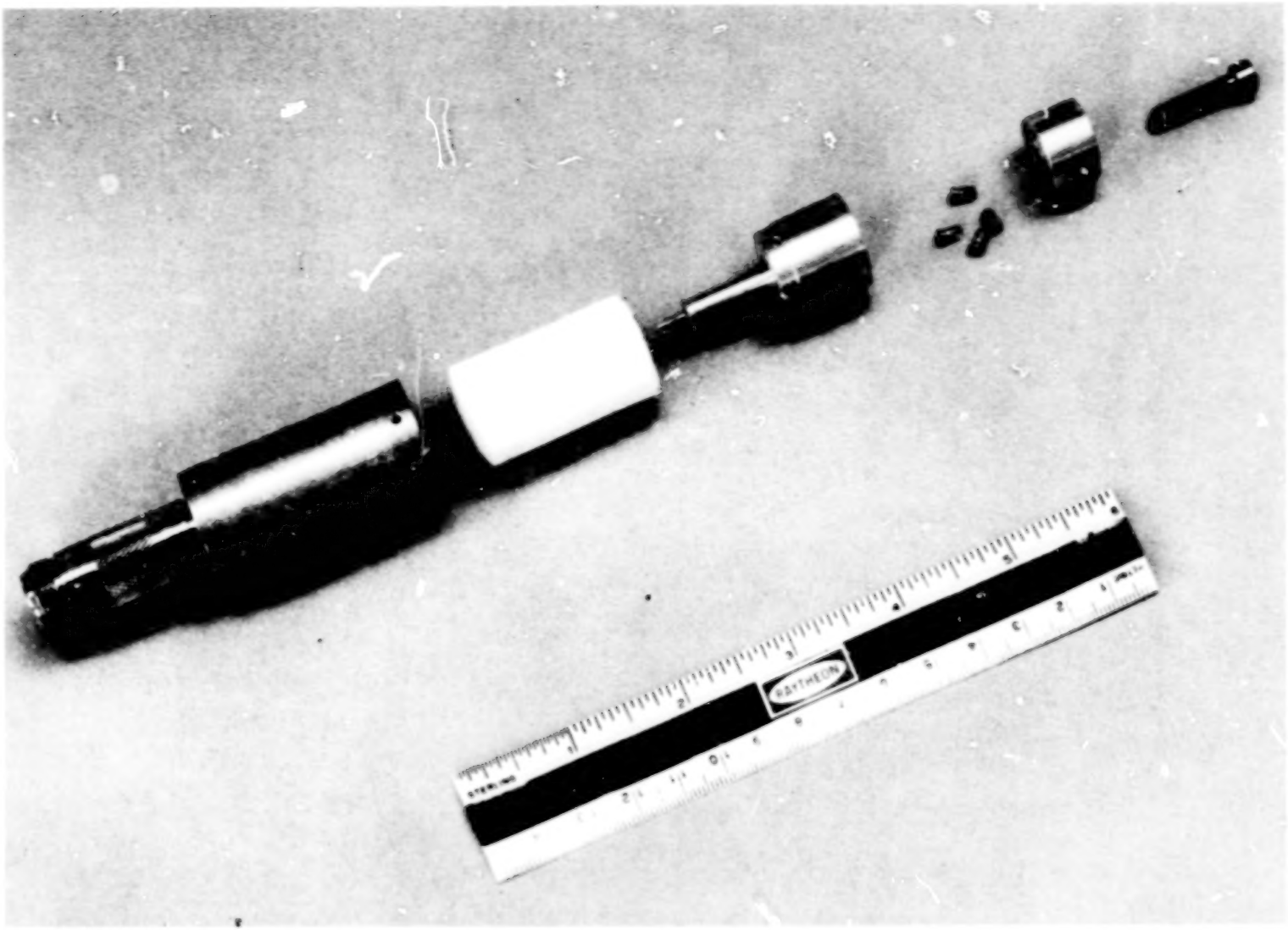

80-2362B

Figure 5-4. Exploded View of the Model of the Proposed Arrangement for Obtaining High Current at Low Voltage from a 50 ohm Source of Microwave Power.

four ohm transmission line matches a 50 ohm line to an impedance of only 0.32 ohms, a typical value for the filament. At the 100 watt operating level the corresponding voltage at the terminals to heat the filament would be 5.5 volts.

To indicate that such a design may be within the state-of-the-art, it may be of interest to see how many diodes of current design would be needed to operate in parallel as suggested by Figure 5-3b. Under a contract with LeRC GaAs Schottky barrier diodes making use of tungsten as the junction element were made and tested.(7) The effective barrier voltage was 0.6 volts and the slope of the voltage current characteristic in the forward conducting state corresponded to a series resistance of 0.7 ohms. The breakdown voltage in the reverse direction was 60 volts and the junction capacitance was 3.8 picofarads.

Let us assume that 20 such diodes are arranged in parallel following the approach shown in Figure 5-3b. The average current through each diode then becomes 0.91 amperes. With an assumed duty cycle of one third (fraction of time spent in the conduction region) the peak current will be 2.73 amperes and the instantaneous dissipation in each diode will be 5.2 watts. The average dissipation will be one third that, or 1.73 watts. To this dissipation must be added the junction loss of (0.7) (0.91) or 0.64 watts for a total dissipation per diode of 2.37 watts. The total dissipation in the 20 diodes then becomes 47 watts, and the efficiency of the device then becomes 69%.

It should be possible to improve upon the projected efficiency by designing the diodes for lower reverse breakdown voltage which will decrease the series resistance by a factor of two without changing the area of the junction. Considerably more junction area could probably be used in the diodes to further decrease the series resistance before encountering skin effect phenomena.

5.3 Scenario of Start-Up Procedure in Subarray that Supplies its Own Auxiliary Power

With the help of this explanation of how auxiliary power can be obtained from a microwave source, we will now develop a scenario in which each subarray has its own built in sources of auxiliary power. This scenario follows closely that in Section 4.0 which develops the architecture and microwave chains for the power modules and the subarray. Figure 5-5 will be used as a reference in the following discussion.

In the subarray there are three relatively small sources of battery standby power which will be needed for startup of the subarray after it has been shut down for any reason. These three battery sources are (1) a 150 watt low-voltage source for the transient heating of the filament of the magnetron directional amplifier which drives all of the power modules as described in Section 4.0; (2) a small 20 watt, 20 volt source with a negative polarity; and (3) a 100 watt, 20 volt source with a positive polarity. These latter two sources are used to initially power the phase control electronics, the solid state driver, and the phase and amplitude control feedback loops of the magnetron directional amplifier.

The filament start-up battery needs to be used for about five seconds while the other two battery sources need to be used only for a few miliiseconds to supply drive to the magnetron directional amplifier during startup. The outputs of all of these batteries are in parallel with microwave-to-DC supplies that are attached to the output of the magnetron directional amplifier, so that as soon as the magnetron directional amplifier starts it supplies power to the phase control electronics, the solid state driver, and its own control circuits for phase and amplitude tracking. At the same time the batteries are kept charged up. No switching is necessary, except for the removal of the external source of heater power from the magnetron filament.

Assuming now that both rf drive and high voltage DC from the photovoltaic array is applied to all radiating units, the next step is to apply transient power to heat the filaments and to supply low voltage DC power for the

BLANK PAGE

BLANK PAGE

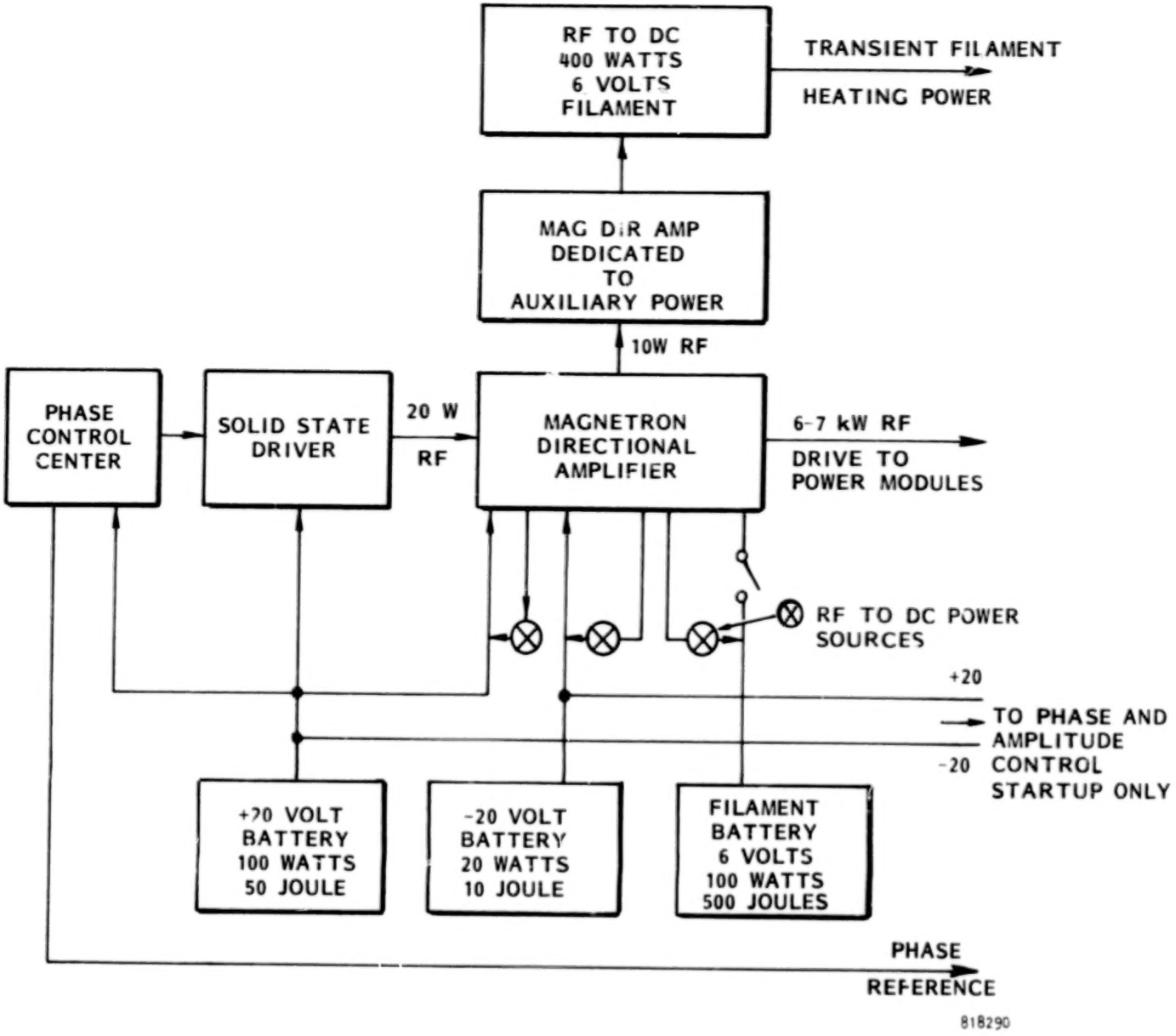

Figure 5-5. Schematic of Arrangement for Containing All Sources of Auxiliary Power within the Subarray.

phase and amplitude control electronics in each of the microwave radiating units. It is proposed that the power for both of these requirements may be initially obtained from a second magnetron directional amplifier that is dedicated to these purposes alone as shown in Figure 5-5.

In the discussion of the starting of the magnetrons, it has generally been considered that they would be started in sequence in some manner. This now needs to be considered in greater detail. One of the issues that needs to be addressed is how much time will be allowed to complete the starting of all tubes. If, for example, only one was started at a time, if there are a total of 256 tubes, and if each took five seconds to start, the total time required to complete the start-up would be 21.3 minutes - probably an elapsed time that is too long. Another issue that needs to be addressed is the reflected microwave power that will have to be absorbed in the drive source in some manner if symmetry is not observed in the start-up of the radiating units. For this reason it would be essential to start at least four radiating units simultaneously. This would reduce the completion of the start-up time by a factor of eight (because there are two tubes in each radiating unit) as well as requiring increased transient heating power by a factor of eight. If 140 watts for each radiating unit is required and there are four radiating units then 560 watts of DC power is required. If the microwave to DC efficiency is 67%, then 840 watts of generated microwave power is required. The total energy that must be dissipated as losses in the microwave to DC power supplies is therefore 44,800 watt-seconds. If aluminum is considered as the heat sink, if there is no short-term heat radiation from the sink, and if the heat sink is permitted to have an increase in temperature by 50°C, then approximately 896 grams of aluminum will be required for the heat sink. This seems a reasonable mass penalty to pay for an otherwise advantageous procedure.

The problem of continuously supplying the radiating units with auxiliary power for phase and amplitude control requirements remains. The problem of supplying the power from a central source seems prohibitive from a heat dissipation point of view. If the assumption is made that 20 watts of DC power may be required for

each tube at some time during the life of the system, then there is a total power requirement of 5.12 kilowatts. If an 80% microwave to DC conversion efficiency is assumed, 1.28 kilowatts of dissipated power must be radiated in the form of heat. Bearing in mind that the radiating surface in which the microwave rectifying diodes are imbedded can go no higher than 100°C, a centralized source of power would seem inadvisable because of the difficulty of finding a place to put the radiator.

The logical answer to this problem is to distribute the burden of producing this auxiliary power throughout the power module itself. As soon as each radiating unit is started in sequence, it is in a position to supply 20 watts of DC power to the next radiating unit to be started. With an efficiency of 80%, it is only necessary to radiate 5 watts at 100°C from the surface of the slotted waveguide array.

The procedure just outlined does not take care of the first radiating unit in each power module. Initially this power must come either from the dedicated auxiliary magnetron directional amplifier or from the magnetron directional amplifier driver as shown in Figure 5-5. But it does not appear that this is a satisfactory permanent source because there are 32 of these radiating units in the assumed total of 128. Fortunately, the solution is to have the units supply their own auxiliary DC power after they are started. This would double the heat radiation burden of these units to 10 watts at 100°C. This additional burden appears to be bearable.

In summary it would appear that a completely autonomous arrangement for auxiliary power sources within the subarray is possible. There would be a considerable amount of switching required but this is at a low power level where both solid state switching and conventional switching may be considered.

1. W. C. Brown, "Free-Space Microwave Power Transmission Study, Combined Phase III and Final Report", Raytheon Report No. PT-4601, September 1975. NASA Contract No. NAS-8-25374.

2. W. C. Brown, "The Technology and Application of Free-Space Power Transmission by Microwave Beam", Proceedings of the IEEE, vol. 62, No. 1, Jan. 1974, pp. 11-25.

3. R.M. Dickinson, "Evaluation of a Microwave High-Power Reception-Conversion Array for Wireless Power Transmission", Tech. Memo 33-741, Jet Propulsion Lab., Cal. Inst. Tech. , Sept. 1, 1975.

4. "Reception - Conversion Subsystem (RXCV) for Microwave Power Transmission System", Raytheon Report No. ER75-4386, JPL Contract No. 953968, Sept. 1975.

5. R.M. Dickinson, W.C. Brown, "Radiated Microwave Power Transmission System Efficiency Measurements", Tech. memo 33-727 Jet Prop. Lab. Cal. Inst. Tech., March 15, 1975.

6. "Microwave Power Transmission System Studies", Raytheon Contractor Report ER75-4368 NASA CR-134886, December 1975.

7. W.C. Brown, "Electronic and Mechanical Improvement of the Receiving Termimal of a Free-Space Microwave Power Transmission System", Raytheon Contractor Report PT-4964 NASA CR-135194, Aug. 1977.

8. J. Nahas, "Final Report, Simulation and Experimental Studies of Microwave-to-DC Energy Conversion Systems", Prepared for NASA, Lewish Research Center, under Grant No. NSG-3070.

9. SPS System Evaluation Phase III Study Document - Executed by Boeing, Raytheon, General Electric-Boeing D180-24635-1.

10. R.J. Gutmann, J.M. Borrego "Solar Power Satellite Rectenna Design Study" Contract NAS 9-15453, December, 1978.

6.0 NOISE MEASUREMENTS

6.1 Introduction and Summary

The objective of one of the detailed tasks under this contract was to improve the sensitivity of measurements of noise in that frequency region which is removed by 10 or more MHz from 2.45 GHz at which the SPS microwave generator is assumed to operate. Of particular significance is a more sensitive measurement of noise immediately adjacent to the ISM band (50 MHz from the carrier).

Although there are a few exceptions noise so far removed from the carrier is of little interest in most radar and communications systems; therefore, provision is not usually made for measuring such noise at very low levels. However, this noise is important in the SPS because of the enormous amount of carrier power involved. In previous noise measurements that have been carried out on the magnetron the level of the background noise even within 10 megahertz of the carrier was below the sensitivity of the measuring equipment that employed a 24 dB notch filter to suppress the carrier. It was therefore desirable to improve the sensitivity of the measuring equipment to determine how much lower the noise level of the magnetron might be.

We have been successful in upgrading the sensitivity of the noise measurements by more than 30 dB, to the point where spectral noise density (the noise in one cycle of bandwidth) that is 195 dB below the carrier level may be sensed. Noise level this low, if it were to be achieved routinely, would appear to provide a sufficiently high safety factor over the present CCIR noise requirements to assure no interference with commercial microwave communication systems.

The availability of this equipment represents a powerful new tool for investigating low level noise that is removed in frequency from the carrier. Some of the preliminary measurements that have been made with it have produced information

that is both significant and surprising. For example, in a magnetron in which the emission of broadband noise had been further discouraged with the use of special external microwave circuits applied to the cathode support, the emitted noise approached the limit of sensitivity of the noise measuring equipment. At a spectral power density level where the RMS noise is 196 dB below the carrier a slight increase in noise above the residual noise in the spectrum analyzer was discernible.

As indicated in Figure 6-1 the noise level that is in the frequency region inside of the ISM band edges is about 40 dB better than has so far been measured on klystrons in this same frequency region. Although klystrons have been predicted theoretically to have low noise levels at frequencies removed substantially from the carrier frequency and their noise has been measured at levels approaching 190 dB below the carrier at a frequency 180 MHz away from the carrier* there have been no noise measurements comparable to the magnetron so close to the carrier.

The significance of such low noise measurements in terms of meeting the CCIR requirements are shown in Table 6-1. A 40 dB safety factor appears to be possible in the case of the magnetron if it can be designed to routinely perform as did the special laboratory model from which the data was obtained.

The use of this improved noise measuring capability has been incorporated into a continuing program of attempting to correlate observed noise with some assumed noise generating mechanism within the magnetron.

In general the noise spectra that we have observed are either of a continuous frequency or discrete frequency type. Occasionally both types of spectra are present although the more general situation is to have one or the other. It is not known to what extent the two types of spectra interact, but it is highly probable that they are caused by different phenomena. Although the discrete spectra are present

*Measurements made by JPL on their klystron transmitting tube in the Goldstone tracking facility at S-band for deep space probes.

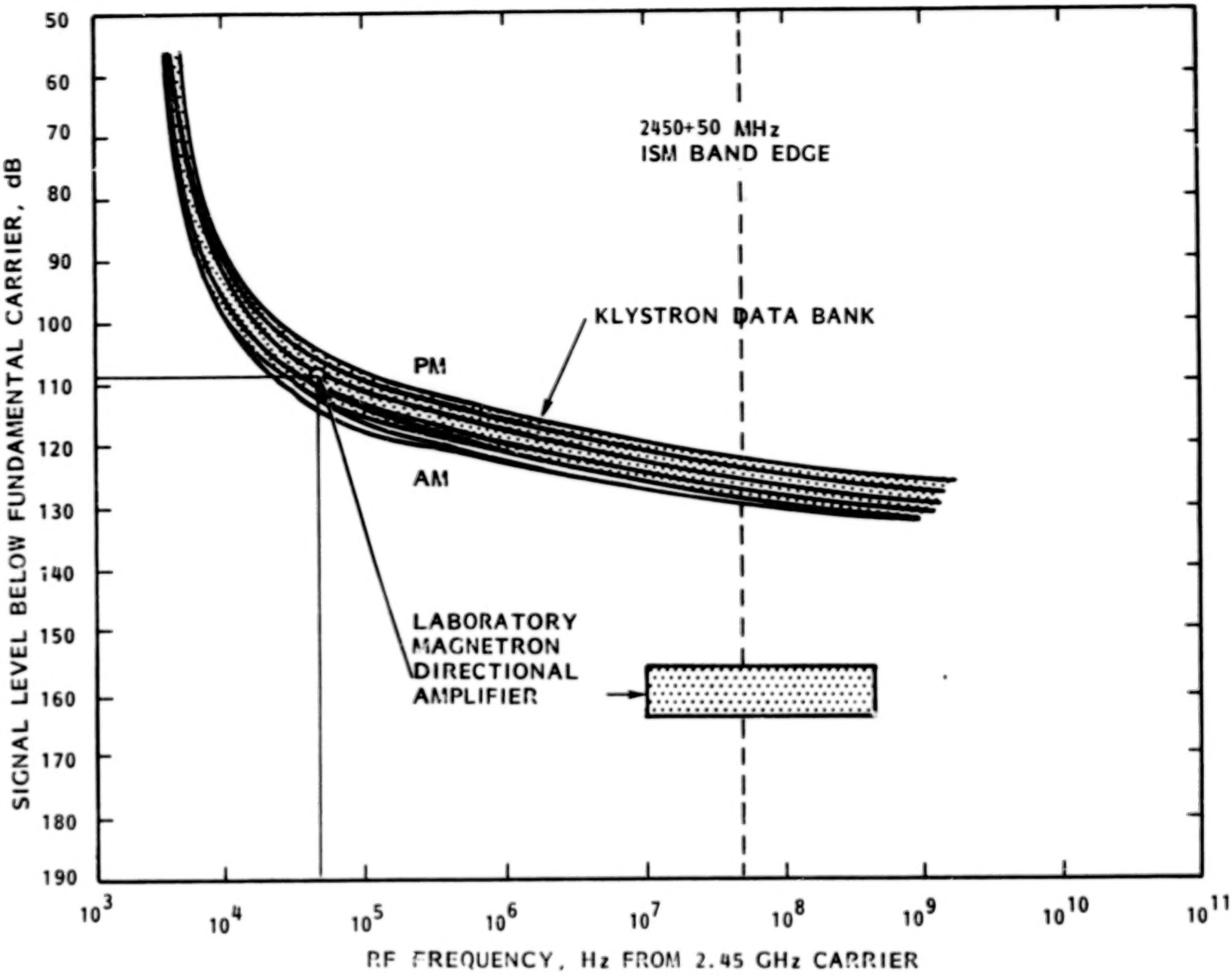

Figure 6-1. DC to RF Converter Spectral Noise Power Density in 4 kHz Bandwidth.

TABLE 6-1

RADIATED NOISE AND CCIR REQUIREMENTS

BASED ON RADIATED POWER

AT ISM BAND (2.4 - 2.5 GHz) EDGES

SUBJECT	KLYSTRON DATA BANK	LABORATORY MAGNETRON DIRECTIONAL AMPLIFIER
TOTAL NOISE RADIATED POWER IN 4 KHz BANDWIDTH FROM 7.7 GIGAWATT TRANSMITTER	0.00239 WATTS	0.00000075 WATTS
RADIATED POWER DENSITY PER SQUARE METER AT EARTH IN 4 KHz BAND ASSUMING UNIFORM RADIATION OVER A HEMISPHERE	0.29×10^{-18} W/M^2	0.93×10^{-22} W/M^2
SAFETY FACTOR OVER CCIR REQUIREMENTS (-154 DBW/M^2/4 KHz)	31.3 DB	66.3 DB
SAFETY FACTOR AFTER TAKING GAIN OF RADIATING APERTURES INTO ACCOUNT	-1.0 DB (4.06 SQ. METERS)	45.5 DB (0.29 SQ. METERS)

usually at low levels only, they are still objectionable in the SPS application. From the viewpoint of understanding the cause, it would seem that the discrete spectra now that they are more discernible with the increased measurement sensitivity, would be more susceptible to finding their cause. The data taken so far indicate that there are several kinds of discrete spectra and that there are a number of potential sources for them, but it has not been possible to identify a particular source with a particular kind of discrete spectra.

Because it is known that the use of external heater power has such an impact upon increasing the noise level and that this must somehow impact the temperature of the filamentary cathode we have also made noise measurements on a magnetron that has an optical window in it so that we can also observe any changes in the average cathode temperature and in the distribution of temperature along the cathode. Some observations that have resulted from these measurements will be incorporated into this report.

In summary, we have evolved a much more sensitive measuring technique for noise of either a continuous frequency or discrete frequency type that is removed from the carrier by 10 MHz or more. Using this equipment on a laboratory version of a magnetron in which special external circuits were added we have made measurements of spectral density noise that is 195 dB below the carrier. The technique is continuing to be used in attempting to correlate noise with assumed noise generating mechanisms within the magnetron.

In the material that follows the noise measuring equipment will be described and some of the measurements that have been made with it will be reported upon. Measurements of noise were measured on two tubes. One of them on which the very low noise was observed and shown in Figure 6-1 was the same tube (Raytheon #13) which had been used for the phase and amplitude demonstration. The second tube had an optical window in it and was of a somewhat different design.

6.2 Description of the High Sensitivity Noise Measuring Equipment

A largely self explanatory schematic of the noise measuring equipment is shown in Figure 6-2. In principle the equipment allows all of the noise that will propagate down the WR 430 waveguide to impinge upon the input of the spectrum analyzer while 66 dB of notch filtering of the carrier prevents the carrier from burning out the rf input of the spectrum analyzer while also adding 66 dB to the dynamic range of the spectrum analyzer.

Figure 6-3 shows several photographs that indicate the frequency characteristics of the combined notch filter that is described in Figure 6-2. Figure 6-3a, where the frequency sweep is 10 MHz per division, indicates that nearly all of the attenuation occurs within 10 MHz of the carrier frequency. Figure 6-3b shows a total sweep of 500 MHz, while Figure 6-3c shows a total sweep of only 20 MHz. The full attenuation at the carrier frequency is obscured in these photographs by the tendency of the electron beam in the image storage mode to "paint in" the deepest part of the cleft. The absolute attenuation at the carrier frequency was determined by static frequency measurements, and there is a full 66 dB of attenuation from 2450 to 2500 MHz. The attenuation is slightly less in going to the lower edge of the ISM band as both Figures 6-3a and 6-3b indicate, although full attenuation is reached at 2430 MHz.

Both the 42 dB and 24 dB notch filters are mechanically tunable over a limited range.

6.3 Description of the First Magnetron Configuration Tested

There was a selection process in determining which magnetrons would be used and what the magnetron interfaces to the test equipment would be. A total of 11 Raytheon, two Hitachi, and two Toshiba magnetrons were examined as candidates with the use of the 24 dB insertion filter alone. While some appeared to be better than others, in the final selection process it was decided to use the same magnetron that had been used in obtaining the phase and amplitude tracking data. This was a Raytheon QKH2000, identified as Raytheon #13.

BLANK PAGE

BLANK PAGE

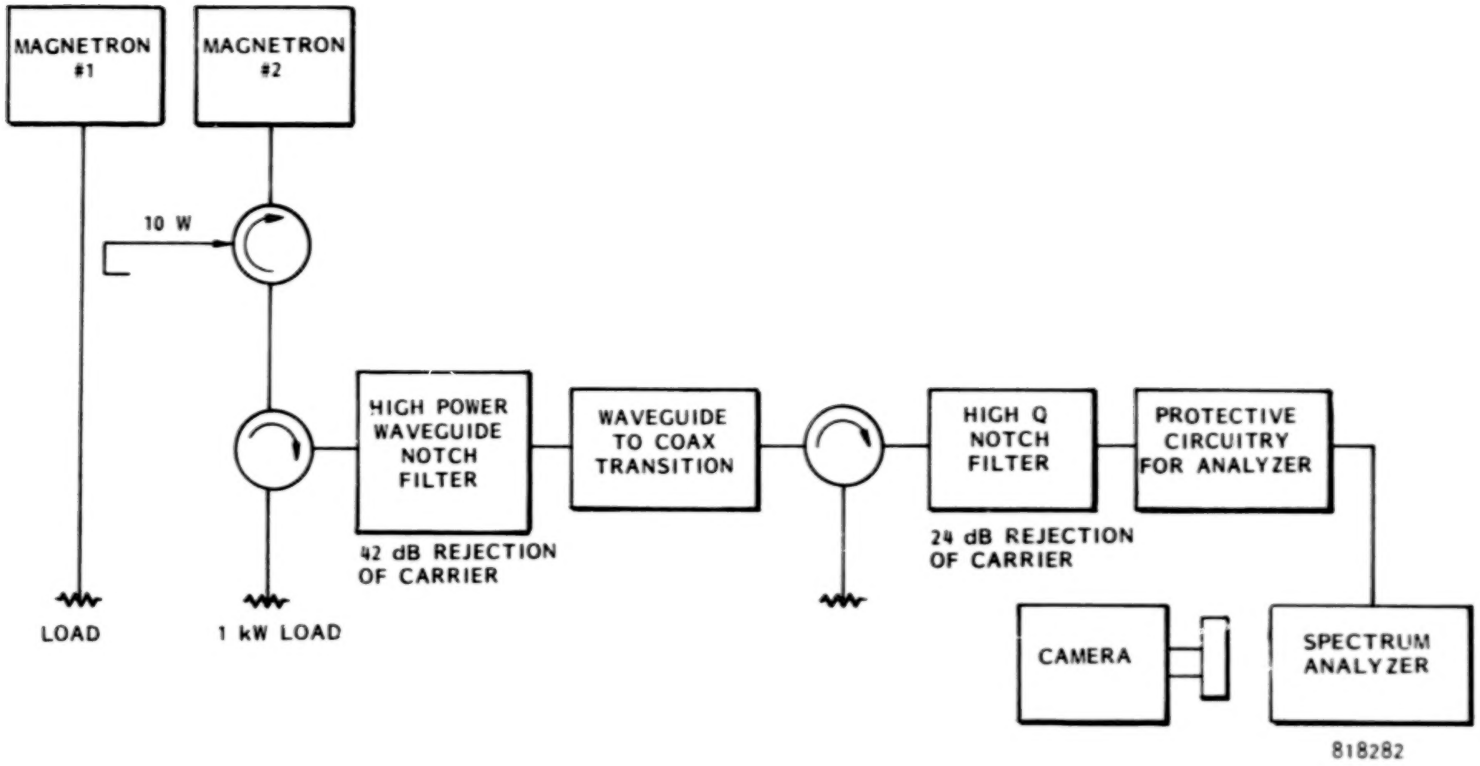

Figure 6-2. Improved Notched Filter Functional Test Block Diagram for Increased Sensitivity of Noise Measurements. Power not getting through high power waveguide filter is reflected back into a ferrite circulator and absorbed. Total filter consists of a cascade combination of a "T" section of WR 430 waveguide with a short in one arm adjusted to give minimum power transmission and a resonate cavity made from WR 284 tightly coupled to 3/4 inch coaxial line. A ferrite circulator is interposed between them to prevent coupling.

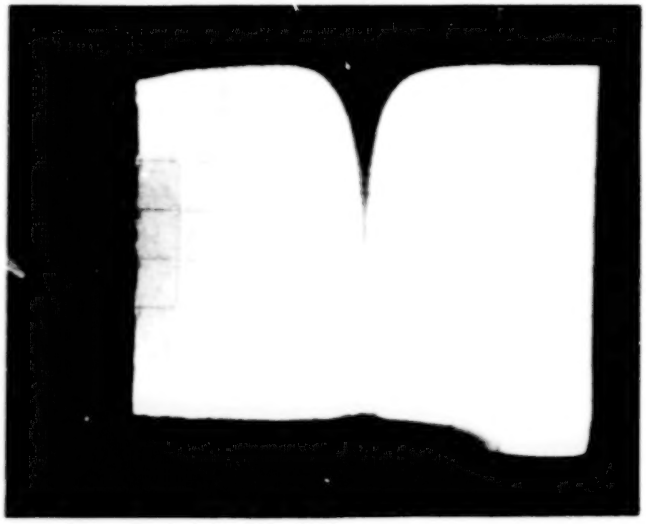

6-3 (a) Total Frequency Sweep = 100 MHz
Center Frequency - 2450 MHz
Vertical Scale - 10 dB/div.

10 MHz/Div IFBW 300 KHz

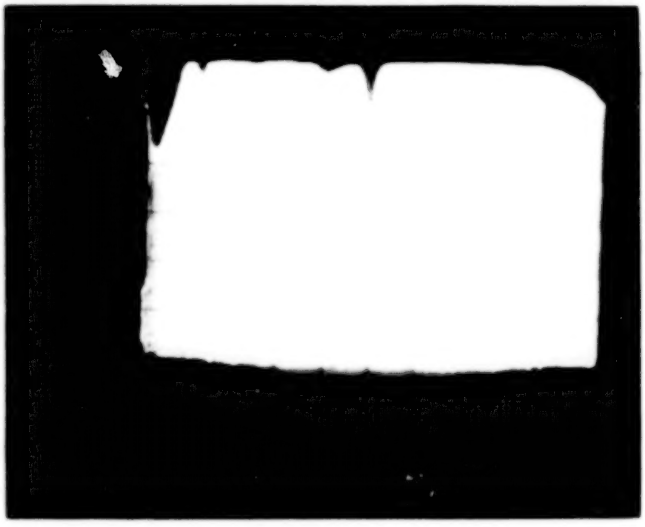

6-3 (b) Total Frequency Sweep = 500 MHz
Center Frequency = 2450 MHz
Vertical Scale - 10 dB/div.

50 MHz/Div.

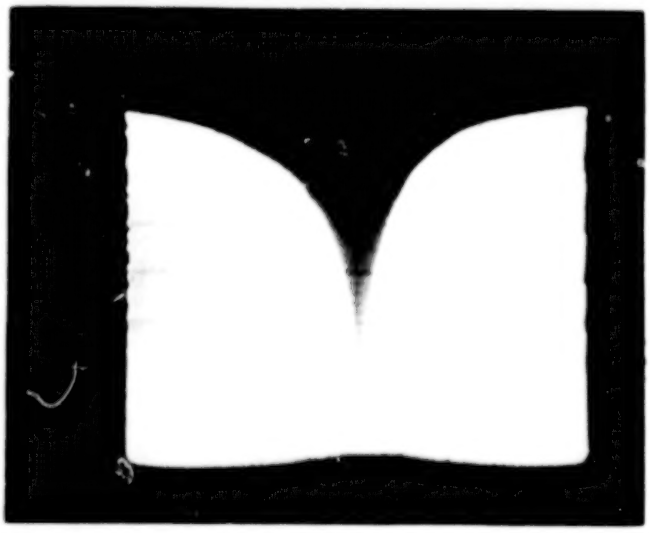

6-3(c) Total Frequency Sweep = 20 MHz
Center Frequency = 2450 MHz
Vertical Scale - 10 dB/div.

2.0 MHz/Div.

Figure 6-3. Attenuation of Notch Filter as Function of Frequency as Viewed on Hewlett Packard Spectrum Analyzer and Using Swept Oscillator as Signal Source.

A principle reason for this was that the tube was already equipped with a water cooled anode and a buck boost coil that could be used to vary the magnetic field. The use and positioning of permanent magnets to supply the basic value of magnetic field in the interaction area assured magnetic field symmetry and the absence of any effects that might be created with a slightly time varying field from the power supply for an electromagnet. The tube was also packaged in a manner that allowed the attachment of an external circuit to the cathode support structure of the tube.

Figure 6-4 shows the tube and its attachment to the waveguide and to the special microwave circuit attached to the cathode support. Figure 6-5 shows a closeup view of the tube itself with its magnetic circuit which includes the two samarium cobalt permanent magnets and the torus surrounding the tube which combines water cooling of the magnetron anode and the windings for the "buck boot" coil. The "buck boost" coil either adds to or subtracts flux from that established by the samarium cobalt permanent magnets. Note that there is no iron flux return path. The large diameter cold-rolled steel end plates couple effectively to a return path through air whose reluctance is relatively low compared to that of the air gap in the interaction area. The use of a cold-rolled steel return shell would increase the flux density in the air gap by only 15%.

Figure 6-6 shows a cross section of the circuit that was attached to the cathode support. The circuit is essentially a coaxial line with a movable microwave short circuit. The center of the coaxial line is attached to the cathode support as close to the tube as possible while the outer conductor is attached to the anode of the tube. A number of considerations complicate the construction of the unit. Provision has to be made for the other lead to the filament, and the shorting plunger must be insulated for at least 4 kilovolts because of the difference in potential of the cathode and the anode. As expected, when the coaxial line is attached to the tube, positions of the shorting plunger can be found where the open end coaxial cavity resonates at 2450 MHz. The travel of the movable short is large enough to traverse two positions of resonance, separated as expected by a physical distance of one-half wavelength. When the tube is operating these resonant regions are detected by a

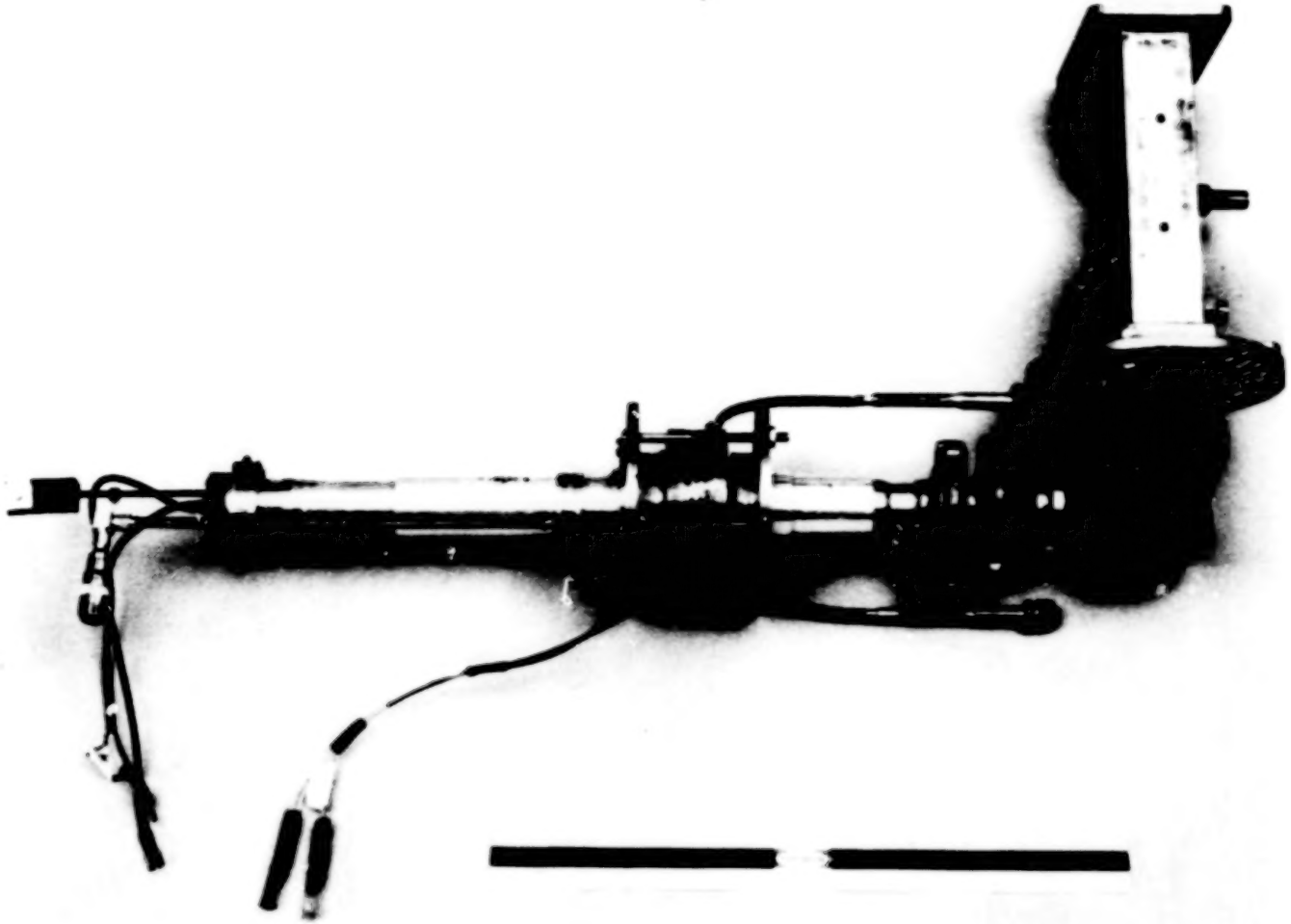

Figure 6-4. Assembly of Tube Under Test. A Special Microwave Circuit is Attached to the Cathode Circuit. The Microwave Output of the Tube Feeds into a Coaxial Circuit which is then Coupled into Waveguide that is Attached to Noise Measuring Equipment.

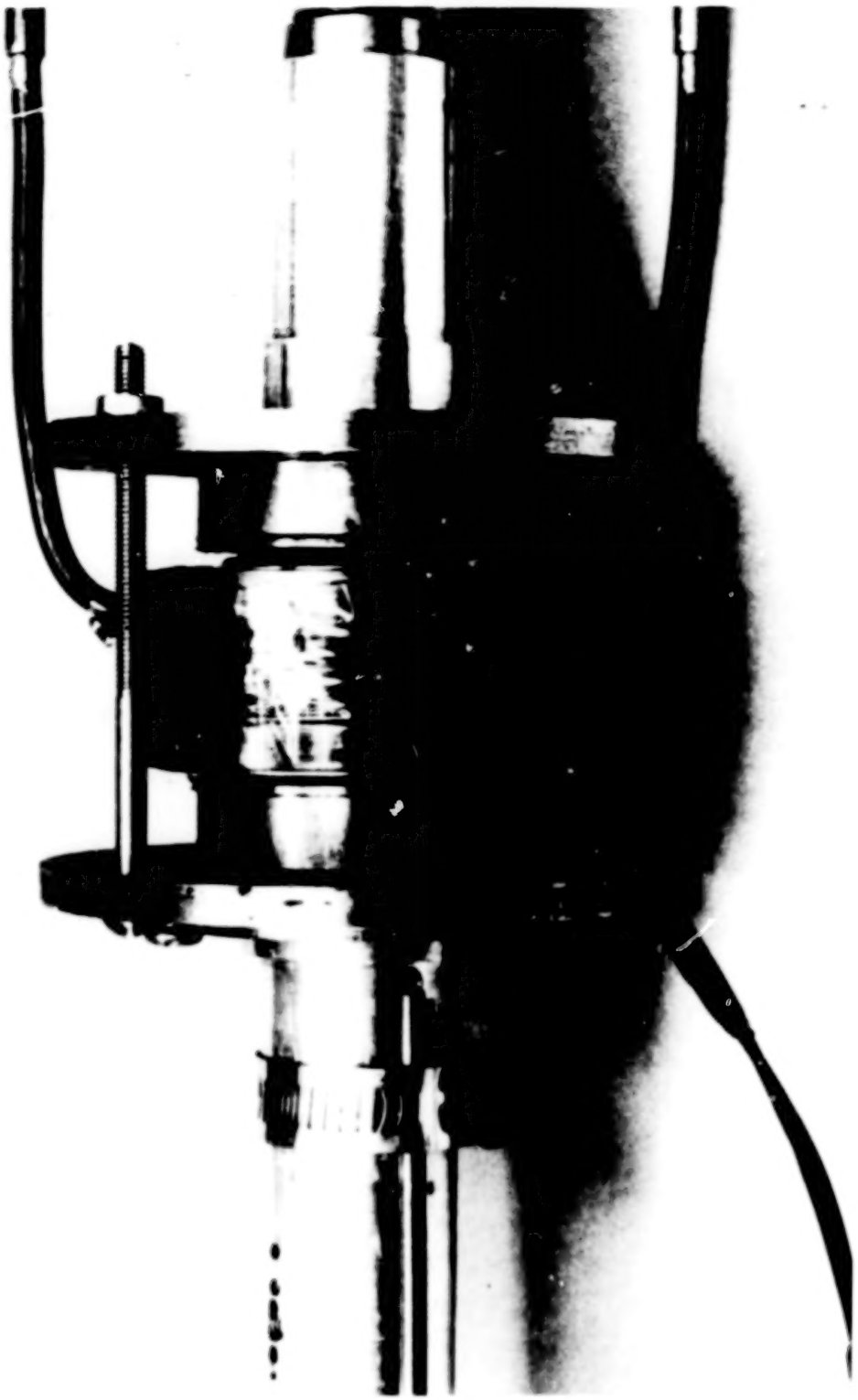

Figure 6-5. Assembly of Tube in its Magnetic Circuit. From Top to Bottom (1) Coaxial Output (2) Top Cold-Rolled Steel Flange, (3) Upper Samarium Cobalt Magnet (4) Torus which is Combination Water Cooling Jacket or Magnetron and "Buck Boost" coil and (5) Lower Samarium Cobalt Magnet, (6) Lower Cold-Rolled Steel Flange (7) Special Circuitry Added to Cathode Lead.

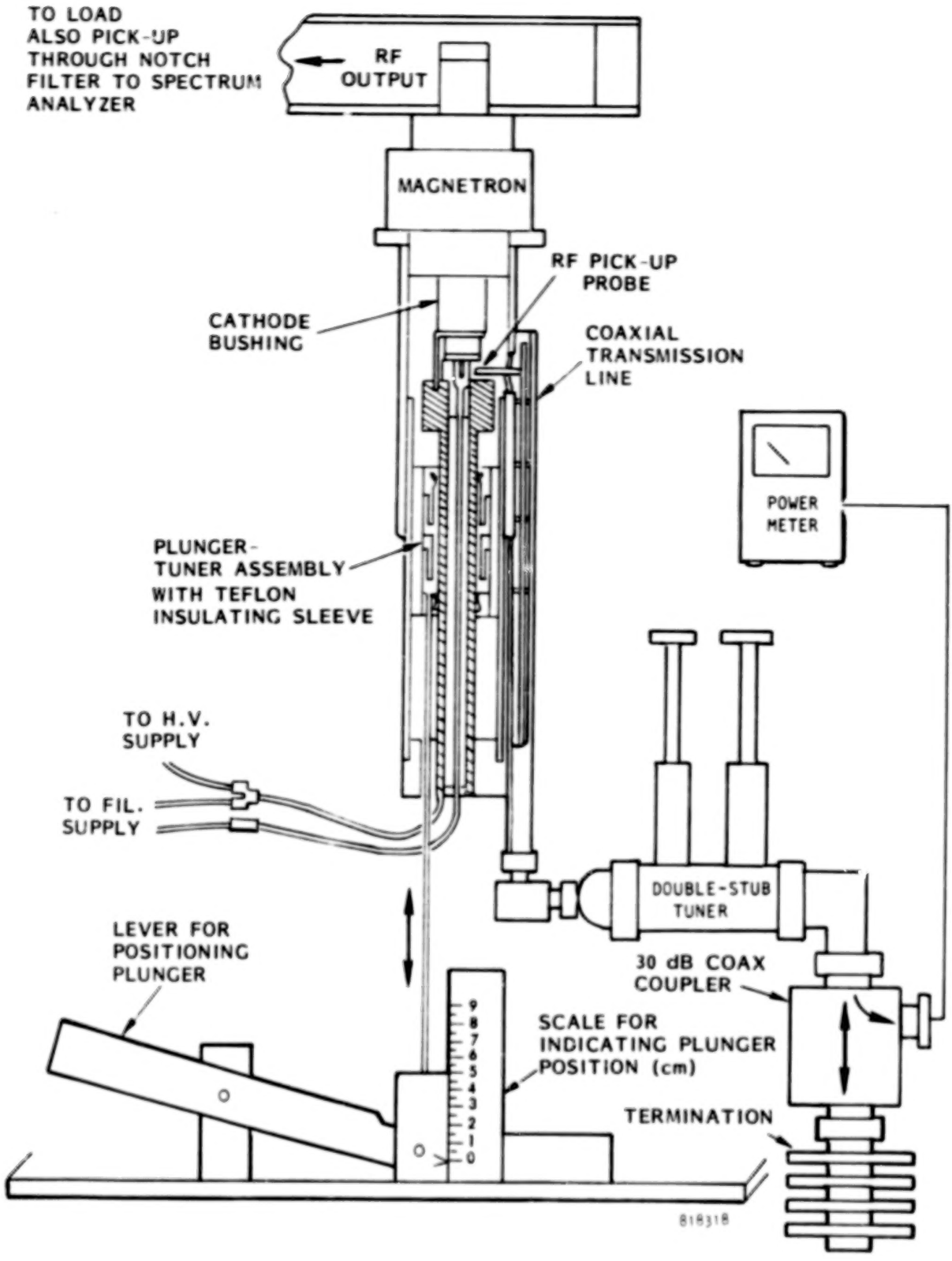

Figure 6-6. Cathode Plunger-Probe Set-Up.

probe which is attached to the side of the coaxial line. The probe is terminated into a matched load through a double stub tuner and may be adjusted to couple as much as 5 watts of power from the tube.

The original motivation for adding this additional circuitry to the tube was to either improve or worsen the field pattern in the interaction area to study the impact upon efficiency. However, it has been found that the plunger can be positioned to improve the signal to noise ratio a substantial amount while at the same time improving the efficiency by perhaps one-half percent.

6.4 Results from the Magnetron Directional Amplifier Using the Raytheon QKH2000 #13

Utilizing the Raytheon QKH2000 #13 in the configuration described in Section 2.1.3 and Figure 6-4, a series of tests were made utilizing the test arrangement shown in Figure 6-2. The results of one of these tests will be shown in the series of photographs in Figure 6-7.

Because of the low level of noise to be detected it was necessary to use a driver that had a very low noise level. The quality of this drive signal after the carrier had been attenuated by the 66 dB notch filter described in Figure 6-2 is shown in Figure 6-7a. The drive level that was a nominal 10 watts was adjusted to a point 20 dB below the top graticule on the HPA spectrum analyzer. The residual noise level of the analyzer was responsible for the noise at the bottom of Figure 6-7a as may be seen in Figure 6-7b which is for the identical settings on the spectrum analyzer but with the carrier signal removed. Figure 6-7c shows the noise level, still with the 66 dB of carrier suppression, after the magnetron directional amplifier has been turned on and giving 20 dB of gain to bring the carrier signal to the top graticule on the scope. It may be seen that the noise level at the edges of the frequency sweep (which corresponds to the 100 MHz width of the ISM band) is about 2 dB above the noise level seen on the scope without any input signal.

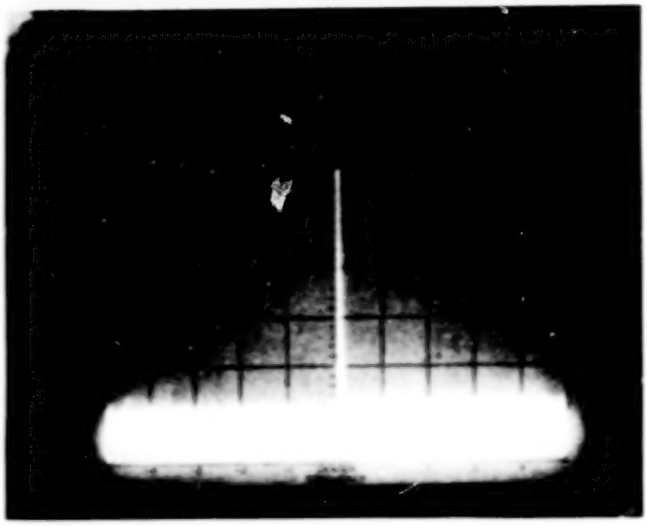

6-7 (a) Appearance of Drive Signal with 66 dB of Carrier Suppression Inserted.

Total Frequency Scan = 100 MHz

Vertical Scale = 10 dB/div.

Frequency - 2450 MHz

Noise at Bottom of Scope is Noise in Analyzer.

10 MHz/Div. IFBW 300 KHz

Log Ref 100 dB + 8.0 dB

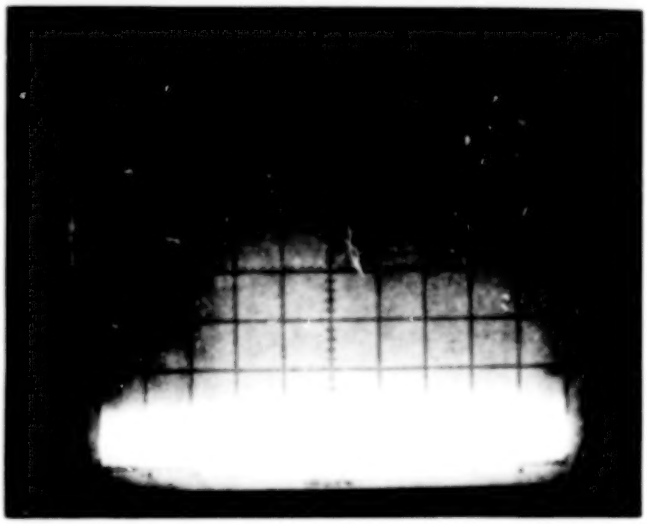

6-7 (b) Same Conditions Imposed on Analyzer as in 7(a) but with Drive Signal Source Removed.

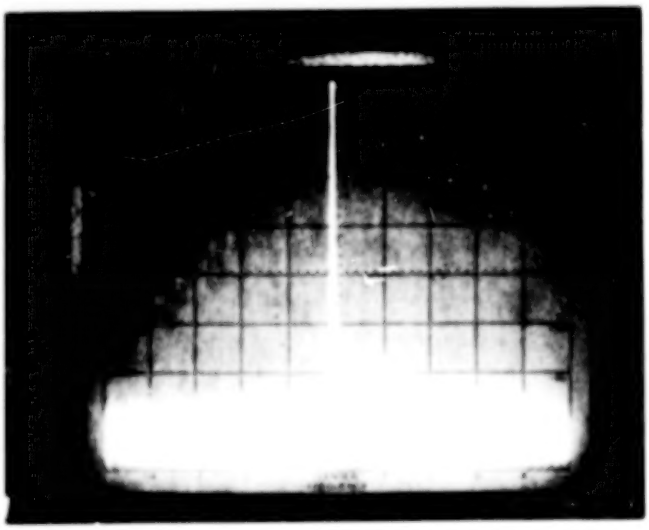

6-7 (c) Presentation on Analyzer with Magnetron Directional Amplifier Using QKH2000 #13 Magnetron and Optimum Position of Short in Cathode Microwave Circuit.

Receiver Bandwidth = 300 KHz

Total Frequency Scan = 100 MHz

Vertical Scale = 10 dB/div.

Carrier Suppression = 66 dB

Signal to Peak Noise = 133 dB/300 KHz

Signal to RMS Noise = 142 dB/300 KHz

Spectral Noise Density = -196.8 dBc

Figure 6-7. Signal to Noise Ratio Measurements of Improved Sensitivity. Spectral Noise Density of 196 dB Below carrier was Measured.

To obtain the actual spectral noise density corresponding to the signal observed on the scope at the band edges, first note that the signal as seen on the screen is 67 dB below the carrier. But the carrier is suppressed by 66 dB so the noise is actually 133 dB below the carrier. But the RMS value of noise is considered to be 9 dB below the observed peak noise leading to a signal to noise ratio of 142 dB but for a bandwidth of noise that is 300 KHz.

When the level of noise is transferred from a 300 KHz bandwidth to a 1 Hz bandwidth an additional 54.8 dB is added, so that the spectral power density of the noise is 142 + 54.8 or 196.8 dB below the carrier. If the noise is referred to a one megahertz bandwidth, then the carrier to noise ratio is 136.8 dB/MHz.

The impact of the positioning of the sliding short in the cathode coaxial circuitry upon the noise level may be observed by a comparison of Figures 6-8a and 6-8b. Figure 6-8a is the same photograph as 6-7c while 6-8b is for unfavorable setting of the cathode plunger. There is a difference of about 20 dB in noise level between the two settings.

For purposes of contrasting the present signal to noise ratio measurements to those that were obtained before the external heater power was removed and before the use of the circuitry on the cathode Figure 6-8c has been added. In this photograph the heater power that is normally used in the microwave oven application was applied. It is seen that the noise level is much higher even though the gain of the noise is reduced by 24 dB because only 42 dB of carrier suppression was used. With 66 dB of carrier suppression the noise would almost fill the screen. It was found that the cathode plunger made little difference for the conditions with full heater power applied.

6.5 Description of and Test Results from the Second Magnetron Configuration

The second magnetron (designated 0-3105) to be tested was made at a much earlier time period than the first one tested and had a special feature of an optical window through which the operating temperature of the cathode could be

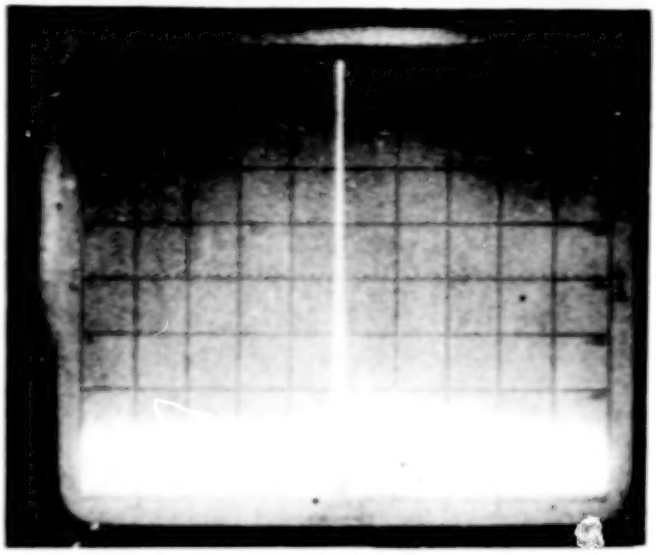

6-8 (a) Same Conditions as 6-7 (c)
Total Frequency Scan = 100 MHz
Carrier Suppression = 66 dB.

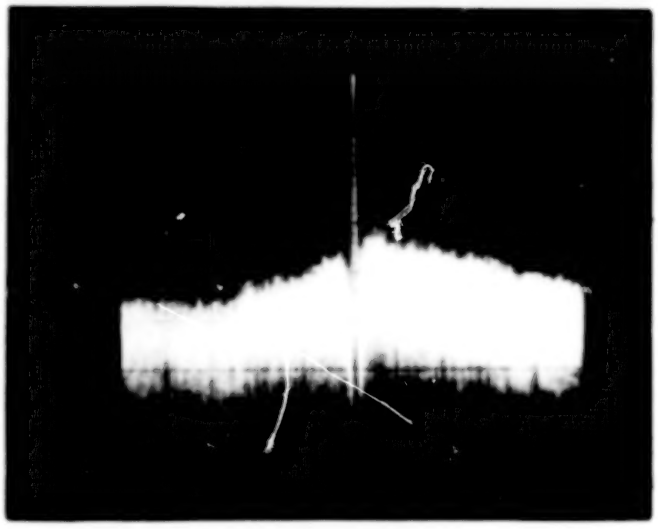

6-8 (b) Same Conditions as for 6-7 (a) but with Non-Optimum Position of Short in Cathode Microwave Circuit.

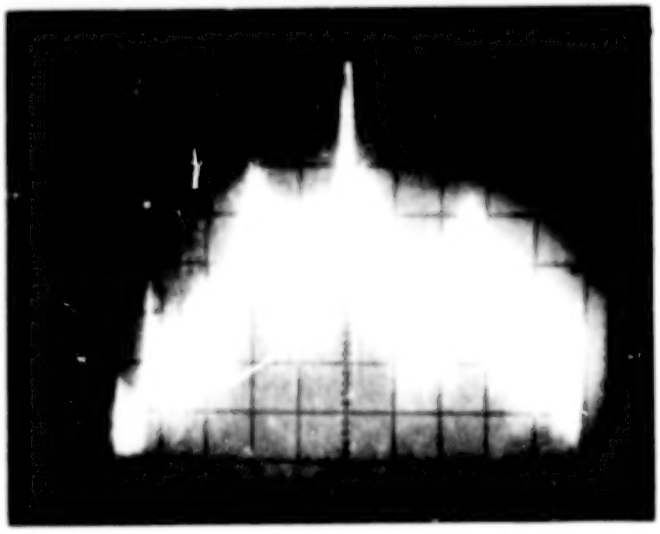

6-8 (c) Noise Level of Same Magnetron Directional Amplifier with Normal Heater Power of 37 Watts from External Power Source Applied.
Total Frequency Scan = 500 MHz
Carrier Suppression = 42 dB.

Figure 6-8. Data Indicating Impact of Positioning Cathode Circuit Short Circuit and Applying Heater Power.

observed while the tube was being operated. The tube is shown in Figure 6-9a. Figure 6-9b shows the standard Leeds and Northrup 8622C optical pyrometer that was used to observe the temperature of the cathode.

This tube was also fitted with the coaxial line circuitry on the cathode support of the tube but there is a substantial difference in the manner in which the cathode is supported. This tube was an all glass tube so that while the filament itself was identical the support was considerably different.

A substantial amount of data was taken with this tube with the major emphasis upon observing any changes in the temperature of the cathode or distribution of temperature along the cathode as a function of operating parameters, including the position of the shorting plunger in the cathode circuitry. In this report, three informative tests will be reported.

The first of these tests was an observation on how the temperature of the cathode, under conditions where no external heater power was applied, varied as a function of the anode current. This was needed as a check upon similar tests that had been run on a second tube with an optical window for viewing the cathode temperature and which had been included in the report of effort performed by Raytheon under contract #JPL 955104. In addition to different tubes, there was also a different operator taking the data. The result of this test is shown in Figure 6-10 where the data is compared with that from the other tube and with the theoretical predictions given by the Richardson-Dushman equation. The new data is seen to be consistent with the previous data and therefore tends to confirm the observation that the magnetron device seems to have built into it a feedback mechanism in which the filament temperature is automatically adjusted to just that value which is needed to supply the required anode current.

The second of these tests was an observation of noise as a function of anode current. Three photographs of spectra for three different anode current

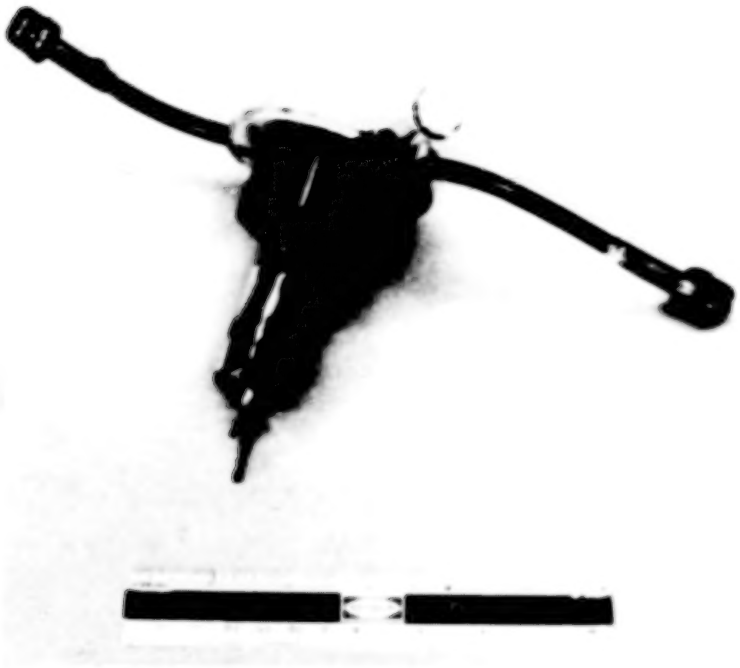

802366B

Figure 6-9a. Magnetron with an Optical Window for Viewing Filament Temperature.

802365B

Figure 6-9b. Leeds and Northrup 86226 Optical Pyrometer.

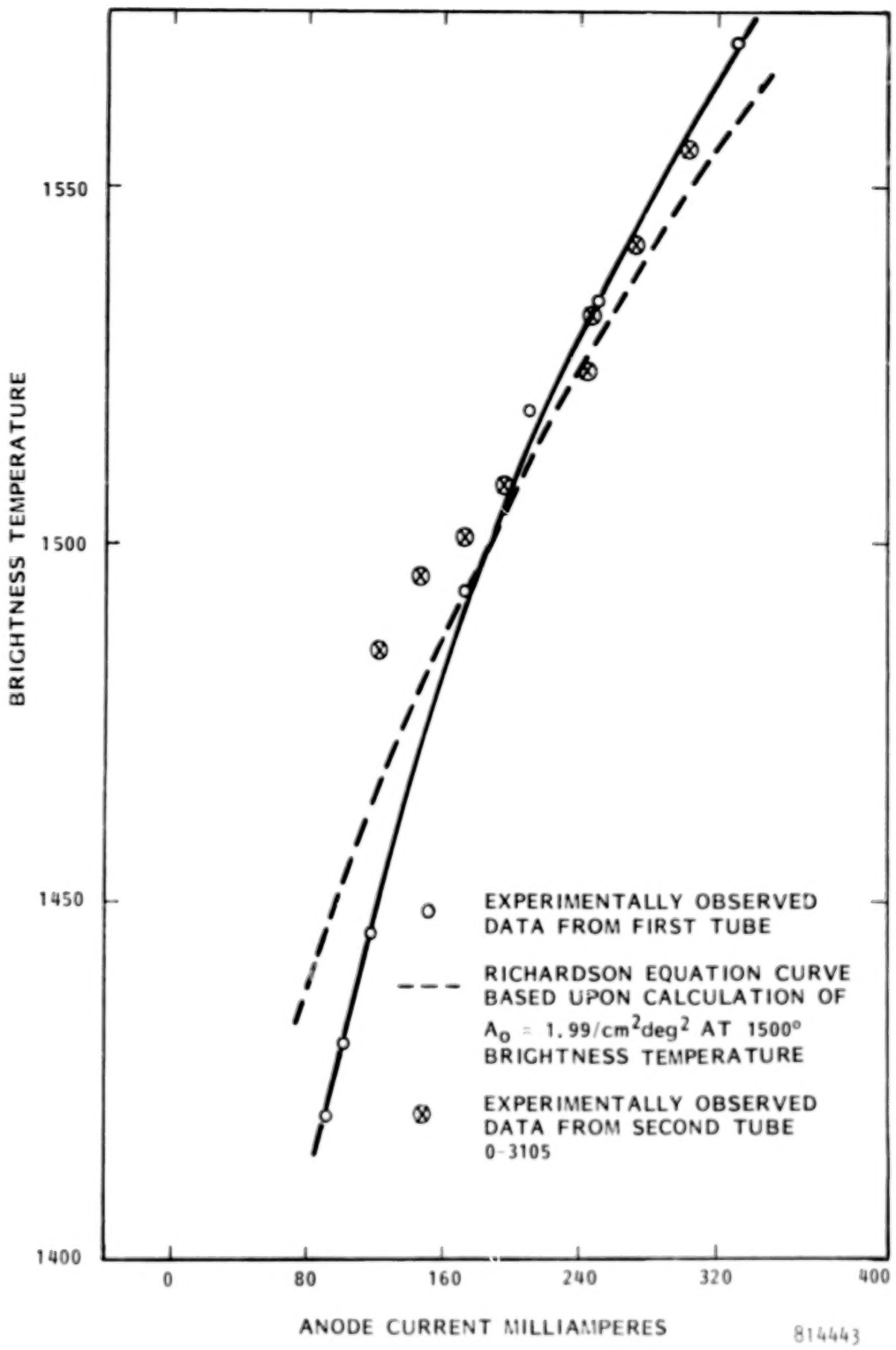

Figure 6-10. Experimentally Observed and Theoretically Predicted Relationship Between Cathode Temperature and Anode Current for Two Magnetrons with Optical Window.

values were selected and are inserted into the report as Figure 6-11. It is seen for values of anode current that ranged from 125 to 300 milliamperes there was no significant change in the appearance of the spectra. In these pictures only 42 dB rather than 66 dB of inserted notch filtering was used.

The third set of data included as Figure 6-12 was for the appearance of the spectra as a function of the positioning of the movable short in the circuit attached to the cathode. The position of the movable short for which resonance occurs is 7.45 cm. Resonance is indicated by maximum power coupled to the external circuit. The spectrum at resonance is shown in Figure 6-12a. As the short is moved by only 0.05 cm the spectrum changes to that shown in Figure 6-12b, the coupled power from the cathode has decreased by a factor of three, and the operating efficiency of the tube is at a maximum. Off resonance at a position of 7.9 cm the output spectra appears as in Figure 6-12c.

To obtain significantly different spectra with 42 dB of notch filter attenuation of the carrier it was necessary to apply 15 watts of external heater power to the filament. The three photographs were selected from sixteen photographs which indicated a rapdily changing picture in the region of resonance. Visual temperature readings of the filament were made and these indicated that the filament temperature changed by perhaps as much as 10^{o} at or near the resonance condition. This is a relatively small amount and its significance is not known.

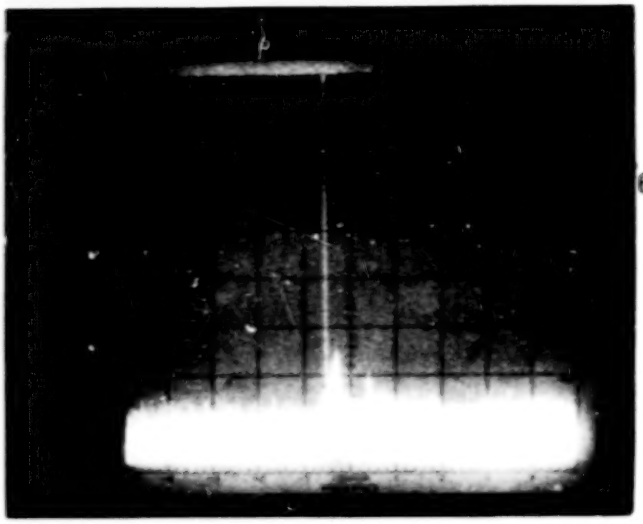

6-11 (a) External Filament Power = 0
Anode Current = 125 mA
Anode Voltage = 4150 Volts
Notch Filter = 42 dB
Total Frequency Sweep = 500 MHz

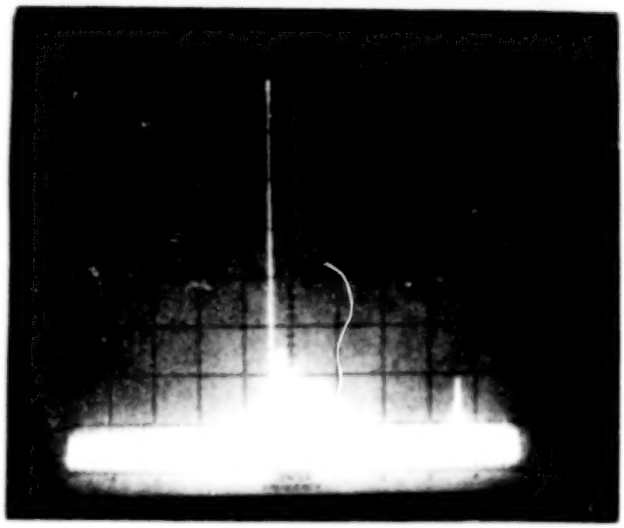

6-11 (b) External Filament Power = 0
Anode Current = 200 mA
Anode Voltage = 4121
Notch Filter = 42 dB
Total Frequency Sweep = 500 MHz

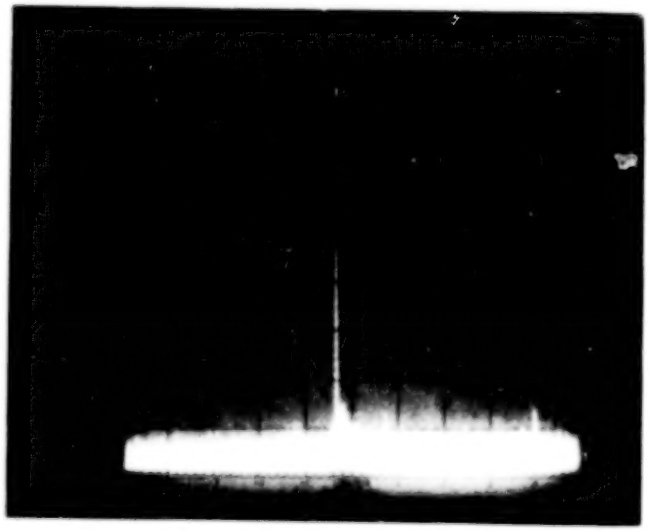

6-11 (c) External Filament Power = 0
Anode Current = 300 mA
Anode Voltage = 4121
Notch Filter = 42 dB
Total Frequency Sweep = 500 MHz

Figure 6-11. Spectra as a Function of Anode Current

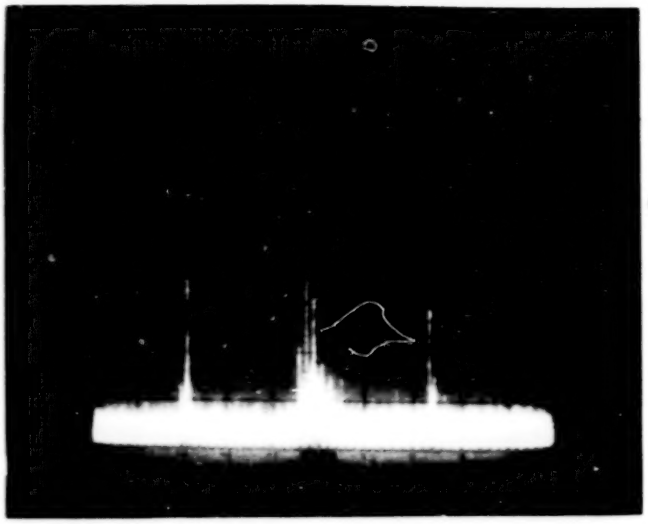

6-12 (a) External Filament Power = 15 W
Anode Current = 250 mA
Anode Voltage = 3698 Volts
Notch Filter = 42 dB
Movable Short at the Resonance Position of 7.45 cm
Total Frequency Sweep = 500 MHz
Cathode Circuit Power

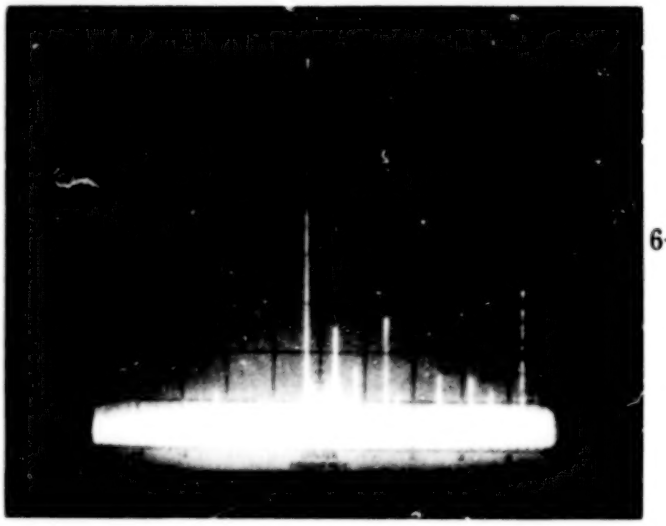

6-12 (b) Same as 12 (a) but with Movable Short at 7.50 cm

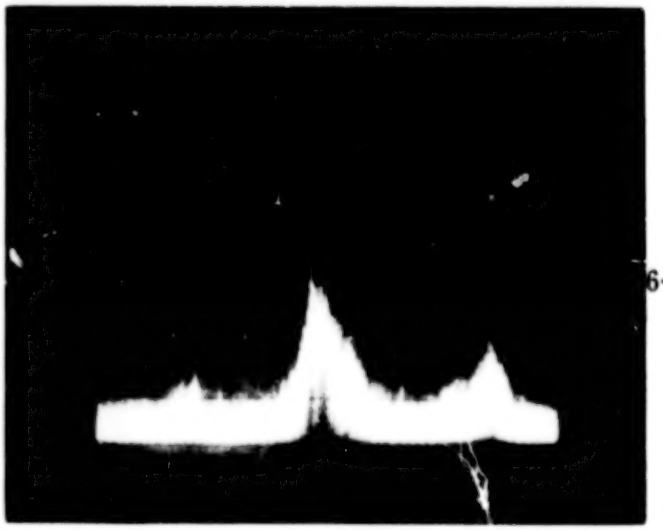

6-12 (c) Same as 12 (a) but with Movable Short at 7.9 cm.

Figure 6-12. Spectrum Appearance as Function of Position of Movable Short in Circuitry Attached to Cathode.

7.0 DESIGN OF THE SPS MAGNETRON

7.1 Introduction

This section will be concerned with the design of the magnetron for the SPS, including the contributions of any supporting technology investigations that have been carried out under this contract. These include the magnetic circuit and pyrographite radiator studies. The final objective of the effort is to project the expected characteristics that the magnetron designed for the SPS would have.

An interesting but complicating and difficult aspect of the magnetron design for the SPS is that within its packaged envelope it must provide for a relatively large number of functions. It must have (1) a microwave input and output port-in the magnetron directional amplifier these are the same; (2) permanent magnets to provide the residual magnetic field; (3) buck-boost coils within the total magnetic circuit for the amplitude tracking function; (4) means for passively radiating any heat resulting from any inefficiency in the device. A recent conceptual development that adds to the complexity of the magnetron design is that the best arrangement for making the phase of the microwave output from the magnetron directional amplifier track the reference phase may be to change the free-running frequency of the magnetron by means of a fast-acting friction-free displacement tuner actuated by the phase control feedback loop. This is because the phase shift through the magnetron directional amplifier is proportional to the difference between the free-running frequency of the magnetron and the frequency of the drive signal as discussed in Appendix A. The advantage of this arrangement is that the operation of the magnetron directional amplifier is no longer restricted to a tradeoff between gain and the range of current over which the magnetron can be operated. In effect, the concept enables the tube to be operated at any value of current or voltage that is within the capabilities of the heat removal system. In addition the arrangement also avoids the deficiencies of many other forms of phase shifters.

After a considerable effort it has been found possible to combine all of these functions into one packaged envelope. The design appears to be a reasonable one and all of the functions except that of passive heat radiation by means of the pyrographite radiator and the tuner to control the phase tracking have been tested out. The keys to the solution of this packaging problem were (1) revert back to operating the cathode above ground, and (2) operate the magnetic circuit at ground potential, made possible by a thin ceramic placed between the large end shield and the samarium cobalt magnet. The general approach to the design of the package is shown in Figure 7-1.

The design of the projected magnetron for the SPS bears a close relationship to two other crossed-field tube designs and is the result of experience with them. One of these, of course, is the microwave oven magnetron which has been used to investigate noise in the CW crossed-field device with considerable success, as discussed in section 6.6. It has also served as a workhorse for the investigation of the more general characteristics of the magnetron directional amplifiers[1], indeed the microwave oven magnetron could be used in its present form for an earth-based phased array for microwave power transmission. The SPS magnetron design is essentially a power and voltage scaled version of the microwave oven magnetron.

The other experience of importance is that gained in the design, construction and testing of an amplitron as the first phase of an intended amplitron development for the SPS.[2] This experience is important because of the close similarity of the magnetron and amplitron in both mechanical construction and sealing.

Measurements that have been made on the operating temperature of the cathode in the microwave oven magnetron as discussed in section 6.1.5 have also been the basis for predicting very long life in the SPS magnetron providing the emission current density from the cathode is scaled down to a value which will permit operation of the filament at a slightly lower temperature than in the microwave oven magnetron. After the scale up in power and voltage for the SPS magnetron is taken into consideration for the SPS tube, the dimensions of the cathode to provide this emission

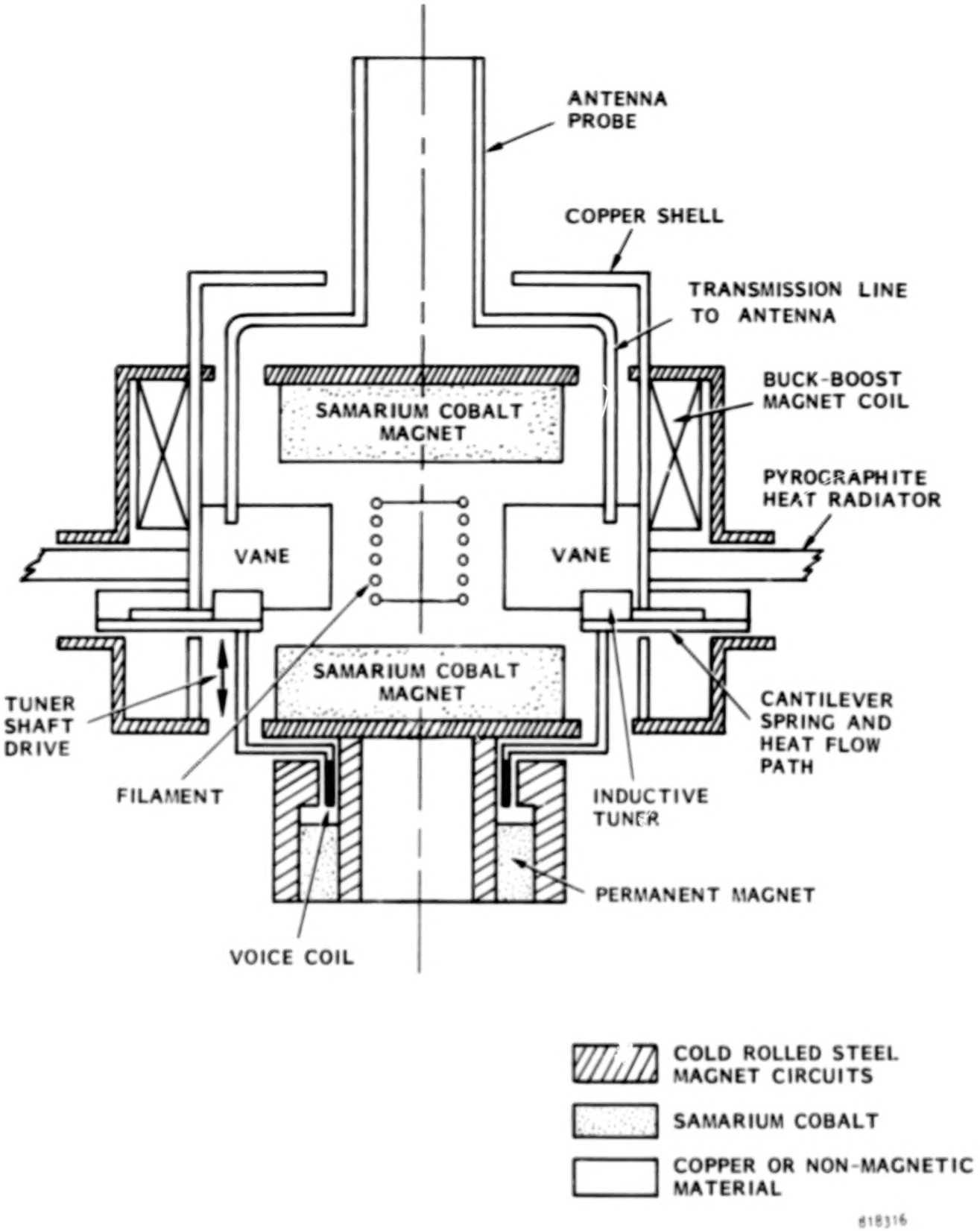

Figure 7-1. Cross Section of Magnetron Design Showing Permanent Magnets, Buck-Boost Coils for Amplitude Control, and "Voice Coil" Driven Tuner for Phase Control. Details of Support Filament are not shown.

current density are projected to be nearly the same as those for the SPS amplitron design. This appears to be a development of coincidental nature, but nevertheless, one of interest and significance. For example, low noise was observed during the operationg of the amplitron at anode current levels of only 84 milliamperes while the projected operating current value for the scaled SPS magnetron is 235 milliamperes. The low noise operation was also at 10 kilovolts or about 2.5 times the voltage level at which quiet operation has been observed in the microwave oven magnetron. Of even greater interest was the fact that external heater power was being applied during this quiet operation, raising the question of why it is considered impossible to obtain quiet operation from the microwave oven magnetron with the application of external heater power.

There were other successes with the amplitron. Among them was the demonstration that the use of pole pieces that were operated at cathode potential resulted in very low leakage current and the establishment of normal tube efficiency at very low values of anode current. The feature of pole pieces operated at cathode potential or the equivalent is therefore one that should be used in the SPS magnetron design. An equivalent arrangement in Figure 7-1 that has not yet been detailed would be a large end shield operating at cathode potential and separated from the pole piece by a disc ceramic.

An important development that has grown out of the Raytheon effort with JPL on the slotted waveguide radiator and its integration with the magnetron directional amplifier into the microwave radiating unit is the quantization of the physical size of the pyrographite radiator. This radiator, together with the operating efficiency of the tube, determines the microwave power rating of the tube and therefore many of its physical characteristics. The expected microwave output at 85% efficiency is 3.2 kilowatts while at 90% efficiency it is 5.0 kilowatts.

The need to avoid the forbidding complexities of large scale DC to DC voltage transformation while holding the I^2r losses and mass of the busses in the solar photovoltaic arrays to an acceptable value forces a high operating voltage upon the microwave generator. It is a well recognized fact, however, that difficulty with arcs within the microwave generator increases dramatically with increased voltage. A safe

upper limit on the SPS magnetron is believed to be about 20 kilovolts. This value of voltage results in bus electrical loss and mass that should be acceptable for the photovoltaic array if the transmitting antenna is placed at the center of the array as originally proposed.[3] Moreover, there is the possibility that the two halves of the transmitting antenna can be run in series which would make it possible to operate the busses in the photovoltaic array at 40 kilovolts and to reduce the bussing losses by a factor of four.

This choice of 20 kilovolts as the operating voltage for the magnetron is desirable in the context that it reduces the amount of anode current that is required for a given level of microwave power output. It is therefore possible to obtain much longer life from the same physical size cathode. These operating parameters and long cathode life are consistent with the physical design of the SPS amplitron, a fact that encourages the use of approximately the same physical dimensions of cathode and anode in the SPS magnetron design.

In the following material in this section we will first review the studies that were made on the pyrographite radiator and the magnetic circuit for the SPS magnetron. Then the magnetron scaling and design formulae will be introduced and dimensions established for three different designs. One of these will then be selected. For the selected design an estimate will be made of the mass of the tube. Finally, the general characteristics of the magnetron will be projected as called for by the work statement.

7.2 Study of Pyrographite Heat Radiator Design and Its Manufacture and Cost

7.2.1 Heat Radiator Design

The earliest studies on the microwave generator tube for the SPS quickly zeroed in on pyrolytic graphite as the preferred material for a passive radiator.[4] In the range of 100° to 300°C the annealed or heat-treated pyrolytic graphite has

a heat conductivity twice that of copper as shown in Figure 7-2 and it has a density of only 2.0 as contrasted to 8.9 for copper. Further, it has a natural emissivity of 0.92 and a negligible vapor pressure at the intended operating temperature. It was also assumed that for purposes of data computation the radiator was radiating into deep space with a temperature of 0^{o} Kelvin. The implications of this assumption will be discussed after the presentation of the computed data.

One of the factors that greatly simplifies the study of the pyrographite heat radiator design is the relationship of its size to that of the slotted waveguide radiator. The dimension of the heat radiator has to match the dimensions of the slotted waveguide radiator associated with it in the microwave radiating unit. The dimensions of the slotted waveguide radiator are quantized. It is assumed that each waveguide stick must have an even number of slots in it, and each set of slots is approximately 18.4 centimeters long. The dimensions of the area occupied by the magnetron directional amplifier and its associated waveguide section could therefore be 18.4 cm., 36.8 cm., 55.2 cm., 73.6 cm., etc. These dimensions are also associated with the number of waveguide sticks in the array of 2, 4, 6 and 8 respectively as suggested in Figure 7-2.

For the same temperature drop in the radiator from the center to outside edge the mass goes up as the fourth power of the diameter while the heat radiated goes up as the square. This relationship causes an unfavorable increase in the specific mass (mass per unit of heat radiated) of the magnetron and its radiator as the size of the radiator is increased. Also the cost of the pyrographite per unit of heat radiated would increase with the diameter as would the cost of transportation into orbit. While the 55.2 cm diameter would be unfavorable from this point of view the 18.4 dimension is probably much too small from the viewpoint of scaling down the mass and cost of the control system circuitry and from the viewpoint of design a magnetron that would operate with a kilowatt of power output at an anode voltage of 20 kilovolts. The magnetron design is therefore based on the dissipation capability of a pyrographite radiator 36.8 cm in diameter.

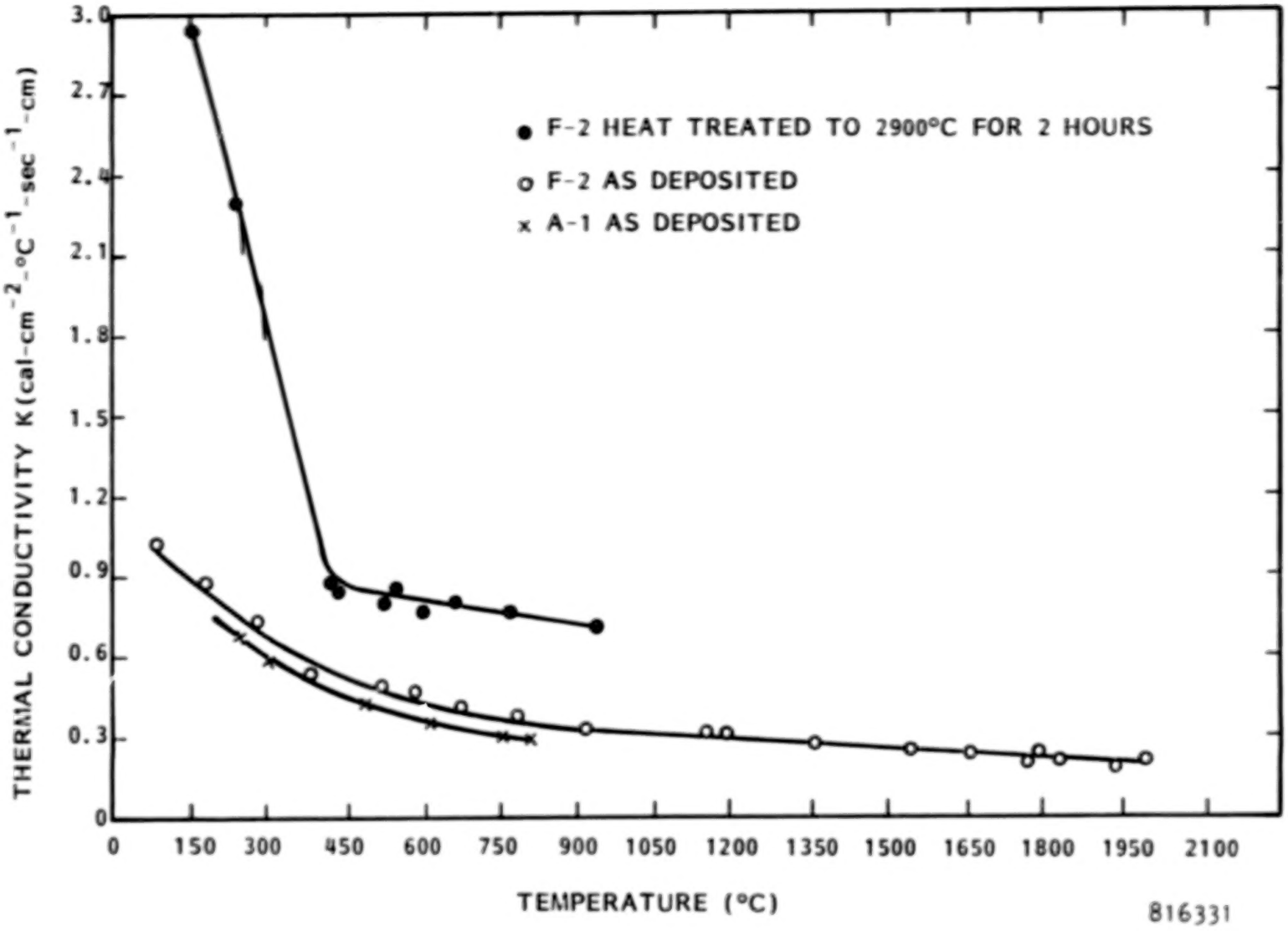

Figure 7-2. Thermal Conductivity of Pyrographite in the "a" Direction as a Function of Temperature.

Given the dimensions of Figure 7-3, an assumption of radiation from one side only, and an emissivity of 0.92, the method of determining the total heat radiated and the temperature drop from the center of the radiator to its outer edge follows: (1) divide the radiator into a large number of radial segments for computation purposes, (2) assume an average temperature for the outermost segment, (3) compute the heat radiated from the outermost segment, (4) compute the temperature drop associated with the radial flow of heat through the ring, (5) add this temperature drop to the radiating temperature of the outermost segment, (6) using the resulting temperature compute the heat radiated by the segment next to the outermost segment, (7) add this heat radiated to that radiated by the outermost segment, (8) using the resulting heat compute the temperature drop associated with its radial flow through the segment, (9) repeat the previous procedure for all segments. As the radius becomes less, the temperature will become greater until the maximum temperature is reached at the inside edge of the radiator. The temperature rise will obviously be a function of the amount of taper and also of the temperature itself as the conductivity varies with temperature, as shown in Figure 7-2. The total heat radiated will be the sum of the heat radiated by the individual segments.

To obtain the appropriate data, it is necessary to run a large number of these computations in which the temperature at the outer edge is varied and in which the degree of taper is varied. From a practical point of view, the outer edge of the radiating fin would have to have some thickness. In the calculations a thickness of 1/2 millimeter or 0.020 inch was used. The results of the computerized computations are shown in Figure 7-4.

Shown in Figure 7-4 are contours of a constant value of temperature at the inner radius, as this may be the limiting condition imposed upon operation. To illustrate the use of the curves, consider a decision to use a maximum temperature of 340°C. The curve shows that this will occur, for example, at a point of power dissipation of 400 watts and a thickness of the inner edge of 0.1 cm, or, as another example, 560 watts and a thickness of 0.35 cm. Shown also on Figure 7-4 is the

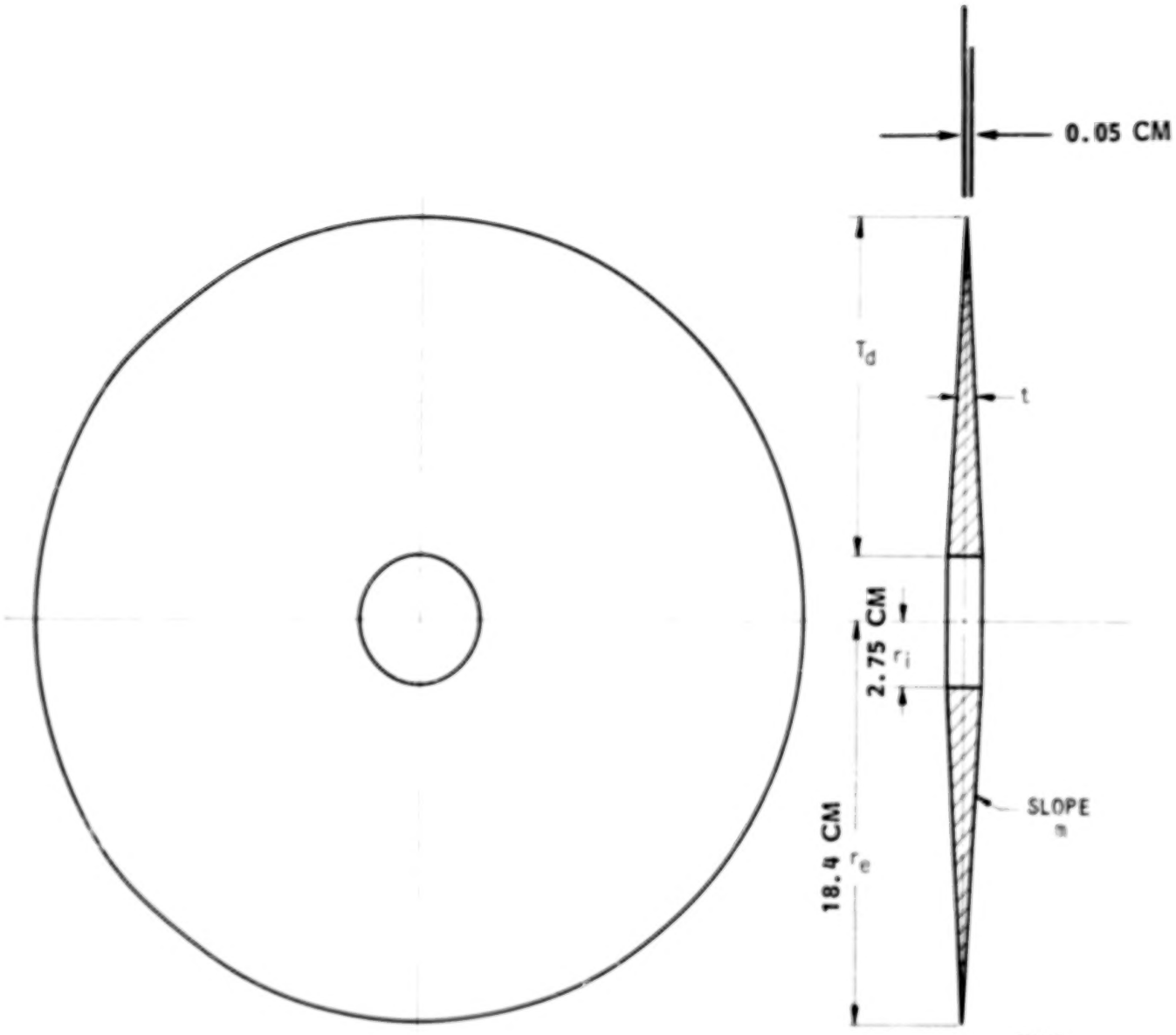

Figure 7-3. Drawing of the Shape of the Cooling Fin for the Microwave Generator. Heat Flows Radially from the Generator at Radius r_i, and is Radiated from the Top Surface. There Will Be a Temperature Drop T_d from r_e to r_i. Diameter of Radiator is Determined by Dimensions of the Slotted Waveguide Radiator.

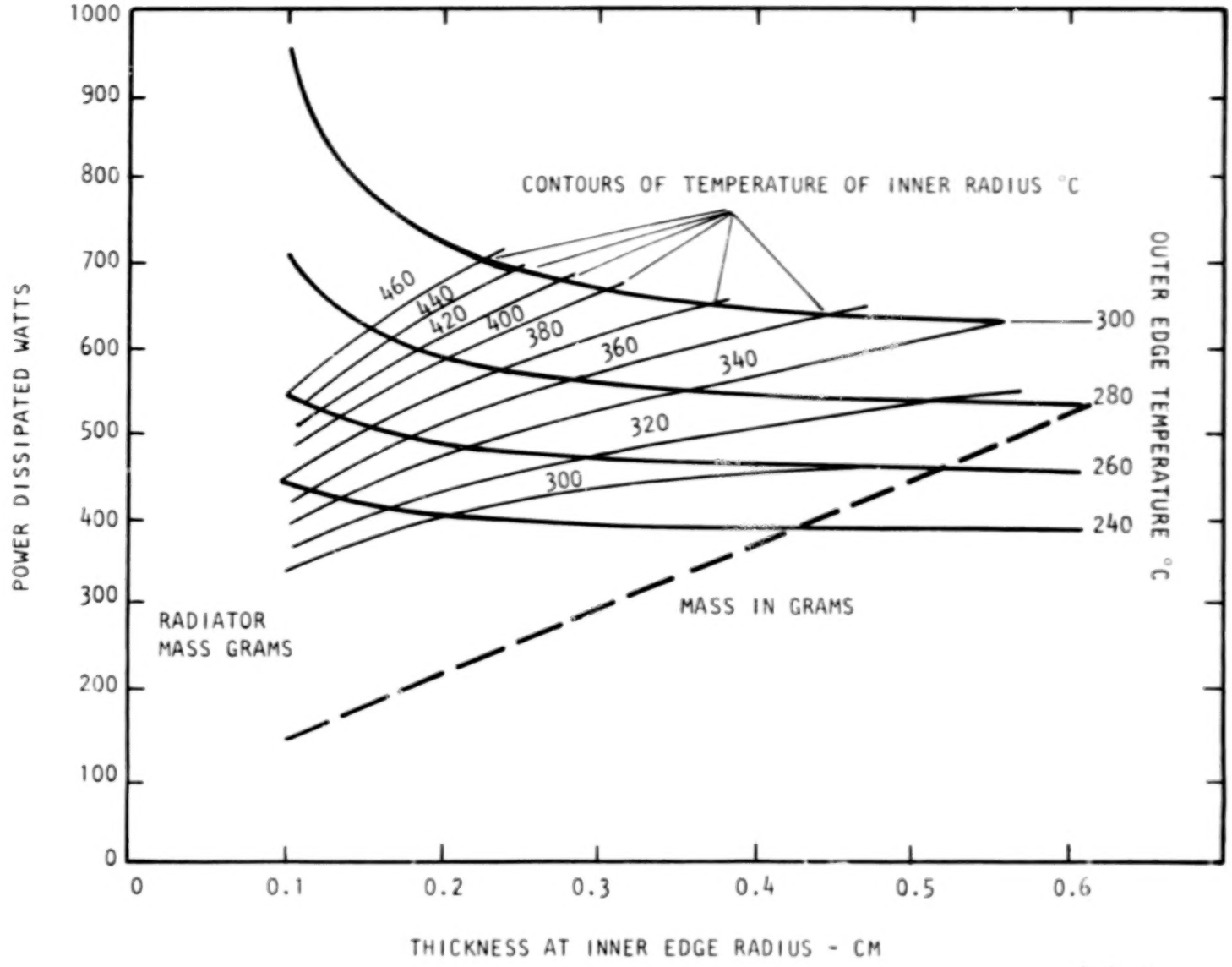

Figure 7-4. Information chart for selection of pyrographite radiator and determination of its mass. First, determine desired temperature at inner radius of radiator. Then select the desired value of power to be dissipated by the radiator and project this value horizontally until it intersects with the inner radius temperature curve. Vertical projection of this point determines both the thickness of the radiator at its inner edge and the mass of the radiator in grams. Temperature at edge of radiator may also be estimated.

relationship between the mass in grams of a radiator and the thickness at its inner radius. Thus, the mass of a radiator operating with an inner radius temperature of 340° that will dissipate 400 watts is 140 grams, while the mass of a radiator that will dissipate 560 watts is 335 grams or 2.39 as much. Thus, radiator mass goes up very rapidly with the dissipation requirements.

The design data arrived at by computer agrees remarkably well with the design data derived several years ago working with considerably cruder tools. Based on the previous approach a dissipation capability of 560 watts corresponded to a mass of 420 grams, whereas the new design data indicates 350 grams for the same 560 watts to be dissipated. However, the new data covers a much wider range of data and will be very useful in future design efforts.

As indicated previously, the data in Figure 7-4 was obtained with the assumption that the pyrographite radiator was radiating directly into deep space and the sun was not shining on it. If the sun were shining directly on it and the absorptance and emittance of the radiator assumed to be equal and independent of the wavelength of the incoming or outgoing radiation, then the heat that is conducted from the magnetron at a fixed temperature of the inner diameter of the radiator will be reduced. On the other hand, under these conditions a considerable amount of heat will be radiated from the slotted waveguide radiators which will be looking away from the sun. Also, the assumption was made that the radiators are round so that an appreciable amount of heat may be reflected from the heat insulation and radiated to space between the radiators. The net result of the tradeoff's between the suns influence to reduce the effective cooling of the tube while the other factors tend to increase it is to indicate that Figure 7-4 is probably close to what will be found in practice.

7.2.2 Bonding Pyrolytic Graphite to the Magnetron Anode

One of the anticipated problems in the use of pyrolytic graphite is bonding it to the magnetron anode. Fortunately a considerable amount of successful experience that appears to be directly applicable to the SPS application has been reported by Lloyd O. Lindquist and Richard Mah of Los Alamos Scientific Lab in report number LA-6928-MS (Informal Report) issued November 1977 and titled "Graphite-to-Metal Bonding Techniques".(5)

According to this report, very successful bonds can be made with thick walled graphite cylinders brazed to copper tubing. This is physically similar to the geometry of the pyrographite radiator brazed to the outside of the magnetron cylinder. The bonds were tested with a heat flux of 600 watts/cm^2 and the bonds successfully withstood 500 heat flux cycles at this flux density without failure. In the SPS applications the heat flux would be lower by a factor of about ten and the cycling would be considerably less severe.

The brazes were made in a conventional vacuum braze furnace. Two bonding alloys were used, Ti-Cu-Ni and Ti-Cu-Si. Both made good bonds and withstood the cycling test at the high flux densities reported above.

It is believed that the demonstration of these satisfactory bonds indicates that the pyrographite to copper bonding of the heat radiator to the magnetron anode should be a relatively straightforward development. However, there is a distinct difference in the geometry of the bond. In the bonds that Lindquist made, the thickness of the pyrographite was greater than the diameter of the copper tubing, while in the SPS case the thickness of the pyrographite radiator will be only a small fraction of the diameter of the magnetron anode.

7.2.3 The Manufacture of Pyrolytic Graphite and Its Fabrication into Radiators

It has long been recognized that an important element of the mass and cost of the satellite portion of the microwave power transmission system is the pyrographite cooling fin for the magnetron. It is imperative that the material be used because of its combination of many desirable properties. In particular, its low density and high heat conductivity makes its mass as a heat radiator far less than any other known material. This is very important in the SPS because of the high cost of transporting mass to synchronous orbit. In addition the material has a naturally high emissivity of 0.92 so that it does not need any surface treatment. Finally, its vapor pressure is negligible at the temperature at which it would be operated.

Pyrographite is a polycrystalline, vapor-deposited, form of carbon which is characterized by a strong anisotropy in its properties.[4] It is formed by passing a carbonaceous gas over a heated surface which is also carbon. In the "as deposited" condition the material has a high density, a high degree of preferred orientation, and is crystallographically similar to lamp black. Heating the material to temperatures above the deposition temperature brings about the process of graphitization which increases preferred orientation, layer order, crystallite size, and decreased microstrain. In the treated condition it is a relatively strong material and may have useful mechanical beam problems. Heat treating it for two or three hours at an elevated temperature provides the material with a heat conductivity about two times that of copper at 300°C as shown in Figure 7-2.

From a fabrication point of view the principal advantages of pyrographite is that the raw material, a carbonaceous gas, is abundant and relatively cheap. A major disadvantage, however, is the relatively expensive furnace in which it is made and the low deposition rate which is about six mils per hour. In addition, the material at present has a limited market and the national annual capacity is of the order of 20 to 30 tons, so that it is necessary to consider what is involved in increasing the capacity tonnage to that needed for the SPS.

To obtain a better perspective on the costs involved in using pyrographite in the SPS the author contacted two experts in the pyrographite area. One of these was Dr. James Pappis in the Raytheon organization who did much of the original work on pyrographite and who is actively engaged in using his substantial laboratory facilities for the pyrolytic deposition of other materials.[4] The other expert was Dr. Froberg of the Minerals, Pigments and Metals Division of the Pfizer Corp. in Easton, Pennsylvania. He is responsible for a manufacturing facility for pyrographite, as distinguished from a laboratory facility. A special trip to Easton to interview him was made by the author.

After interviewing these two people, the author concluded that an accurate costing of a manufacturing facility of the size needed for the SPS and the resulting unit cost of the radiators would require a substantial effort on the part of a qualified person. However, some ball park estimates can be made based upon the size of the furnace size used in the Raytheon laboratory facility. This is a good size furnace costing approximately $400,000 with automated controls.

Dr. Pappis estimated that material for approximately 260 pyrographite radiators of the size needed for the SPS magnetrons could be made in one 100 hour run in his furnance. It therefore would appear that after allowing for loading, heating up, cooling, and unloading one weeks time (168 hours) would be ample for a single run. This single furnace could then make material for 13,520 radiators per year. The approximate mass of the raw material would be 14,380 kilograms or approximately 15.8 tons. Assuming the use of 2,500,000 magnetrons in a single satellite (3 kilowatts of microwave power from each magnetron) 185 furnaces of the same size would be needed. At a cost of $400,000 per furnace a total investment cost in furnaces alone would be $74,000,000.

Using such equipment, a rough estimate of $20.00 was made for the pyrographite blank from which the radiator would be made. To this would be added the cost of machining and the heat treating costs which were roughly estimated at $20.00. The total cost would then be $40.00. In the opinion of the author this represents an upper limit because all of the cost cutting factors that take place when large production occurs were not taken into account.

Dr. Frobergs' estimates for facilities was considerably higher than that estimated above. He uses a different method of heating the furnace. He uses inductive heating which may make the equipment considerably more expensive. This illustrates again, the need for a more definitive study.

One of the possible added interesting applications of pyrographite in the SPS magnetron design is as a cantilever spring member to support the proposed mechanical tuner. The mechanical properties are interesting, a Young's modulus that is quite low, about 2 x 10^6, and a tensile strength that is about 20 x 10^6 lbs/sq. inch. It would therefore appear practical to make cantilever springs to support the tuner with pyrographite that would have the distinct advantage over copper or other metals of relatively short length, large cross section, and a higher coefficient of heat conduction.

7.3 Magnetic Circuit Study

The purpose of the magnetic circuit study was to narrow down the range of expected mass of the magnetic circuit for the SPS tube by analytical and experimental techniques. The analytical approach makes use of a special computer program at Raytheon that provides quantitative results and plots flux and equipotential lines. The program has been developed for general magnetic circuit problems and has been found to give accurate results for magnetic circuits for electron tubes. The program provides analytical results only. The experimental approach made use of available samarium cobalt magnets, specially machined cold-rolled steel parts for the magnetic circuits, and magnetic field measuring equipment.

The design of the magnetic circuit, the prediction of magnetic fields by computer program, and experimental measurements of these fields were based upon the selection of the magnetron interaction area to consist of an anode 1 cm long, 2 cm in diameter, a cathode 1.25 cm in diameter, and a separation of pole pieces of 1.75 cm. The magnetic circuit is shown in cross section in Figure 7-5. These dimensions are substantially the same dimensions as those selected in the final design which is described in section 7.4.

The permanent magnets that were used experimentally were solid discs of samarium cobalt, 3.3 cm in diameter and 0.75 cm thick. The experimentally measured fields were 2575 gauss on the axis of the tube and 2240 gauss at the center of the cathode-anode interaction area. The computed values arrived at by assuming

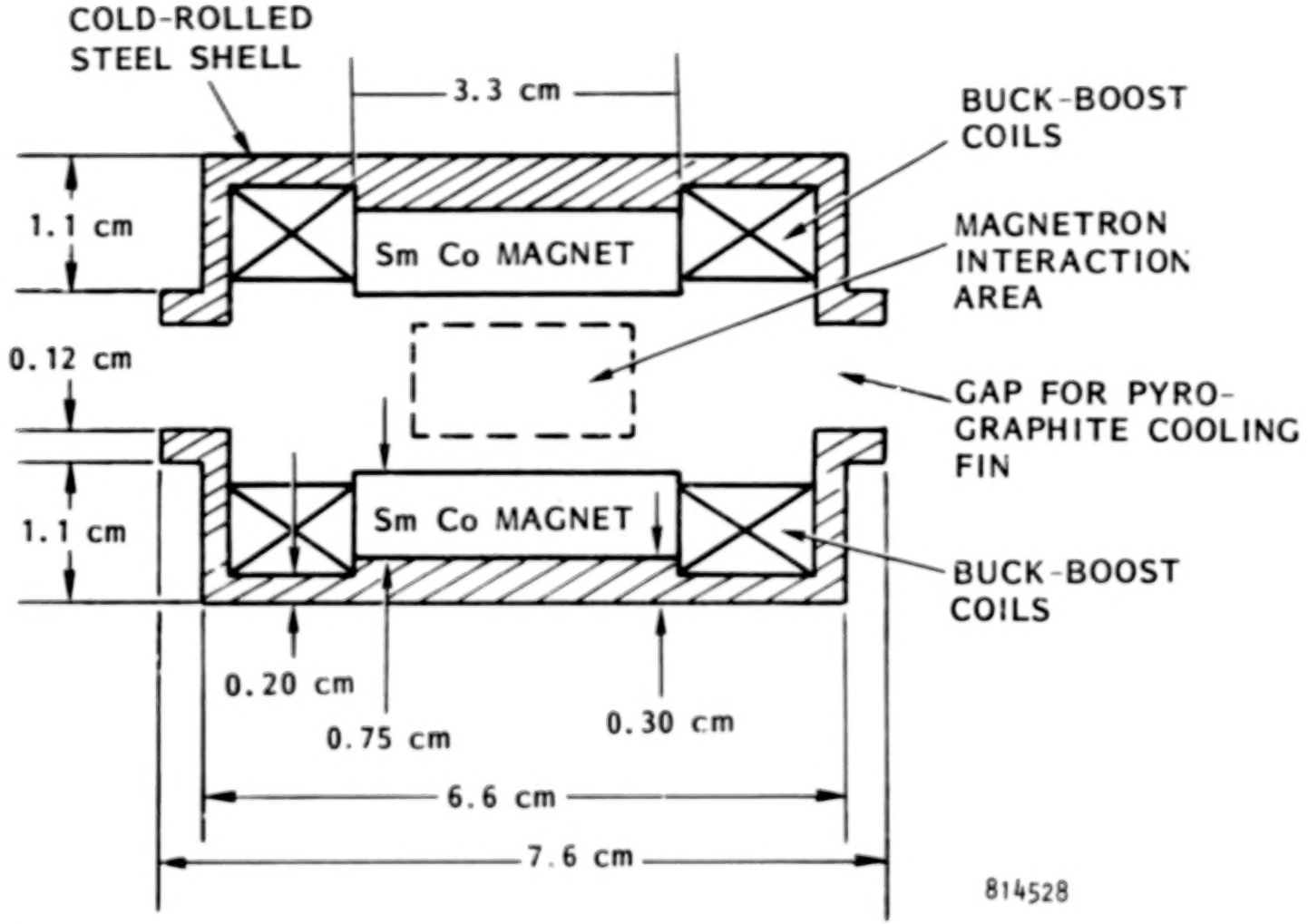

Figure 7-5. Magnetic Circuit Used for Computer Simulation and Experimental Measurement of Field in Interaction Area by Probe. The scale of the Illustration is 40% Oversize.

that the energy product of the samarium cobalt material was 14,000,000 were 2393 on the axis of the tube and 2070 at the center of the cathode-anode interaction area.

The value of 2070 is consistent with a value of 2700 to be obtained from samarium cobalt with an energy product of 24,000,000 which has been achieved in some laboratories. It is believed that such a material will be available by the time the SPS development is started. As of June 1980 magnets with an energy product of 22,000,000 were being contracted for commercially.

The value of 2700 gauss in the interaction area is consistent with the final design selection of a B/B_0 ratio of 7 as discussed in section 7.4. As shown in Section 7.4 the increase in theoretical conversion efficiency is very little once a ratio of B/B_0 of 7 has been reached. Once constructed, however, the tube can be evaluated for higher ratios than this by increasing the magnetic field beyond the design value.

The measured mass of the experimental circuit as shown is 266 grams, inclusive of the permanent magnet weight. The weight of the buck-boost coil was not included.

The magnetic circuit shown in Figure 7-5 that was analyzed and experimentally confirmed was the result of substantial improvements over the initial design. The initial design made use of a cooled-rolled steel pole piece of appreciable thickness and a relatively large hole in the magnet and pole piece. It is probable that the final design will have a small hole in the middle of the permanent magnet to make contact to the filament from an external lead. It should not impact the amplitude of the magnetic field appreciably.

For documentation purposes, Figure 7-6 shows the field plots that were obtained from the computer program.

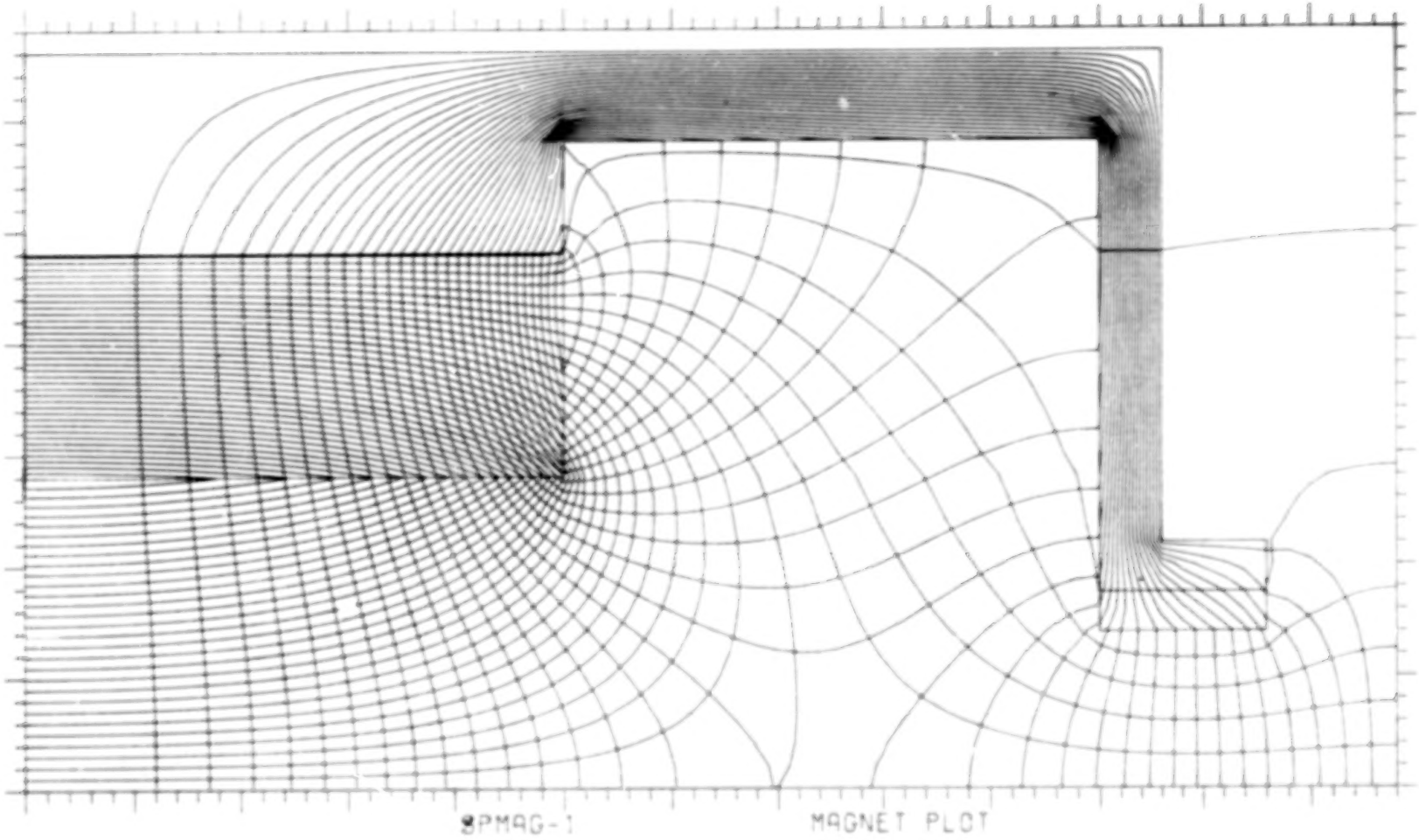

Figure 7-6. Computer Field Plots for Magnetic Circuit.

7.4 Design of Interaction Area of Magnetron

The relationship between applied magnetic field and operating voltage that has been established for the magnetron is based upon the physical dimensions of the anode and cathode and the number of space charge spokes that are established in the interaction area.(6)

The voltage at which current is first initiated in the magnetron (or Amplitron) is called the Hartree Voltage, V_H. The Hartree Voltage is given by:

$$V_H = V_o \left(\frac{2B}{B_o} - 1\right) \tag{1}$$

where B is the applied magnetic field in the interaction area and V_o and B_o are constants defined as follows:

$$B_o = \frac{21{,}200}{n\lambda\left(1 - \frac{r_c^2}{r_a^2}\right)} \quad \text{gauss} \tag{2}$$

$$V_o = 253{,}000 \left(\frac{2\pi\ r_a}{n\lambda}\right)^2 \text{ volts} \tag{3}$$

where:

n = number of spokes of space charge

λ = wavelength of operation in centimeters

r_c = radius of cathode in centimeters

r_a = radius of anode in centimeters

In general, the Hartree Voltage V_H is not the same as the magnetron operating voltage but in CW magnetrons the difference is very small and the V_H value can be assumed to be the operating voltage.

Another formula of importance is the generally used relationship between the cathode to anode diameter ratio and the number of spokes of space charge. This is:

$$r_c/r_a = \frac{n/2 - 1}{n/2 + 1} \qquad (4)$$

The theoretical DC to microwave conversion efficiency is also a function of the B/B_o ratio and is given by:

$$\text{Efficiency} = \frac{2B/B_o - 2}{2B/B_o - 1}$$

This expression suggests operating at a high B/B_o ratio for high efficiency and indeed this is necessary in the SPS application. However, as the below tabulation indicates, the improvement in efficiency is slight after a moderate value of B/B_o is reached.

Ratio	Theoretical DC to Microwave Conversion Efficiency	Incremental Increase
3	80%	
4	85.7%	5.7%
5	88.8%	3.1%
6	90.9%	2.1%
7	92.3%	1.4%
8	93.3%	1.0%
9	94.1%	0.8%
10	94.7%	0.6%

Although there is a slight improvement in the conversion efficiency for values of B/B_0 in excess of seven the efficiency increase may be offset by some drop in circuit efficiency since the microwave circuits will be smaller in volume for a given anode voltage. It is also probable that efficiency peaking techniques such as vane contouring will have more impact upon conversion efficiency that an increase in B/B_0.

As a result of these conditions we will assume a value of B/B_0 of 7 in the design of an SPS magnetron.

Having assumed a value of 7 for B/B_0 as well as an imposed anode voltage requirement of 20 kilovolts, it is possible to use equations 1, 2, 3 and 4 to determine the dimensions of the anode interaction area. It is instructive to consider several that are differentiated by the number of spokes of space charge. Table 7-1 gives the anode and cathode dimensions as a function of 6, 7 and 8 space charge spokes.

A selection of a design with 12 vanes or 6 space charge spokes was made. Although the selection is not irrevocable and can be changed if there are new inputs, the 12 vane design has good justification. In the first place, the prior use of a larger number of vanes in the LeRC design was based upon the anticipation of a higher power tube than the 3 to 5 kilowatts for the current SPS design that is quantized by the size of the pyrographite radiator that matches the projection area of the slotted waveguide array. The slightly higher unloaded Q of the 12 vane tube will provide it with a higher circuit efficiency. The physical size will be somewhat smaller and the mass a little less. The smaller size of the cathode will require less backbombardment power to heat it and therefore the overall efficiency will be a little higher. Yet the cathode area as analyzed in section 7.5 should be adequate for very long life.

TABLE 7-1

Cathode and Anode Diameter Dimensions for Magnetrons Operating at 20 Kilovolts and a B/B_0 Ratio of 7 with Different Number of Space Charge Spokes.

B/B_0	No. of Space Charge Spokes	Anode Voltage kV	Cathode Diameter		Anode Diameter		No. of Vanes	B_0 Gauss	B Gauss
			Inches	cm	Inches	cm			
7	6	20	0.358	0.910	0.716	1.820	12	384	2688
7	7	20	0.464	1.180	0.872	2.126	14	358	2506
7	8	20	0.574	1.458	0.956	2.430	16	338	2366

7.5 Design of Cathode for Long Life

Very long life is one of the requirements imposed upon the microwave generator in the SPS. Fortunately, the carburized thoriated tungsten cathode is capable of very long life if it is run in a good vacuum at emission current densities that permit low operating temperature of the cathode. In a recent investigation sponsored by NASA[1] and confirmed in section 6.1.5 of this report, it was discovered that the operating temperature of the carburized thoriated tungsten cathode in the microwave oven magnetron was apparently controlled by an electron backbombardment mechanism that allowed the cathode to operate at the minimum temperature to provide the required anode current. The cathode temperature varied with the anode current in a manner predicted by the Richardson-Dushman equation for temperature limited emission as shown in Figure 6-11 of that report.

The Richardson-Dushman equation gives the relationship between saturated thermal emission current and the absolute temperature of the cathode as follows:

$$J_S = A_O T^2 e^{-\frac{\phi}{kT}}, \text{ where}$$

J_S = Saturated thermal emission current density in A/cm^2

A_O = Dushman's constant; the theoretical value is $120.4/cm^2\ deg^2$

T = Temperature in degrees Kelvin

e = 2.71828

ϕ = True work function in electron volts

κ = Boltzmann's constant = $8.6 \times 10^{-5} eV/^oK$

The experimentally observed value of A_O is always much less and the effective area of the emitting surface of the filament is not accurately known. If it is assumed that the emitting area is 1 square cm in the microwave oven magnetron then a value for A_O of 1.99 is obtained.

What should be the life expectancy of the cathode in the SPS magnetron design if the tube operates at 3.5 kW of microwave power output, at an efficiency of 85% and at an anode voltage of 20 kilovolts so that it requires an anode current of 235 milliamperes? The emitting area of the cathode in the SPS is 1.82 times that of the microwave oven magnetron, based upon the ratio of cathode diameters.

The comparable emission current density in the SPS magnetron is therefore 129 milliamperes per square cm. Using the value of A_o = 1.99/cm^2/deg^2 and a work function ϕ of 2.85 electron volts, we obtain an operating temperature of 1862^o Kelvin. This is a low operating temperature for carburized thoriated tungsten but not much less than the 1900^o and excellent life experience described in reference 1.

Life also depends upon the amount of carburized material or upon the depth of carburization.[7] If we assume 0.030 inch diameter tungsten wire that is 40% carburized the design charts in references 1 or 8 indicate that at a temperature of 1860^o Kelvin life should be in excess of sixty (60) years.

It may therefore be concluded that the proposed design has ample cathode emitting area to provide very long life under the highly controlled operating conditions in the SPS.

7.6 Mechanical Design of the Magnetron

The schematic of the mechanical features of the proposed magnetron design are shown in Figure 7-1. The design as shown is a composite of some design features that have been carefully analyzed and experimentally verified while other design features are more conceptual in nature. Those design features of the former class are (1) the basic magnetron itself, involving cathode and anode dimensions and number of vanes, (2) the pyrographite radiator design, (3) the magnetic circuit involving the permanent magnet alone. Good estimates of the mass represented by these design features can be made.

The "voice coil" tuning arrangement, on the other hand, is a concept recently introduced to remove the restrictions imposed upon the useful power range over which the magnetron directional amplifier could be operated. While the inductive tuner is a well established method for mechanically tuning magnetrons and the "voice coil" arrangement is a standard one for moving audio speaker diaphragms, the proposed combination has not been designed and analyzed from a control circuit point of view. Its mass is not expected to be large and probably would be less than that for a phase shifting device in the circuitry elsewhere.

The arrangement shown for the buck-boost coil represents a temporary element of confusion. Although the principle of the buck-boost coil has been amply demonstrated, (Section 2.0) and its low power consumption for a given change in magnetic field and corresponding operating voltage of the microwave oven magnetrons has been well documented (see Figure 2-12), it has not been evaluated as a buck and boost aid to the magnetic field and circuit provided by the design shown in Figure 7-1. Its incorporation into the final SPS magnetron design could change the physical placement of the samarium cobalt magnets. The obvious procedure to resolve this confusion is to use the magnetic-circuit computer program after incorporating both permanent magnets and the buck-boost coil into the model. Successive changes could then be made to optimize the magnetic circuit from a mass point of view. Unfortunately the realization of the possibility of the inapplicability of the data from Figure 2-12 has come too late in the program to resolve the confusion.

In the layout of Figure 1, connections to the filament, ceramic support of the samarium cobalt magnets and end shields have not been shown. These are important sub-elements of design but their incorporation into the figure obscures the principle features of the design. The straps in the microwave anode circuit have also been omitted. The construction features that are needed, however, to incorporate these mechanical design details, have largely been worked out in the amplitron development project (2).

One of the features of the design that should effect a considerable improvement in circuit efficiency over the conventional microwave oven magnetron is the use of an antenna probe output which is symmetrically fed by several legs attached to the anode structure rather than just the one. The single leg approach, used in the microwave oven magnetron because of its low cost, has the disadvantage that all of the microwave power that is generated has to flow along the straps to be transmitted to the antenna, and the transmission loss through the straps is not negligible. It is of interest that the proposed design arrangement is the same that was originally used for microwave oven magnetrons; so in a sense it is a proven technology.

The new output arrangement may also improve the existing field pattern in the interaction area which is known to depart from the ideal. In this regard it is of interest that the field pattern in the early microwave oven magnetrons which used the symmetrical output was considerably better than in the existing microwave oven magnetron. A poor field pattern is known to be often associated with a less than ideal efficiency in the magnetron.

Table 7-2 gives the estimated mass for the various functions that the magnetron package provides. In terms of percentage of the total mass, the purely power generation function represents 39.6%, the cooling function represents 34.3% while the amplitude and power conditioning represent 19.6% and the phase control function represents 6.2%. The power generation function is broken down into its various components with the magnetic field circuit being the largest. The specific mass for the various functions in terms of the ratio of kilograms of mass to kilowatts of power is also provided. It will be noted that these figures are very dependent upon the overall efficiency achieved by the device.

7.7 Projection of the Characteristics of the Magnetron Package

One of the tasks of the work statement was to project the characteristics of the magnetron. As the project evolved in the context of the descending hierarchies of the designs of the subarray, the power module, the microwave radiating unit, the

TABLE 7-2

ESTIMATED MASS OF PACKAGED MAGNETRON INCLUDING COOLING, AMPLITUDE CONTROL, PHASE CONTROL AND POWER CONDITIONING FUNCTION

Function	Item	Mass	% of Total	Accuracy Estimate of Final Weight	How Estimated	Total Mass of Function	% of Total	KG/KW		Power Output	
								85%	90%	85%	90%
Power Generation	Antenna Probe	11	1.0	±20	Computed	404	39.6	0.13	0.08	3.2	5.0
	Copper Vanes	44	4.3	± 5	Computed					3.2	5.0
	Copper Shell	45	4.4	±20	Computed					3.2	5.0
	Ceramics	30	2.9	±10	Measured					3.2	5.0
	Filament	8	0.8	±10	Measured					3.2	5.0
	Magnetic Circuit Including Sm Co Magnets	266	26.1	±10	Measured					3.2	5.0
Phase Control	Voice Coil & Inductive Tuner	64	6.2	±30	Computed	64	6.2	0.02	0.01	3.2	5.0
Amplitude Control Power Conditioning	Buck-Boost Coil	200	19.6	-50 +100	Roughly	200	19.6	0.06	0.04	3.2	5.0
Cooling	Pyrographite Radiator	350	34.3	±10	Computed	350	34.3	0.11	0.07	3.2	5.0
All Functions		1018	100%			1018	100%	0.32	0.20	3.2	5.0

magnetron directional amplifier, and finally the magnetron itself, the magnetron became a package that included not only the power generation function and the heat dissipation function but also an arrangement in the form of a buck-boost coil to provide amplitude control and an arrangement in the form of a "voice coil" actuated magnetron tuner to provide phase control. For several reasons these additional functions are built into the tube package. It therefore follows that the "projection of the characteristics of the magnetron" should be expanded to the "projection of the characteristics of the magnetron package".

Table 7-3 gives the projection of the electrical characteristics of the magnetron package while Table 7-4 gives the "projection of the mechanical characteristics of the magnetron package".

TABLE 7-3

PROJECTED ELECTRICAL CHARACTERISTICS OF THE MAGNETRON PACKAGE

Item No.	Characteristics	Value	Determined By	Comments
1	Maximum Operating Anode Potential	20 kV	System Design Choice	
2	Minimum Anode Potential	15 kV	Limits of Amplitude Control	Depends Upon Magnetron Tuning for Phase Control
3	Operating Current	100 to 400 milliamperes	Dissipation Rating and Backheating of Cathode	Depends Upon Magnetron Tuning for Phase Control
4	Microwave Power Output at 85% Eff.	3.2 kW	0.56 kW Dissipation Rating and Efficiency	
5	Microwave Power Output at 90% Efficiency	5.0 kW	0.56 kW Dissipation and Efficiency	
6	Maximum Dissipation	0.56 kW	Radiator Dimensions 340°C Maximum Temp.	See Section 7.2 of this Report
7	Minimum Efficiency at 20 kV	85%	Present Design Capability	
8	Minimum Efficiency at 15 kV	82%	Reduced Because of Reduced B/B_o	See Section 7.4 of this Report
9	Maximum Efficiency at 20 kV	90%	Inherent Capability of Crossed Field Device	Much Development Needed
10	Maximum Efficiency at 15 kV	87%	Reduced Because of Reduced B/B_o	See Section 7.4 of this Report
11	Nominal Power Gain	20 dB		
12	Power Gain Range	0-30 dB	Selection of Phase Compensating Method	See Section 2.7 of this Report
13	Noise 30 MHz from Carrier	-120 DBC*/ MGZ	Unresolved Determination of Noise Sources and Their Elimination	See Section 6.0 of this Report

*DBC - decibels relative to carrier power.

TABLE 7-3

PROJECTED ELECTRICAL CHARACTERISTICS OF THE MAGNETRON PACKAGE (Continued)

Item No.	Characteristics	Value	Determined By	Comments
14	Added Phase Modulation Noise 50 KHz from Carrier	-114 DBC/	Measured	
15	Starting Filament Power	70 Watts	Filament Properties	See Section 3.0 of this Report
16	Operating Filament Power	0	Reduction of Noise	See Section 6.0 of this Report
17	Emission Life of Filament, 3.2 kW Output, 85% Eff.	>50 Years	3.2 kW Output, Anode Current Requirement	See Section 7.5 of this Report
18	Emission Life of Filament 5.0 kW Output, 90% Eff. Related to Life at 3.2 kW	0.8	Anode Current and Filament Temperature are Greater	See Section 7.5 of this Report
19	X-Ray Radiation	Negligible	Principle of Magnetron when Operating at Relatively Low Voltage	
20	Max. DC Power Consumed in Voice Coil	2 Watts	Tuner Design	See Section 7.6 of this Report
21	Max. DC Power Consumed by Buck-Boost Coil	20 Watts	Estimated	See Section 7.6 of this Report
22	Nominal Loaded Q of Magnetron	50	Needed High Circuit Efficiency	

TABLE OF CONTENTS

Section			Page	
0		EXECUTIVE SUMMARY	0-1	1/B2
1.0		INTRODUCTION	1-1	1/B14
	1.1	Background Information	1-4	1/C4
2.0		PHASE AND AMPLITUDE TRACKING DEVELOPMENT AND DEMONSTRATION	2-1	1/D3
	2.1	Introduction and Summary of Results	2-1	1/D3
	2.2	Phase and Amplitude Tracking Data	2-5	1/D9
	2.3	Description of the Demonstration Test Bed, the Integration of the Magnetron with the Buck-Boost Coil, and Other Supporting Data	2-13	1/E5
	2.3.1	Physical Description of the Demonstration Test Bed	2-13	1/E5
	2.3.2	Description of the Magnetron with Buck-Boost Coil; Buck-Boost Coil Characteristics	2-15	1/E7
	2.3.3	Description of the Sensors, Comparators, and Other Components in the Phase and Amplitude Feedback Control	2-18	1/E11
	2.4	Analysis of the Microwave Power Amplitude Control System	2-23	1/F2
	2.5	Analysis of the Microwave Power Phase Control System	2-31	1/F10
	2.6	Documentation of the Electronic Circuits in the Amplifier for Phase and Amplitude Control Circuitry	2-31	1/F10
	2.7	Suggested Approach for a Phase Shift Device in the SPS Architecture	2-34	1/G1
3.0		MAGNETRON STARTING	3-1	1/G5
4.0		CONCEPT OF THE POWER MODULE AND ITS INTERFACE WITH THE REST OF THE SATELLITE	4-1	1/G9
	4.1	Definition of the Power Module and Its Interface with the Subarray	4-1	1/G9
	4.2	Interface of the Power Module with the Thermal Environment and with the Auxiliary DC Power Sources	4-6	2/A6
5.0		AUXILIARY POWER SOURCE STUDY	5-1	2/A13
	5.1	Introduction	5-1	2/A13
	5.2	Application of Microwave-to-DC Power Conversion as a Source of Auxiliary Power	5-3	2/B3
	5.3	Scenario of Start-Up Procedure in Subarray that Supplies its Own Auxiliary Power	5-10	2/B13

TABLE OF CONTENTS (Continued)

Section			Page
6.0		NOISE MEASUREMENTS	6-1 2/C6
	6.1	Introduction and Summary	6-1 2/C6
	6.2	Description of the High Sensitivity Noise Measuring Equipment	6-6 2/C13
	6.3	Description of the First Magnetron Configuration Tested	6-6 2/C13
	6.4	Results from the Magnetron Directional Amplifier Using the Raytheon QKH2000 #13	6-13 2/D9
	6.5	Description of and Test Results from the Second Magnetron Configuration	6-15 2/D11
7.0		DESIGN OF THE SPS MAGNETRON	7-1 2/E5
	7.1	Introduction	7-1 2/E5
	7.2	Study of Pyrographite Heat Radiator Design and Its Manufacture and Cost	7-5 2/E9
	7.2.1	Heat Radiator Design	7-5 2/E9
	7.2.2	Bonding Pyrolytic Graphite to the Magnetron Anode	7-11 2/F3
	7.2.3	The Manufacture of Pyrolytic Graphite and Its Fabrication into Radiators	7-12 2/F4
	7.3	Magnetic Circuit Study	7-15 2/F9
	7.4	Design of Interaction Areas of Magnetron	7-19 2/F13
	7.5	Design of Cathode for Long Life	7-23 2/G4
	7.6	Mechanical Design of the Magnetron	7-24 2/G5
	7.7	Projection of the Characteristics of the Magnetron Package	7-26 2/G7
8.0		HARMONIC SUPPRESSION BY COAXIAL STUB FILTERS	8-1 3/A7
9.0		THE USE OF THE AMPLITUDE CONTROL FEATURE IN THE MAGNETRON DIRECTIONAL AMPLIFIER TO OPTIMIZE THE OVERALL SYSTEM EFFICIENCY AND TO PROVIDE DIRECT CONTROL OF SPS SYSTEM DC POWER OUTPUT BY THE ELECTRIC UTILITY	9-1 3/B6
	9.1	Experimental Verification with a Simulated Voltage-Current Characteristic of the Solar Cell Array	9-6 3/B11

TABLE OF CONTENTS (Continued)

Section			Page	
10.0		DEFINITION OF TECHNOLOGY DEVELOPMENTS FOR THE MAGNETRON PACKAGE AND MAGNETRON DIRECTIONAL AMPLIFIER	10-1	3/B14
	10.1	Introduction	10-1	3/B14
	10.2	Unresolved Issues and Additional Investigations	10-2	3/C1
	10.3	The Proposed Development Program for the Magnetron Package	10-5	3/C4
	10.4	The Proposed Development Program for the Magnetron Directional Amplifier	10-5	3/C4
11.0		ESTIMATED MAGNETRON PACKAGE PRODUCTION COSTS	11-1	3/C10
APPENDIX A		THEORY OF OPERATION OF THE MAGNETRON DIRECTIONAL AMPLIFIER	A-1	3/C13
APPENDIX B		DATA COMPARISON	B-1	3/C14

TABLE 7-4

PROJECTED MECHANICAL CHARACTERISTICS OF THE MAGNETRON PACKAGE*

Item No.	Characteristics	Value	Determined By	Comments
1	Mass	1.018 kG ±0.2 kG	Design of Tube	See Section 7.6 of this Report
2	Radiator Diameter	36.8 CM	Design of Tube	See Section 7.2 of this Report
3	Axial Length	10 CM	Design of Tube	See Section 7.2 of this Report
4	Microwave Output	Antenna Probe	Design of Tube	
5	Maximum Operating Temperature of Pyrographite Radiator	350°C		

*See Table 7-2 for Additional Detail.

1. W.C. Brown "Microwave Beamed Power Technology Improvement", Final Report PT-5613 for JPL contract No. 955104, dated May 15, 1980.

2. W.C. Brown "Design, Fabrication and Testing of a Crossed-Field Amplifier for Use in the Solar Power Satellite", NASA CR-159410, Raytheon PT-5528, August 1978.

3. "Microwave Power Transmission System Studies", NASA CR-134886, Raytheon ER75-4368, Contract NAS 3-17835, December 1975.

4. "Final Report on Pyrographite Research and Development", August 1961, Sub-Contract PO 18-2259 to Raytheon Company from Lockheed Missiles and Space Company, Prime Contract No. rd 17017, written by High Temp. Materials Department, Research Division, Raytheon Company.

5. Lindquist, L.O. and Mah, R., "Graphite to Metal Bonding Techniques", LA-6928-MS (Internal Report), November 1977.

6. G.B. Collins, "Microwave Magnetrons", McGraw-Hill Book Company, Inc. 1948. Page 416 (This book is part of Radiation Laboratory Series).

7. R.B. Ayer, "Use of Thoriated Tungsten Filaments in Transmitting Tubes", Proc. of I.R.E., Volume 40, May 1952, pp. 591-94.

8.0 HARMONIC SUPPRESSION BY COAXIAL STUB FILTERS

One of the interesting aspects of the use of a relatively low power microwave generator is that the power from the tube can be brought out through a coaxial line of relatively small diameter as shown in Figure 8-1. It may then be possible to use simple coaxial stubs placed along the line to reflect the harmonic power. The purpose of the work under this contract was to obtain some initial data on the performance of such filters and to make an initial evaluation of whether such a procedure is practical.

The general procedure on how this was accomplished is shown in Figure 8-2.

The simple approach being taken to an initial evaluation of the stub filter is shown in Figure 8-3. This was arrived at after reviewing other possible approaches with our consultant. In principle the position of the shorting plunger in the top stub is adjusted until the maximum power is reflected at the second harmonic frequency. The position of the shorting plunger is then secured by drilling a hole for a holding pin. The length of the conductor protruding from the other side of the center conductor of the main coaxial transmission line is then adjusted to give maximum reflection of the third harmonic. The rejection of the second harmonic frequency is then checked again to see if there has been any perturbation of that adjustment by adjusting for the third harmonic rejection.

However, it was not possible to optimize both second and third harmonic reflection on cold test. It was therefore decided to remove the stub for the third harmonic filter and to concentrate upon the second harmonic filter. In particular it was desired to see how the filter would behave on hot test.

The physical arrangement that was used for hot test is shown in Figure 8-4. The magnetron and its coaxial output is at the left of the picture. The coaxial output feeds into a 6 inch section of 7/8 inch coaxial line that contains the second harmonic reflecting stub. That, in turn, feeds into a coaxial water load. Two coupling outputs are shown on the water load. They are positioned on the load at locations before power absorption by the load begins.

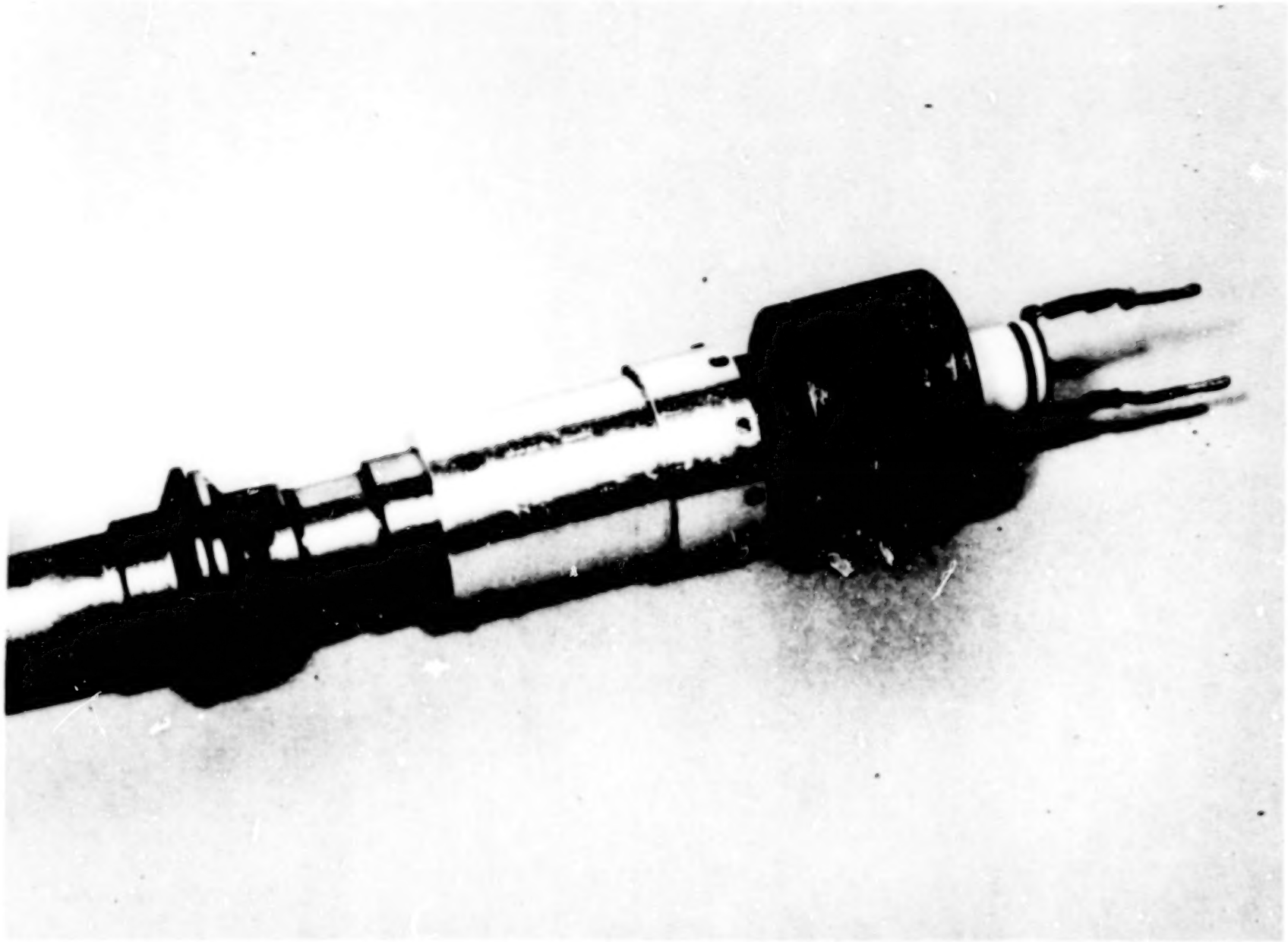

80-1038B

Figure 8-1. Coaxial Output Fitted Directly to the Microwave Oven Magnetron.

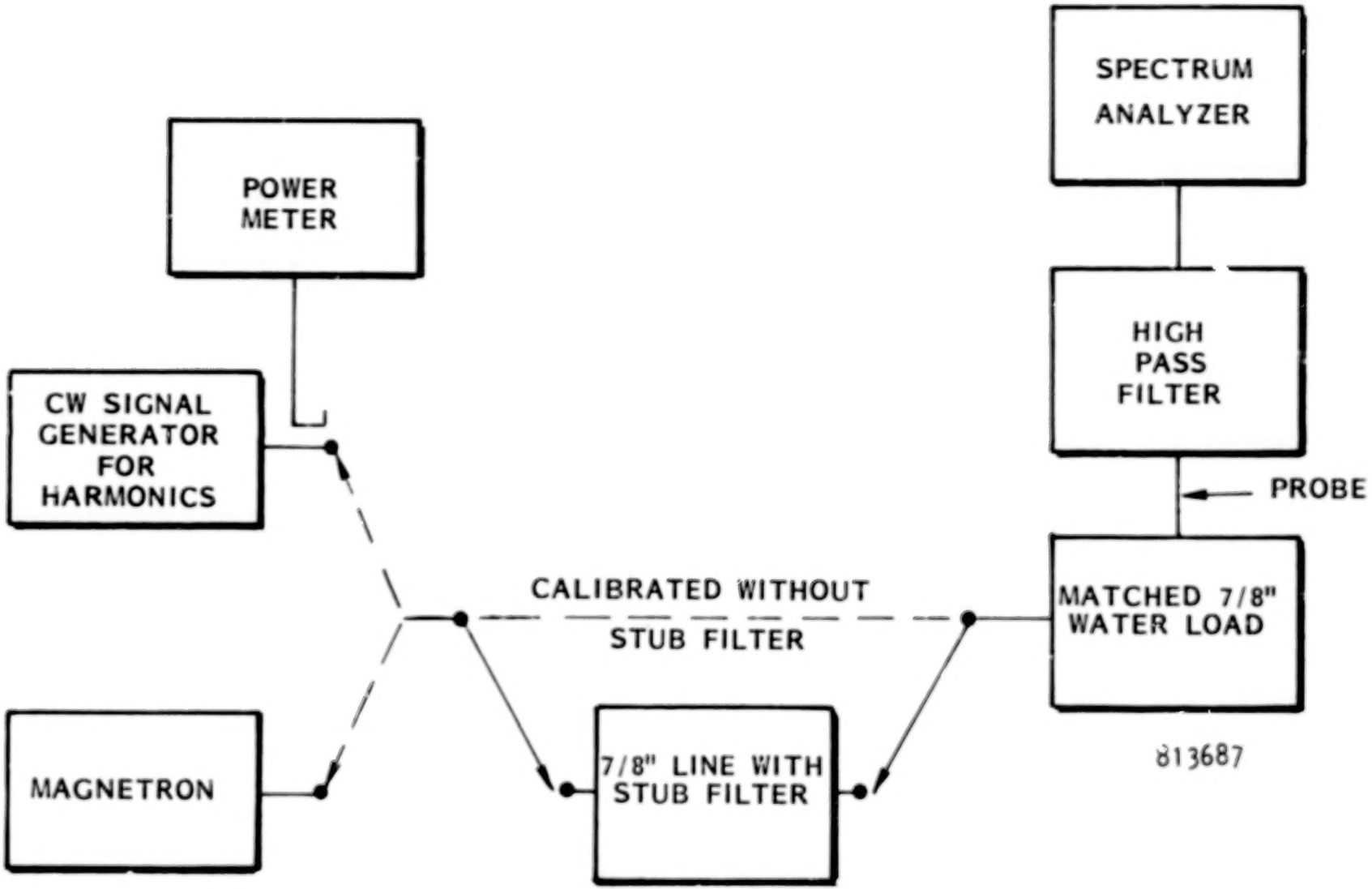

Figure 8-2. Arrangement for Investigating Stub-Type Filter for Reducing Harmonic Level.

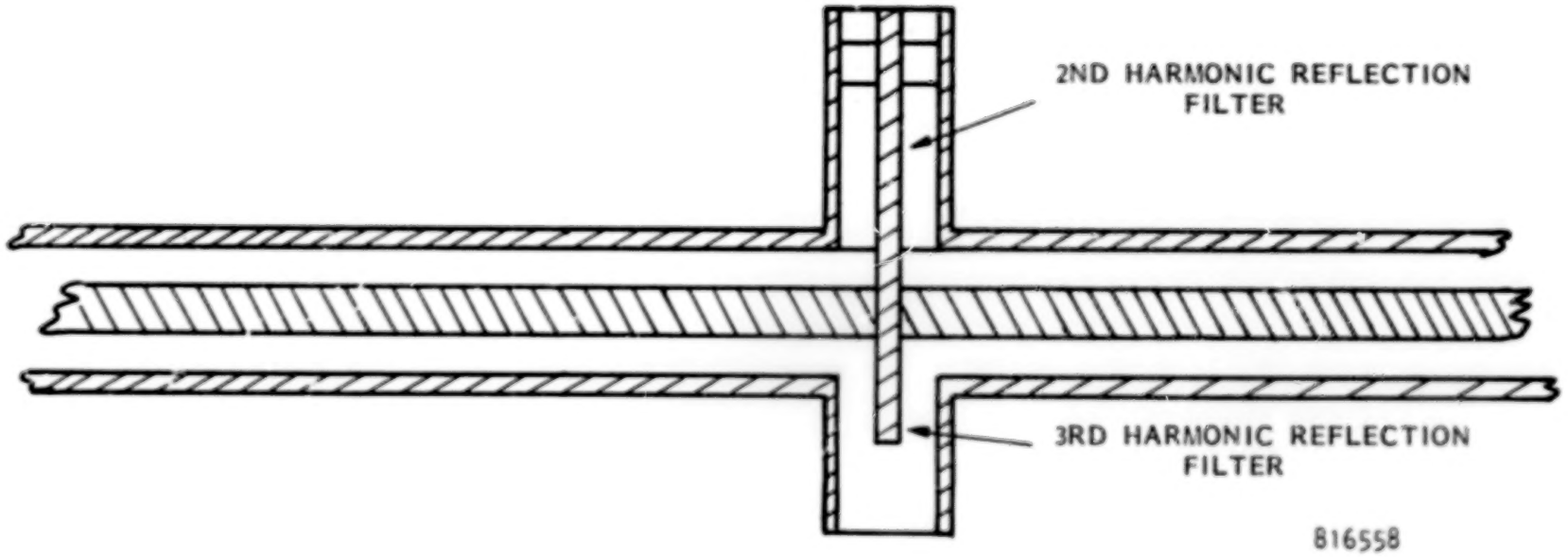

Figure 8-3. Proposed Reflection Filters to Minimize Second and Third Harmonic Power.

BLANK PAGE

BLANK PAGE

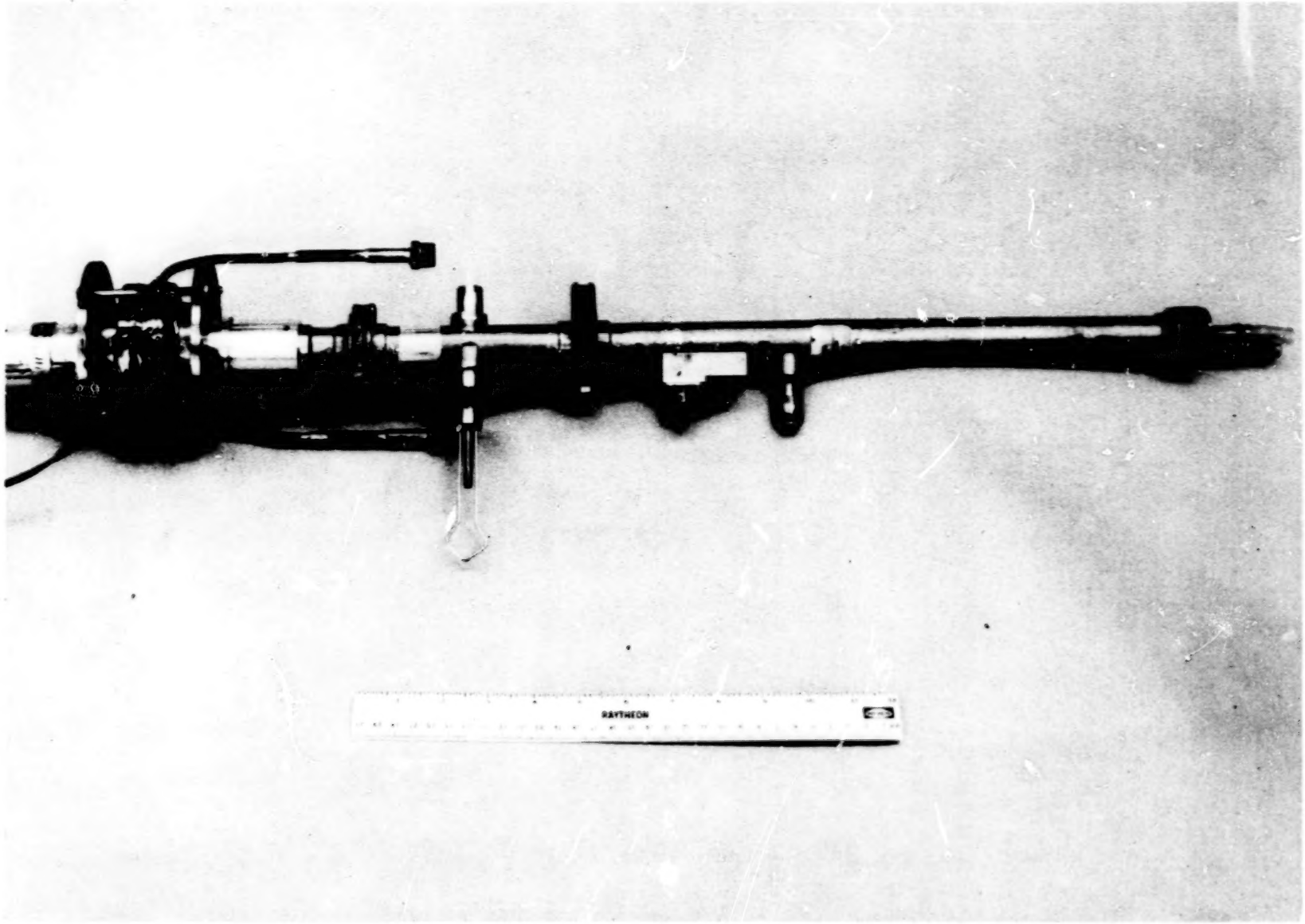

80-2367B

Figure 8-4. Experimental Arrangement for Measuring Additional Attenuation of Second Harmonic Power by Coaxial Stub in 7/8 Inch Coaxial Line Tuned to Reflect Second Harmonic Power.

The hot test data was informative. It was determined that the stub could be adjusted to reduce the second harmonic flow into the load by 40 dB. Because the second harmonic output was approximately 60 dB below the carrier without the use of the stub-line filter, the level of the second harmonic signal with the use of the filter was approximately 100 dB below the carrier.

It therefore appears that the use of a stub filter is a viable method of reducing the second harmonic content of the output of the magnetron. Additional effort may also indicate that it is satisfactory for the reduction of the third harmonic content as well. Considerable additional effort is indicated to fully evaluate the use of such filters in the SPS.

It is interesting to observe the accumulative effects of (1) a relatively low harmonic output of the tube, (2) the additional reduction that can be made with the use of a reflective stub filter, and (3) the attenuation and angular scattering of these harmonics that results from the slotted waveguide radiator. At the receiving sets of the rectenna all these factors reduce the harmonic power to density levels that are equal to or less than the CCIR requirement of -154 dBm/meter^2/4 KHz. An exercise with the measurements made on the second harmonic shows a safety factor of 40 dB at the earth. The exercise is carried through in Table 8-1.

TABLE 8-1

HARMONIC LEVELS IN SPS SYSTEM BASED UPON (1) HARMONIC MEASUREMENTS ON OUTPUT OF MICROWAVE OVEN MAGNETRON, (2) FILTER REJECTION, AND (3) RADIATING ANTENNA PATTERN FOR HARMONICS.

HARMONIC ORDER	HARMONIC MEASURED AT TUBE OUTPUT DBC		MEASURED STUB FILTER REJECTION dB	MEASURED GAIN REDUCTION IN ANTENNA SECTION DBC	RATIO OF HARMONIC TO CARRIER PWR PER SOLID ANGLE DBC	HARMONIC LEVEL AT EARTH FOR ANTENNA SECTION DBW/SQ. METER	HARMONIC LEVEL AT EARTH FOR ENTIRE SPS SATELLITE DBW/SQ. METER	CCIR REQUIREMENT DBW/M^2/4 kHz
	JPL	RAYTHEON						
	(1)	(2)	(3)	(4)	(5)	(6)	(7)	(8)
2ND	-54	-70	40	65	-166	-261	-204	-154
3RD	-65	-91	NO DATA	50				
4TH	-67	-89	NO DATA	50				
5TH		-63	NO DATA	65				

(1) FIGURE 2-4 JPL PUBLICATION 80-11, JUNE 15, 1980, "BEAMED MICROWAVE POWER TRANSMITTING AND RECEIVING SUBSYSTEMS RADIATION CHARACTERISTICS". RICHARD DICKINSON. METHOD OF MEASUREMENT WAS IN WAVEGUIDE WITH "PORCUPINE".

(2) PAGE 4-22 RAYTHEON COMPANY FINAL REPORT ON JPL CONTRACT NO. 955104 "MICROWAVE BEAMED POWER TECHNOLOGY IMPROVEMENT" 15 MAY 1980. W.C. BROWN. METHOD OF MEASUREMENT WAS IN 7/8" COAXIAL LINE ATTACHED DIRECTLY TO TUBE OUTPUT.

(3) SECTION 8.0 "HARMONIC SUPPRESSION BY COAXIAL STUB FILTERS", OF RAYTHEON DRAFT REPORT PT-5653 ENTITLED "SATELLITE POWER SYTEM (SPS) MAGNETRON TUBE ASSESMENT STUDY" ON CONTRACT NAS8-33157. W.C. BROWN.

(4) FIGURE 3-3 AND 3-4, JPL PUBLICATION AS IN (1). AREA OF ANTENNA SECTION IS 0.55 SQUARE METERS AND CORRESPONDING GAIN IS 26.7 dB.

(5) BASED ON AVERAGE OF JPL AND RAYTHEON MEASUREMENT OF HARMONIC OUTPUT OF 61 dB, 40 dB STUB FILTER REJECTION, AND 65 dB MEASURED GAIN REDUCTION OF 2ND HARMONIC IN ANTENNA RADIATOR.

(6) BASED UPON POWER OUTPUT OF 13 KILOWATTS FROM 0.55 SQUARE METER RADIATOR WITH 26.7 dB GAIN AND -166 DBC HARMONIC LEVEL PER SOLID ANGLE.

(7) BASED UPON A TRANSMITTING ANTENNA WITH 7.5 GIGAWATTS OF POWER OUTPUT COMPRISED OF 576,000 RADIATORS OF 0.55 SQUARE METER AREA. IT IS ASSUMED THAT THERE IS NO COHERENCE OF THE PHASE OF THE HARMONIC OUTPUT FROM THE RADIATORS.

9.0 THE USE OF THE AMPLITUDE CONTROL FEATURE IN THE MAGNETRON DIRECTIONAL AMPLIFIER TO OPTIMIZE THE OVERALL SYSTEM EFFICIENCY AND TO PROVIDE DIRECT CONTROL OF SPS SYSTEM DC POWER OUTPUT BY THE ELECTRIC UTILITY

It has been previously pointed out in Section 2.1 that the amplitude control feature of the magnetron directional amplifier permits the device to be placed across the DC buss that originates in the solar photovoltaic array, with only a small resistance of 100 ohs or less in series to allow for a fuse and some possible small inductance to permit burning off of "whiskers" should such a pheonomenon be present, as explained in Section 2.3. This arrangement eliminates the bulk of the power conditioning that would otherwise be necessary for the microwave power generation.

However, the amplitude control feature can also be combined with a logic and control center to optimize the overall system efficiency and to provide direct control of the DC power output from the rectenna to match the needs of the electric utility user. This latter feature is of great interest to the electric power system engineer because of the fast response time which is virtually only the time that it takes to transmit a signal from the earth to the SPS satellite, about 0.2 seconds.

To understand better the basic principles involved consider Figure 9-1 which is a simplified block diagram for the overall amplitude control system. The desired system load reference is the voltage level at which it is desired to operate the input to the power utility grid. The voltage level at the output of the rectenna is then sensed and compared with the reference level. Any voltage difference represents an error which is relayed to the satellite. This error is distributed throughout the satellite and added or substracted to the reference power level (also in the form of a DC voltage) for each of the magnetrons. When the proper reference voltage is reached the microwave power reaching the ground is just sufficient to match the power requirements of the grid.

Figure 9-2 shows a more detailed format in which the adjustment in reference level is distributed to each of the step-taper levels from which the reference level

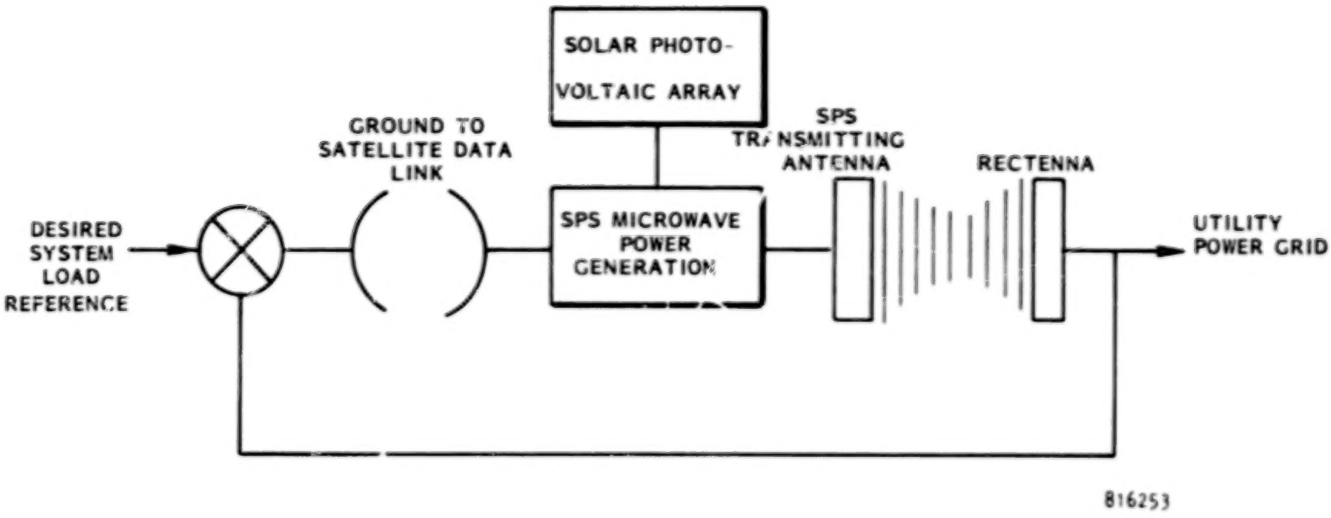

Figure 9-1. Overall Control System Showing How the Varying Demands of the Utility Power Grid can be Interfaced with the SPS Facility.

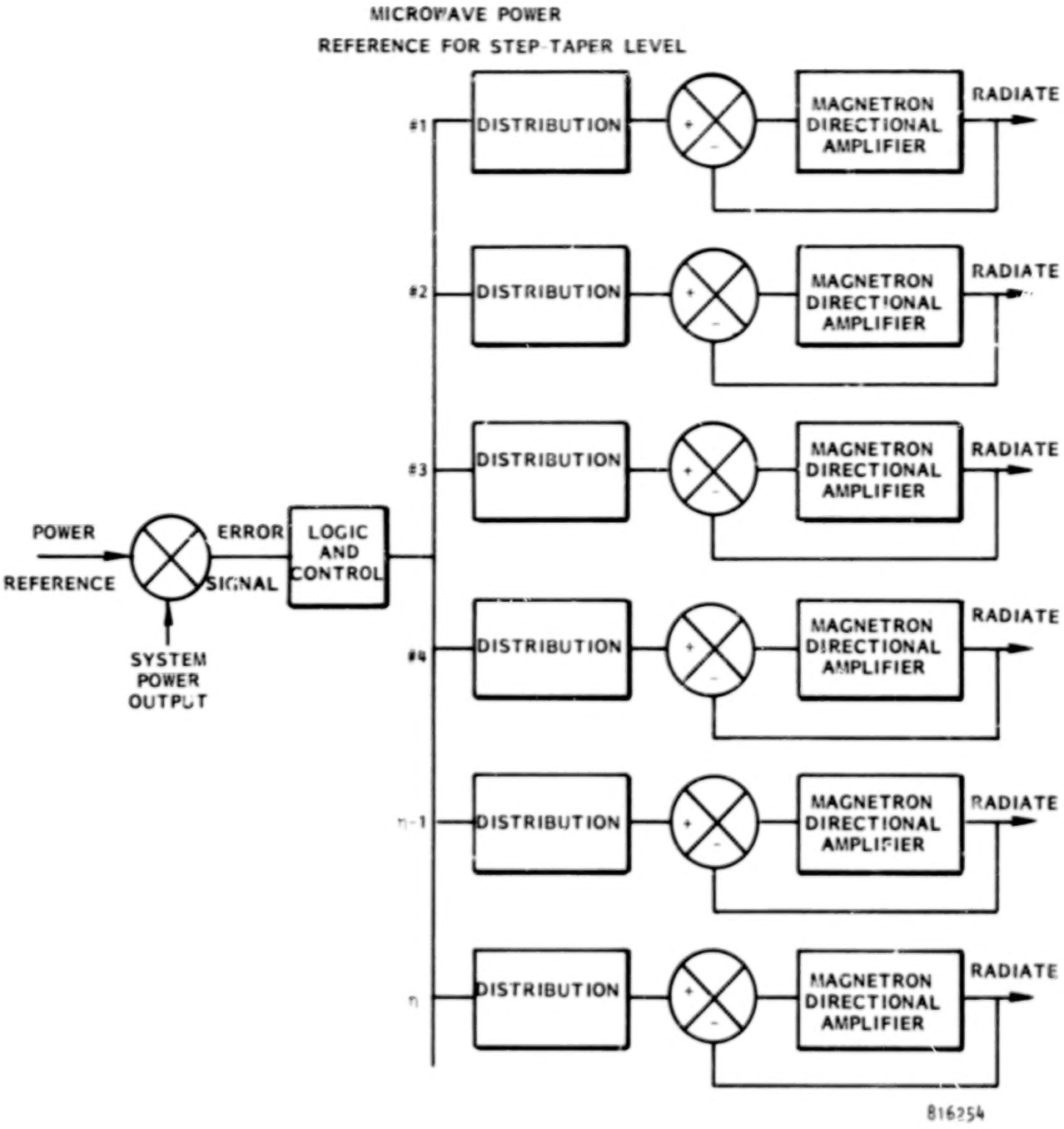

Figure 9-2. Control of Illumination Distribution by Logic and Control Center to Command Amount of Power Radiated from Each Step-Taper Level.

is distributed, first to the subarrays and then to the power modules and finally to each magnetron which has its own buck-boost coil. The logic and control center shown in Figure 9-2 has potentially many functions. In addition to optimizing the efficiency of the SPS system and being indispensible in the overall power control loop, it may also be used to change the illumination taper across the transmitting antenna. It is expected that this flexibility will be useful in maximizing aperture transfer efficiency and in minimizing troublesome grating lobes if they should occur.

Figure 9-3 shows the interface of the microwave power generation function in the SPS with the solar cell array. Three cases are considered. Case I is the situation in which the voltage-current characteristic of the solar cell array remains constant but where it is desired to change the power output from the rectenna to meet varying utility demands on the Earth. Each of the constant load curves labeled 1, 2 and 3 represents a different constant settting of the microwave power output reference. Operation of the system occurs at the point where the load curves represented by the magnetron cross the voltage-current characteristic of the solar cell array.

To obtain maximum power output from the solar array the load-line of the microwave generator bank needs to be located close to the knee of the voltage-current characteristic of the solar cell array since this "knee" represents the most efficient point of the solar array.

Case II shows the situation in which the load is constant but in which there is a change in the voltage-current characteristic of the solar cell array either in the short term or in the long term, and that is caused either by a change in the solar illumination intensity or a change within the solar cells themselves. For example, when the satellite comes out into the sunlight after occultation by the earth there will be drastic changes in the values of the current which the solar cell array can supply. If the dynamic range of the microwave generators is limited, the logic and control center can issue commands to start the magnetrons in some sequence.

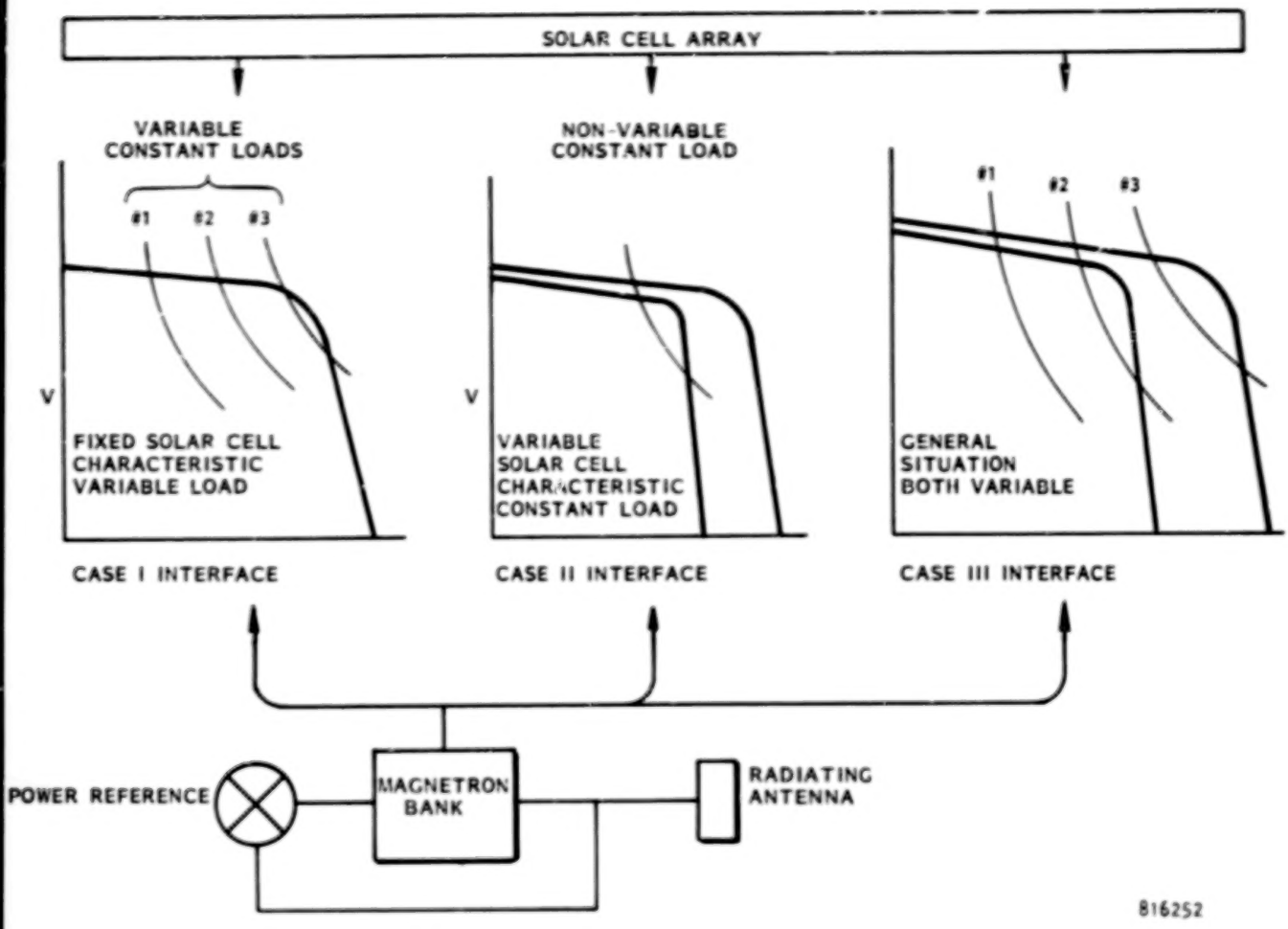

Figure 9-3. Interface Between Solar Cell Array and Magnetron Directional Amplifier.

Finally, Case III shows the general situation in which both the load requirements and the voltage-current characteristic of the solar cell array are variable with time. The great flexibility of the logic and control center to deal with many different situations by simply transmitting a reference signal of low voltage and negligible power to each magnetron directional amplifier should be of great value in the SPS power system.

9.1 Experimental Verification with a Simulated Voltage-Current Characteristic of the Solar Cell Array

To simulate the interaction of the whole bank of magnetron directional amplifiers with the solar cell array, the slope of the voltage-current characteristic of the solar cell array was simulated with an 810 ohm resistor in series with the voltage-regulated power supply as shown in Figure 9-4. A single magnetron directional amplifier represented the total bank of generators. Figure 9-5 shows how the curves of constant power output as determined by the reference voltage intersect with the voltage-current characteristics of the solar cell array which are determined by the open circuit voltage of the power supply and a series resistance of 810 ohms.

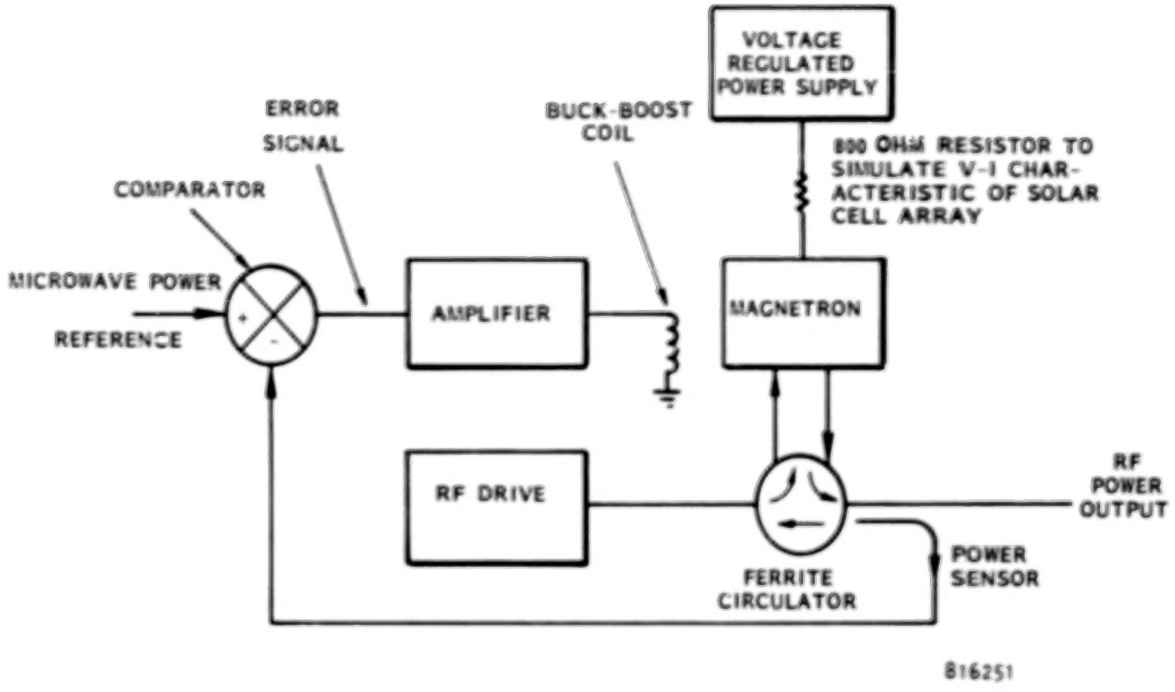

Figure 9-4. Test Arrangement for Evaluation of Amplitude Control. See Also Figures 2-1 and 2-3.

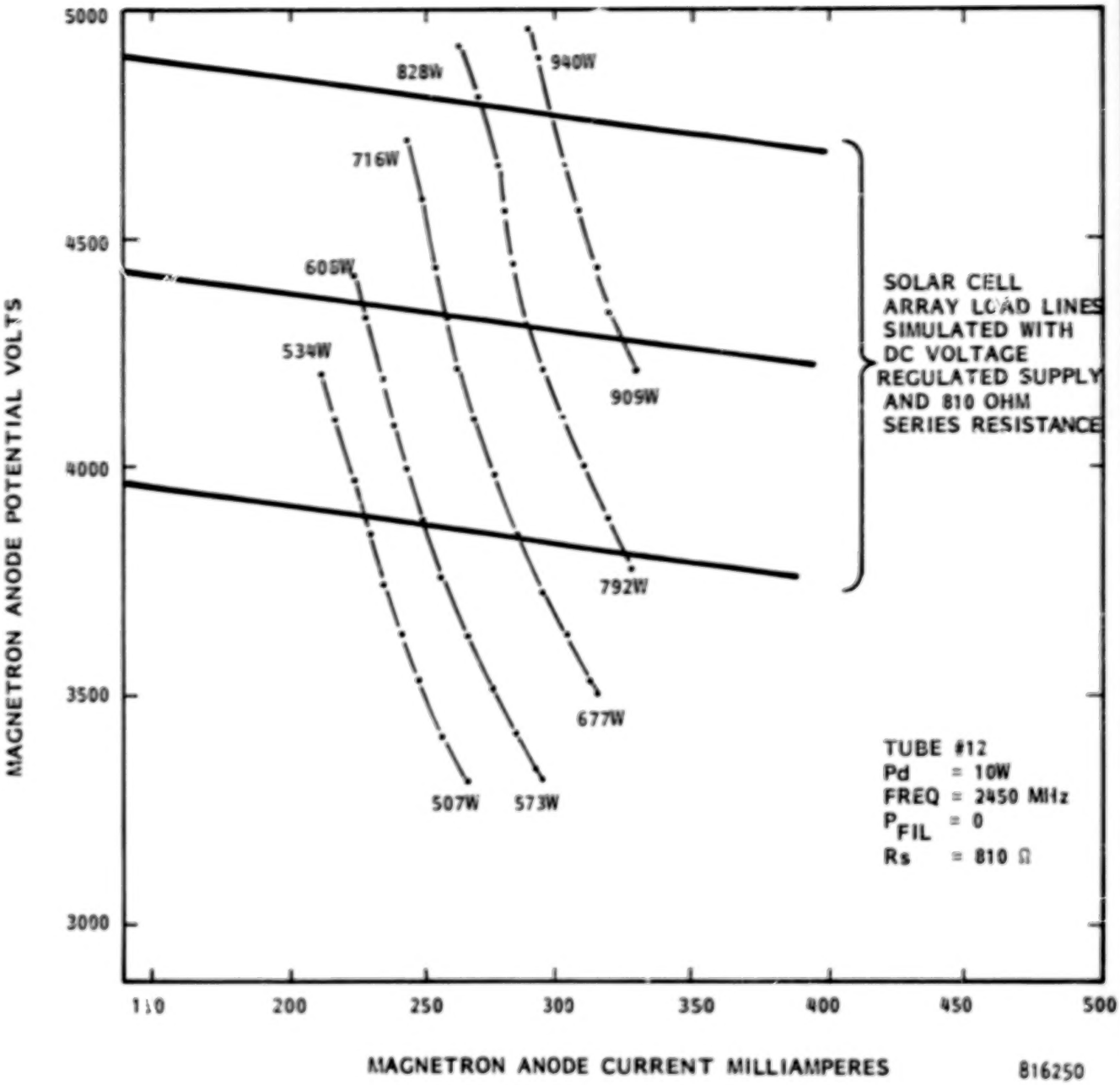

Figure 9-5. Experimental Data on the Amplitude Control System Shown in Figure 9-4 and in More Detail in Figures 2-1 and 2-3.

10.0 DEFINITION OF TECHNOLOGY DEVELOPMENTS FOR THE MAGNETRON PACKAGE AND MAGNETRON DIRECTIONAL AMPLIFIER

10.1 Introduction

In this section we will define the technology developments for both the magnetron package and the magnetron directional amplifier and estimate the effort in terms of time and constant 1980 dollars. The "magnetron package" is defined as a package that contains (1) the basic device for DC to microwave energy conversion, including the permanent magnets, (2) the pyrographite radiator that disposes of the waste heat, (3) a buck-boost coil that is used in conjunction with the control of the amplitude of the output, and (4) a "voice coil" driven tuner that is used in conjunction with the control of the phase of the output. These are shown in Figure 7-1.

The magnetron directional amplifier, on the other hand, is defined* to include, in addition to the magnetron package, the passive directional device, the output sensors and comparators for both phase and amplitude tracking, and the feedback control circuits. The form of the passive directional device in the magnetron directional amplifier can be either a ferrite circulator or a "magic-T" (or its equivalent). The magnetron package itself need not be different for the two different forms of magnetron directional amplifier, but two tubes are used in the "magic-T" format while only one is used with the ferrite circulator.

In some respects it is difficult to specify a technology development program for the magnetron directional amplifier without also involving the slotted waveguide array since it is combined with the magnetron directional coupler to form the basic radiation unit. Even the next level of integration, the power module, may be involved.

*See Appendix A for further explanations.

The present study has helped to resolve a number of important issues and has led to a better quantification of many items, the mass of the microwave system, for example. However there are still several unresolved issues and a number of additional investigations that should be discussed as background for the outline of the technology development programs. In the following section items 1, 2 and 4 are closely related to the technology development program for the magnetron package while 2 and 3 are related to the technology development program for the magnetron directional amplifier.

10.2 Unresolved Issues and Additional Investigations

1. Mass and Power Required for the Buck-Boost Coil as a Function of Change in Operating Voltage

It was pointed out in Section 7.6 of this report that we may have been misled by the data obtained on the use of a buck-boost coil on the microwave oven magnetron. Although the power requirements for buck-boost coils as applied to the magnetic circuit designs of Figures 7-1 and 7-5 could be readily obtained, there was not time to obtain this data before submitting the final report. When the data is obtained and if it is objectionable in terms of mass and power consumption there will be need to work out a compromise design which will incorporate magnetic pole pieces in the design similar to those in the microwave oven magnetron. Until this issue is resolved, the mass and power requirements of the buck-boost approach to power conditioning for the overall system cannot be accurately estimated.

2. Evaluation of the Concept of Retuning the Magnetron to Cause the Phase of the Output of the Magnetron Directional Amplifier to Follow the Reference Phase

If the tuning range involved is about 1% of the carrier frequency, the magnetron directional amplifier should be able to operate over the same range of current and voltage as if the tube were operating as a free-running oscillator limited only by dissipation ratings and a minimal input power level to supply the cathode backbombardment. Such a tuning range can be easily obtained if the tuning method shown in Figure 7-1 is used. Ten percent tuning is a typical figure for a tunable magnetron.

It is probable that there will be considerable skepticism about such an arrangement and a demonstration would therefore be desirable. However, such a demonstration must probably be initially accomplished with a tuning cavity which is attached to the output of the tube because a tunable CW magnetron with an integral tuner as shown in Figure 7-1 is not available.

3. Resolution of the Preferred Passive Directional Device to be Combined with the Magnetron to Form the Magnetron Directional Amplifier

In the interests of demonstrating the general principles of phase and amplitude tracking with the magnetron directional amplifier, the ferrite circulator was used as the passive directional device. While the use of the ferrite circulator for terrestrial use is sound, its use in space may be objectionable because currently available ferrite circulators will not operate in an environment of 300°C. Thus an investigation needs to be made to see if new or different materials could be used to solve this problem.

Because of the potential difficulty with the ferrite circulators in the SPS application, the conventional wisdom has been to use the "Magic T" or its equivalent (other forms may be preferable)* to perform the same functions with high efficiency and with no need for temperature sensitive materials. The "Magic T" is also well adapted to the architecture of Figure 4-1.

Several complications arise in applying the "Magic T" to the SPS application. A set of sensors is needed to sense reflected power at the rf input and feedback control loops are needed to minimize the reflected power. The sensors would be required to function at high temperature. AT the same time the output of the "Magic T" now sensed at the slotted waveguide radiator needs to track phase and amplitude references. There are also special problems in starting to assure simultaneous operation in both tubes and a rapid balancing of phase and amplitude of the individual tube outputs. Although it may be possible it does not seem reasonable to rely upon matched tubes for phase balancing at the output terminals of the "Magic T" and it certainly would be necessary to have buck-boost coils on each tube. The problem appears to be too complicated to be solved simply, and further study seems necessary.

*For example, a symmetrical 3 dB hybrid combiner as proposed by A. Love at Rockwell.

Therefore, in addition to the investigation of the ferrite circulator it becomes necessary to investigate what is involved in a practical solution to the use of the "Magic T" or equivalent in the SPS environment.

4. Understanding the Low Level Noise and Reduced Efficiency in the Microwave Oven Magnetron as a Necessary Input to the SPS Magnetron Development

Although it is now known that the noise emissions from the microwave oven magnetron can be very low and that they can be made even lower by manipulating the external cathode circuit, the mechanisms responsible for a seemingly large variety of observed noise have not yet been identified. A better understanding of these mechanisms may be considered essential to any SPS magnetron development program. In addition it is known that the efficiency of the microwave oven magnetron, although high by most standards, is not as high as it should be, as has already been demonstrated with another magnetron type.

Although this situation has been repeatedly pointed out, the only supported activity toward a better understanding of the causes of noise and reduced efficiency was a Raytheon Independent Research program which has contributed significantly to the bank of data that will be valuable in solving the complex problem.

It should also be pointed out that the complete understanding of these problems and changes in tube design to effect improvements in performance will need experimentation involving the construction of tubes.

Because the design of the SPS magnetron is essentially a scaled version of the microwave oven magnetron design it would seem better to study these problems in connection with the microwave oven magnetron than to proceed immediately to the development of the full scale SPS magnetron.

10.3 The Proposed Development Program for the Magnetron Package

The technology development program as shown in Figure 10-1 is conceived as a four phase development program that starts with the use of the microwave oven magnetron as a desirable and economical intermediate vehicle, proceeds to a "terrestrial" version of the SPS magnetron, then to a "space" version that operates only in a good vacuum and at high temperature, and finally to a program of life test and small lot manufacture of the magnetron. The general description of these developments as well as the uses to which the end product may be put is given in Figure 10-1. Estimated time and cost of each of the phases is also shown.

10.4 The Proposed Development Program for the Magnetron Directional Amplifier

Once the decision is made as to whether the format of the magnetron directional amplifier includes the "Magic-T" or the ferrite circulator, the development program can proceed quite rapidly in comparison with that of the magnetron package and at much lower cost. The major effort is that of determining which of the passive devices will be used in the magnetron directional amplifier.

The cost and required time for determining which passive approach is best depends chiefly upon the cost of constructing a magnetron directional amplifier in the "Magic-T" format and testing its ability to track an amplitude and phase reference. Any sensor, comparator, or other device that is used in the region of the tube or "Magic-T" rather than on the face of the slotted waveguide array should have the capability of being able to operate at 300 to 350^{o}C.

A preliminary estimate of the cost of first analyzing what is involved and then designing, constructing and testing the magnetron directional amplifier in the "Magic-T" format with fully operative phase and amplitude tracking circuits and with a tuning capability given to the magnetron by means of a closely coupled external cavity is in the 100 to 200 thousand dollar range.

PHASE I DEVELOPMENT	PHASE II DEVELOPMENT
• Use of Microwave Oven Magnetron to Understand Sources of Low Level Noise and Inefficiency and Their Correction	• Basic SPS Design Parameters
• Involves:	• Basic Format of Figure 7-1, but;
IA - Measurement and Use of Existing Magnetrons	• Vacuum Envelope
IB - Design Changes and Tube Construction	• Water Cooled
	• No Permanent Magnets
	• Mechanically Tuned through Bellows
USES	USES
1. Understand Sources of Low Level Noise and Their Control	1. Obtain Basic Operating Data
2. Find Sources of Inefficiency and Their Correction	2. Identify Problem Areas and Reiterate Design to Remove Them.
3. Demonstration of Low Noise and High Efficiency	3. Use in Ground Test Demonstration of Power Module and/or Subarray
TIME 18 Months	24 Months
COST A - $60,000 B - $150,000	$800,000

Figure 10-1. Proposed Development of SPS Magnetron Package.

PHASE III DEVELOPMENT	PHASE IV DEVELOPMENT
• Design & Test to All Space Requirements • Samarium Cobalt Magnets • No Vacuum Envelope • Pyrographite Radiator • Test in Vacuum Tank • Operate at 350°C	• Manufacture of Significant Numer of Tubes • Life Test Program
USES	USES
1. Obtain All Data Needed for Space Except Life Test Data. 2. Impact of High Temperature Operation 3. Identify Problem Areas & Reiterate Design 4. Space Tests	1. Search for Long-Term Phenomena 2. Verify Adequacy of Design for Space Use
24 Months	36 Months
2,000,000*	2,000,000*

TOTAL
102 Months 8.5 Years
$4,910,000

*Does Not Include Test Facility.

Figure 10-1. Proposed Development of SPS Magnetron Package. (Continued)

In addition to that effort, it is possible that a study will reveal that the passive ferrite device may still be competitive if new materials are used in its construction. It is then possible that it would be necessary to construct some of these devices, should their feasibility be shown. That could be expensive if substantial development were to be involved.

Once the matter of the form of the magnetron directional amplifier is resolved and one of the units demonstrated, it would seem that further development of the magnetron directional amplifier should occur in the context of putting a number of them together to form a power module. In this format it would then be possible to demonstrate the deployment of the amplitude and phase reference systems and to set up the sources of auxiliary DC power and to start the tubes by energizing their filaments sequentially. It is probable that a microprocessor could be used to advantage in determining the starting sequence and performing a number of other functions.

11.0 ESTIMATED MAGNETRON PACKAGE PRODUCTION COSTS

Magnetron package production costs for large volume production have been estimated. These estimated costs use the current production costs of the microwave oven magnetron modified by the addition of the extra features of the pyrographite cooling fin, the buck-boost coil, the magnetron tuner with solenoid, and the samarium cobalt magnets.

The estimated cost of that portion of the SPS magnetron package that represents the basic generation of microwave power is actually less than the $25.00 price of the conventional microwave oven magnetron which includes a vacuum envelope, the processing of the tube, and relatively expensive packaging parts including the magnets. However, the extra features rapidly increase the cost of the tube. Even so, because of the increased power rating of the tube, the estimated costs per kilowatt of power generated are relatively low, ranging between $12.00 per kilowatt and $32.20 per kilowatt depending upon the range of cost estimates for the tube and its operating efficiency. The operating efficiency should be relatively independent of production costs, and depend only upon the cleverness of the engineer to achieve the potential efficiency of the crossed-field device.

These low costs are additionally significant in that the buck-boost coils provide a system power conditioning function and the "voice coil" tuner provides a phase tracking function that replaces a phase shifting device that would otherwise be needed in the power module.

A breakdown of the estimated production costs is given in Table 11-1.

BREAKDOWN OF COSTS FOR SPS MAGNETRON PACKAGE.

Elements of Cost	Cost Estimate in 1980 Dollars		Specific Cost $/kW			
			3.2 kW Tube 85%		5 kW Tube 90%	
	Low	High	Low Cost	High Cost	Low Cost	High Cost
Basic Tube	12	15	3.75	4.69	2.40	3.00
Pyrographite Fin	20	40	6.25	12.50	4.00	8.00
Buck-Boost Coil	3	8	0.94	2.50	0.60	1.60
Samarium Cobalt Magnets	20	30	6.25	9.38	4.00	6.00
Tuner Including Solenoid	5	10	1.56	3.13	1.00	2.00
Complete Package	60	103	18.75	32.20	12.00	20.60

APPENDIX A

APPENDIX B

DATA COMPARISON

The purpose of adding this appendix is to compare the data that was taken on the magnetron directional amplifier with an amplitude tracking capability made possible by the buck-boost coil with data that had been taken previously without such a capability.

The essential difference between the two sets of data is that the relationship between magnetron anode voltage and current in the amplifier without tracking ability is nearly flat horizontal line above a sharp "knee" that occurs near zero anode current.

The amplitude tracking feedback loop eliminates this flat relationship between anode voltage and current and reestablishes it to provide nearly constant power output as the anode voltage is varied over a wide range.

The figures in this appendix were taken from the final report on "Microwave Beamed Power Technology Improvement", JPL Contract No. 955104, Raytheon Report PT-5613, 15 May 1980.

1. REPORT NO.	2. GOVERNMENT ACCESSION NO.	3. RECIPIENT'S CATALOG NO.
NASA CR-3383		

4. TITLE AND SUBTITLE	5. REPORT DATE
Satellite Power System (SPS) Magnetron Tube Assessment Study	February 1981
	6. PERFORMING ORGANIZATION CODE

7. AUTHOR(S)	8. PERFORMING ORGANIZATION REPORT #
William C. Brown	

9. PERFORMING ORGANIZATION NAME AND ADDRESS	10. WORK UNIT NO.
Raytheon Company Microwave and Power Tube Division Waltham, Massachusetts 02254	M-331
	11. CONTRACT OR GRANT NO. NAS8-33157
	13. TYPE OF REPORT & PERIOD COVERED
12. SPONSORING AGENCY NAME AND ADDRESS	Contractor Report
National Aeronautics and Space Administration Washington, DC 20546	14. SPONSORING AGENCY CODE

15. SUPPLEMENTARY NOTES

Marshall Technical Monitor: Woolsey Finnell III

16. ABSTRACT

The objectives of this study were two-fold: (1) to extend the data base with respect to the magnetron directional amplifier and its operating parameters that are pertinent to its application in the solar power satellite, and (2) on the basis of the resulting extended data base to outline the design of a magnetron that would meet the requirements of the SPS application and then to define a technology program that would result in its development. The incentive for this study was the favorable findings from previous studies that indicated the potential of the magnetron directional amplifier for the SPS application.

This report summarizes the considerable accomplishments of the study, and concludes with the remaining things that need to be investigated or demonstrated to provide high confidence that the magnetron directional amplifier will meet all of the requirements of the SPS system. The ultimate objective is to define the system and investigating the interactions between the system and the microwave generator may well lead to modifications of previous system and tube configurations.

The portions of this study which involved experimental data made use of the microwave oven magnetron that is readily available for test. However, the proposed magnetron design for the SPS is a close scale of the microwave oven magnetron, and resembles it closely physically and electrically.

17. KEY WORDS	18. DISTRIBUTION STATEMENT
Magnetron Directional Amplifier Microwave Power Amplitude Control System Microwave Power Phase Control System	Unclassified - Unlimited Subject Category 44

19. SECURITY CLASSIF. (of this report)	20. SECURITY CLASSIF. (of this page)	21. NO. OF PAGES	22. PRICE
Unclassified	Unclassified	192	A09

For sale by National Technical Information Service, Springfield, Virginia 22161

NASA-Langley, 1981

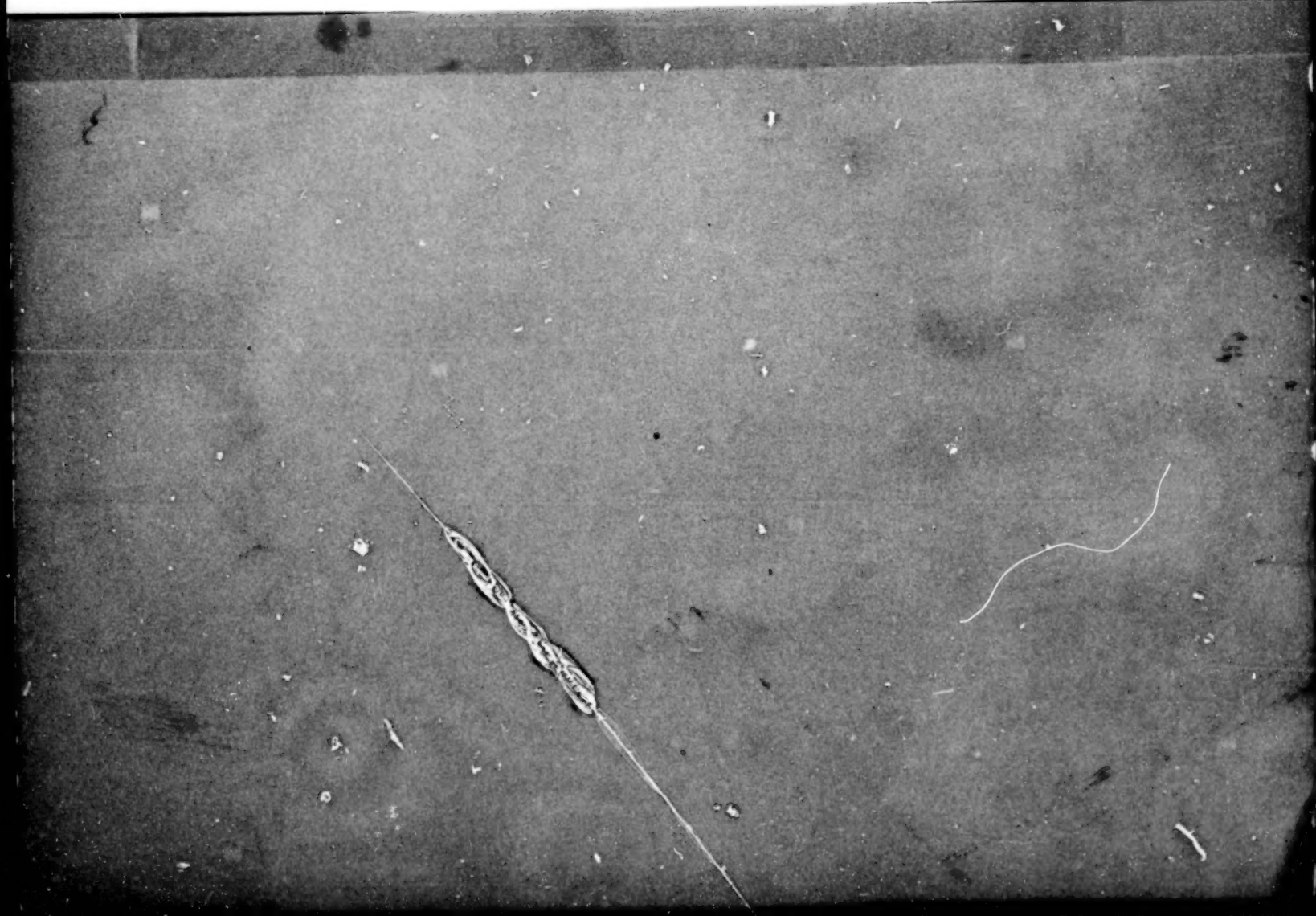

END

April 20, 1981